

An Electrochemical Study of Hydrothermal Reactions
at Elevated Temperatures

Edward Kazimierz Mroczek

Submitted for the degree of
Doctor of Philosophy in Chemistry
at Victoria University of Wellington
June, 1984.

ABSTRACT

A high temperature hydrogen electrode concentration cell based on a design published by Macdonald, Butler and Owen¹, was constructed and used to study the following protolytic equilibria. Thermodynamic equilibrium constants were derived by the usual method of extrapolation to zero ionic strength.

1. The ionization of water at temperatures from 75 to 225 °C in 0.1, 0.3, 0.5 and 1.0 mol kg⁻¹ KCl solution.

$$pK_W^0 = 7229.701/T + 30.285 \log T - 85.007$$

2. The pH calibration of 0.01 and 0.05 mol kg⁻¹ sodium tetraborate at temperatures from 75 to 250 °C in 0.1, 0.3 and 0.5 mol kg⁻¹ NaCl solution.

0.01 mol kg⁻¹ Sodium Tetraborate Solution

$$pH = -0.4830t_1 + 5.5692t_2 + 7.7167t_3 + 8.6983$$

0.05 mol kg⁻¹ Sodium Tetraborate Solution

$$pH = -0.0455t_1 + 8.3987t_2 + 0.2123t_3 + 8.8156$$

3. The second dissociation of sulphuric acid at temperatures from 75 to 225 °C in 0.1, 0.3 and 0.5 mol kg⁻¹ KCl solution.

$$pK_2^0 = 5.3353t_1 - 15.9518t_2 - 111.4929t_3 + 3.8458$$

$$pK_2^0 = 6.1815t_1^* + 12.7301t_2^* + 3.0660 \text{ (up to 150 °C)}$$

where the t_1 to t_3 and t_1^* and t_2^* are the Clark-Glew temperature variable terms at reference² temperatures of 423.15 and 373.15 K respectively.

4. The acid hydrolysis of K-feldspar to K-mica and quartz at a temperature of 225 °C. The determination of the hydrolysis equilibrium constant was limited to one temperature because of the very slow reaction rate at temperatures less than 300 °C.

$$\log(m_{K^+}/m_{H^+}) = 4.2 \text{ (at 225 °C)}$$

Where a comparison could be made, the results of this study agreed well with previously published work, with the exception of the second dissociation constant of sulphuric acid at temperatures above 150 °C. Accurate values for the molal dissociation constant of the HSO_4^- ion pair are required at elevated temperatures before the pK_2^0 results can be fully evaluated.

This research was severely restricted by the unpredictable loss of electrical continuity between the two cell compartments at temperatures above 150 °C. The problem appeared to be associated with the non-wettability of the porous Teflon plug which formed the liquid junction.

ACKNOWLEDGEMENTS

I would like to thank my supervisors Professor J.W. Tomlinson and Dr P.J. Pearce for their continued help, advice and support during the progress of this work. Also greatly appreciated were the many friendly discussions and helpful suggestions of Dr A.J. Read and Dr T. Seward of the Chemistry Division of the Department of Scientific and Industrial Research.

The indispensable technical work of Mr I. Crighton, Mr E. Haldezos, Mr E. Millington and the staff of the University Workshops, Mr L. Morton, Mrs M. Povey, Mr C. Taylor, Mr E. Stevens and in particular of Mr C. Snell is gratefully acknowledged.

Thanks are also due to the Department of Scientific and Industrial Research and the Chemistry Department (VUW) for financial assistance and to the Computing Services Centre (VUW) for providing the statistical, plotting and manuscript preparation facilities.

Finally I would like to thank my parents for their continued support throughout this project.

CONTENTS

ABSTRACT	ii
ACKNOWLEDGEMENTS	iii

PART I -- Introduction

<u>Chapter</u>	<u>page</u>
1. INTRODUCTION	2
1.1 Hydrothermal Solutions.	2
1.2 The Importance of Acidity Measurements at Elevated Temperatures.	3
1.3 High Temperature EMF Measurements.	4
1.4 Proposed Research.	6
1.4.1 Introduction.	6
1.4.2 Ionization of Water.	7
1.4.3 Sodium Tetraborate Buffer.	7
1.4.4 Second Dissociation of Sulphuric Acid.	7
1.4.5 K-feldspar Hydrolysis.	8

PART II -- Experimental and Data Analysis

<u>Chapter</u>	<u>page</u>
2. ELECTROCHEMICAL CELL, MATERIALS AND PROCEDURES	10
2.1 Electrochemical Cell.	10
2.1.1 Introduction.	10
2.1.2 Requirements For The Cell.	10
2.1.3 Cell Design.	10
2.1.4 Electrodes.	13
2.2 Thermostating Baths.	13
2.2.1 Temperature Control.	13
2.2.2 Oil Bath.	14
2.2.3 Salt Bath.	14
2.2.4 Stirring.	15
2.2.4.1 Oil Bath.	15
2.2.4.2 Salt Bath.	15
2.3 Experimental Preparation.	17
2.3.1 Electrodes.	17
2.3.2 Electrode Leads.	17
2.3.3 Chemicals.	17
2.3.4 Porous Teflon Plug.	19
2.4 Experimental Techniques.	22
2.4.1 Electrochemical Equipment.	22
2.4.2 Experimental Procedure.	23
2.4.3 Equilibrium and Reversibility.	24
2.4.4 Time Required For a Complete Experiment.	25

2.4.5 Problems.	26
3. DATA REDUCTION AND ANALYSIS	27
3.1 Thermodynamic Relationships.	27
3.1.1 Potentiometric Determination of Acidity.	27
3.1.2 Liquid Junction Potentials.	29
3.1.3 Activity Coefficients.	31
3.1.4 Standard State.	38
3.2 Dependence of Equilibrium Data on Temperature.	38
3.2.1 Introduction.	38
3.2.2 Valentiner Equation.	39
3.2.3 Clark and Glew Equation.	40
3.3 Statistical Treatment of Data.	41
3.4 Assignment of Uncertainties.	43
3.4.1 Systematic Errors.	43
3.4.2 Random Errors.	46
3.4.3 Derived Functions.	47

PART III -- Results and Discussions

<u>Chapter</u>	<u>page</u>
4. IONIZATION CONSTANT OF WATER	50
4.1 Introduction.	50
4.2 Results.	50
4.3 Errors.	53
4.4 Previous Work.	56
4.4.1 Studies That Employed the Silver/Silver Chloride Electrode.	56
4.4.2 Conductivity Methods.	56
4.4.3 Hydrogen Electrode Concentration Cell Studies.	57
4.5 Discussion and Comparison with Other Work.	57
4.5.1 Introduction.	57
4.5.2 Studies Employing the Silver/Silver Chloride Electrode.	57
4.5.3 Conductivity Measurements.	60
4.5.4 Macdonald, Butler and Owen's Study.	60
4.5.5 Sweeton, Mesmer and Baes's Flowing Cell Results.	61
4.5.6 Mesmer and Co-workers, Static Cell Studies.	63
4.5.7 IAPS Equation.	65
4.5.8 Conclusion.	65
4.6 Thermodynamic Parameters.	66
4.7 Recommended Values for the Ionization Constant of Water.	68
5. CALIBRATION OF SODIUM TETRABORATE BUFFERS	70
5.1 Introduction.	70
5.2 Previous Work.	71
5.3 Results.	72
5.3.1 Activity Coefficients.	79
5.4 Errors.	80
5.5 Discussion and Comparison with Other Work.	83
5.5.1 0.01 mol kg ⁻¹ Sodium Tetraborate Solution.	83
5.5.1.1 Between 75 and 150 °C	86
5.5.1.2 Between 150 and 250 °C	87

5.5.2	Mesmer, Baes and Sweeton's Study.	88
5.5.3	Comparison with Mesmer, Baes and Sweeton's Results, as Calculated by Seward.	89
5.5.4	Boric Acid Dissociation.	93
5.5.5	Assumptions Made in Deriving the pOH Values.	96
5.6	Recommended pH Values for the Sodium Tetraborate Buffers.	99
5.6.1	0.01 mol kg ⁻¹ Sodium Tetraborate Solution.	99
5.6.1.1	Between 75 and 150 °C.	99
5.6.1.2	Between 150 and 250 °C.	99
5.6.2	0.05 mol kg ⁻¹ Sodium Tetraborate Solution.	100
6.	SECOND DISSOCIATION CONSTANT OF SULPHURIC ACID	101
6.1	Introduction.	101
6.2	Previous Work.	101
6.3	Results.	102
6.4	Errors.	105
6.5	Discussion.	109
6.5.1	Comparison with Other Work.	109
6.5.2	Trends of the Dissociation Constants with Temperature.	114
6.5.3	Ion Pair Formation.	116
6.5.4	Reduction of Sulphate by Hydrogen.	119
6.6	Thermodynamic Parameters.	120
6.6.1	Trends with Temperature.	120
6.6.1.1	CG3 Equation.	121
6.6.1.2	CG4 Equation.	121
6.7	Predicted Thermodynamic Trends.	122
6.8	Recommended Values for the Second Dissociation Constant of Sulphuric Acid.	124
7.	ACID HYDROLYSIS OF K-FELDSPAR TO K-MICA AND QUARTZ.	126
7.1	Introduction.	126
7.1.1	Previous Work.	127
7.1.2	Limitations of This Work.	127
7.2	Results.	128
7.3	Iron Correction.	130
7.4	Error.	131
7.5	Discussion.	131
7.5.1	Experiments at Low pH.	131
7.5.2	Experiments at High pH.	133
7.5.3	Previously Published Work.	136
<u>Appendix</u>		<u>page</u>
A.	WATER RESULTS	139
B.	SODIUM TETRABORATE BUFFER RESULTS	151
C.	SULPHURIC ACID RESULTS	178
D.	FELDSPAR HYDROLYSIS RESULTS	195
REFERENCES	200

LIST OF FIGURES

<u>Figure</u>	<u>page</u>
2.1 Electrolyte Concentration Cell.	12
2.2 Salt Bath Stirring Assembly.	16
2.3 Voltage Measurement Connections.	22
4.1 The Variation of pK'_W with Ionic Strength at Various Temperatures.	52
4.2 The Deviation Between the pK^O_W Values Found in This Study and Previously Published Work.	59
5.1 The Variation of pOH of 0.01 mol kg ⁻¹ Sodium Tetraborate Solution with Ionic Strength at Various Temperatures. . . .	77
5.2 The Variation of pOH of 0.05 mol kg ⁻¹ Sodium Tetraborate Solution with Ionic Strength at Various Temperatures. . . .	77
5.3 Literature Results for the Variation in pH of 0.01 mol kg ⁻¹ Sodium Tetraborate Solution with Temperature.	85
5.4 The Variation in pH of 0.05 mol kg ⁻¹ Sodium Tetraborate as Found in This Study and From Swards Calculations.	91
5.5 The Ionic Strength Dependence of $\log Q_b$ in 0.01 mol kg ⁻¹ Sodium Tetraborate Solution at Various Temperatures.	94
6.1 The Variation of pK'_2 as a Function of Ionic Strength at Various Temperatures, CG4 Equation to 225°C.	103
6.2 Literature Results for the Variation of the Dissociation Constant of the Bisulphate Ion with Temperature.	110
7.1 The Variation of $\log(m_{K^+}/m_{H^+})$ with Time of the Feldspar Hydrolysis Reaction at 225°C.	129
7.2 The Variation of $\log(m_{K^+}/m_{H^+})$ with Temperature Derived by Different Workers.	137
A.1 The Temperature Dependence of pK'_W in 0.1 mol kg ⁻¹ KCl Solution.	142
A.2 The Temperature Dependence of pK'_W in 0.3 mol kg ⁻¹ KCl Solution.	143

A.3	The Temperature Dependence of pK'_W in 0.5 mol kg ⁻¹ KCl Solution.	144
A.4	The Temperature Dependence of pK'_W in 1.0 mol kg ⁻¹ KCl Solution.	145
B.1	The Temperature Dependence of pOH of 0.01 mol kg ⁻¹ Sodium Tetraborate in 0.1 mol kg ⁻¹ NaCl Solution.	160
B.2	The Temperature Dependence of pOH of 0.01 mol kg ⁻¹ Sodium Tetraborate in 0.3 mol kg ⁻¹ NaCl Solution.	161
B.3	The Temperature Dependence of pOH of 0.01 mol kg ⁻¹ Sodium Tetraborate in 0.5 mol kg ⁻¹ NaCl Solution.	162
B.4	The Temperature Dependence of pOH of 0.05 mol kg ⁻¹ Sodium Tetraborate Solution, No Added NaCl.	169
B.5	The Temperature Dependence of pOH of 0.05 mol kg ⁻¹ Sodium Tetraborate in 0.2 mol kg ⁻¹ NaCl Solution.	170
B.6	The Temperature Dependence of pOH of 0.05 mol kg ⁻¹ Sodium Tetraborate in 0.4 mol kg ⁻¹ NaCl Solution.	171
C.1	The Variation of pK'_2 as a Function of Ionic Strength at Various Temperatures, CG3 Equation to 150°C.	182
C.2	The Temperature Dependence of pK'_2 in 0.1 mol kg ⁻¹ KCl Solution.	185
C.3	The Temperature Dependence of pK'_2 in 0.3 mol kg ⁻¹ KCl Solution.	186
C.4	The Temperature Dependence of pK'_2 in 0.5 mol kg ⁻¹ KCl Solution.	187

LIST OF TABLES

<u>Table</u>	<u>page</u>
4.1 pK'_W Values a Function of Ionic Strength and Temperature. . . .	51
4.2 Thermodynamic Values for the Ionization of Water.	53
4.3 Estimated Errors in pK'_W as a Function of Ionic Strength at 75° and 225°C.	54
4.4 Contributions to the Final Error in pK'_W at I=0.1 and at 75° and 225°C.	55
4.5 Potentials (mV) and Calculated Errors in pK'_W as a Function of Ionic strength at 75° and 225 °C.	55
4.6 Literature Results for the Temperature Dependence of the Ionization Constant of Water.	58
4.7 pQ'_W in 1 mol kg ⁻¹ KCl Solution, Various Studies.	63
4.8 Comparison of the Thermodynamic Parameters for the Ionization of Water at 25, 75 and 225°C.	68
5.1 pOH Values of 0.01 mol kg ⁻¹ Sodium Tetraborate Solution as a Function of Ionic Strength at Various Temperatures. . . .	74
5.2 pOH Values of 0.05 mol kg ⁻¹ Sodium Tetraborate Solution as a Function of Ionic Strength and Temperature.	75
5.3 pOH Values Using NaCl Activity Coefficients, as a Function of Ionic Strength at Various Temperatures.	76
5.4 Extrapolated pOH Values Calculated Using the Bates- Guggenheim Convention.	78
5.5 Extrapolated pOH Values Calculated Using The NaCl Activity Coefficient Data.	79
5.6 Potentials (mV) and Calculated Errors of the Sodium Tetraborate Solutions as a Function of Ionic Strength at 75° and 250°C.	81
5.7 Contributions to the Final Error in pOH of 0.01 mol kg ⁻¹ Sodium Tetraborate at I=0.11 and at 75°C.	82
5.8 Estimated Errors in pOH as a Function of Ionic Strength at 75° and 250°C.	82

5.9	Literature Results for the Temperature Dependence of the pH of Sodium Tetraborate Buffers.	84
5.10	Temperature Dependence of the First Equilibrium Constant of Boric Acid.	95
5.11	Changes in pOH Caused by a 10% Variation in the Calculated Molar Conductivity of the Chloride Ion at 250°C.	97
6.1	pK'_2 Values as a Function of Ionic Strength and Temperature, CG4 Equation.	104
6.2	Thermodynamic Values for the Dissociation of the Bisulphate Ion, CG4 Equation To 225°C.	105
6.3	Calculated Potentials (mV) and Errors in pK'_2 as a Function of Ionic Strength at 75°, 150° and 225°C.	106
6.4	Estimated Errors in pK'_2 as a Function of Ionic Strength at 75°, 150°, and 225°C.	106
6.5	Contributions to the Final Error in pK'_2 at $I=0.11$ and at 225°C.	107
6.6	Literature Results for the Temperature Dependence of the Dissociation Constant of the Bisulphate Ion, pK_2^0	109
6.7	Sensitivity of pK'_2 to the Measured Hydrogen Ion Concentration in 0.10M KCl Solution.	115
6.8	Calculation of the KSO_4^- Molal Ion Pair Dissociation Constant in 0.10 mol kg^{-1} KCl Solution and at 200°C.	117
6.9	Thermodynamic Values for the Dissociation of the Bisulphate Ion at 25°C.	120
6.10	Thermodynamic Values for the Dissociation of the Bisulphate Ion at 75° and 150°C.	122
7.1	Initial Solution Concentrations of the Feldspar Hydrolysis Experiments.	130
7.2	Summarized Results for the Feldspar Hydrolysis Experiments I, J and K at Low pH.	132
7.3	Summarized Results for the Feldspar Hydrolysis Experiments A, B, C and D at High pH.	135
A.1	Terms Contributing to the Final Smoothed Ionization Constants of Water as a Function of Ionic Strength and Temperature.	140
A.2	Equation Coefficients for the Ionization Constant of Water.	141
A.3	Solution Concentrations used in Determining the Ionization Constant of Water.	146

A.4	Experimental Data of the Ionization Constant of Water in 0.1 mol kg ⁻¹ KCl Solution.	147
A.5	Experimental Data of the Ionization Constant of Water in 0.3 mol kg ⁻¹ KCl Solution.	148
A.6	Experimental Data of the Ionization Constant of Water in 0.5 mol kg ⁻¹ KCl Solution.	149
A.7	Experimental Data of the Ionization Constant of Water in 1.0 mol kg ⁻¹ KCl Solution.	150
B.1	Activity Coefficients at Ionic Strengths of 0.02 and 0.1, as a Function of Temperature.	152
B.2	Clark-Glew Temperature Variable Terms.	153
B.3	Terms Contributing to the Final Smoothed pOH's as a Function of Ionic Strength and Temperature.	154
B.4	Equation Coefficients For the 0.01 mol kg ⁻¹ and 0.05 mol kg ⁻¹ Sodium Tetraborate Buffers.	157
B.5	Solution Concentrations Used in Determining the pOH's of 0.01 mol kg ⁻¹ Sodium Tetraborate.	159
B.6	Experimental pOH data of 0.01 mol kg ⁻¹ Sodium Tetraborate in 0.1 mol kg ⁻¹ NaCl Solution.	163
B.7	Experimental pOH data of 0.01 mol kg ⁻¹ Sodium Tetraborate in 0.3 mol kg ⁻¹ NaCl Solution.	165
B.8	Experimental pOH data of 0.01 mol kg ⁻¹ Sodium Tetraborate in 0.5 mol kg ⁻¹ NaCl Solution.	167
B.9	Solution Concentrations used in Determining the pOH's of 0.05 mol kg ⁻¹ Sodium Tetraborate.	168
B.10	Experimental pOH data of 0.05 mol kg ⁻¹ Sodium Tetraborate Solution, No Added NaCl.	172
B.11	Experimental pOH data of 0.05 mol kg ⁻¹ Sodium Tetraborate in 0.2 mol kg ⁻¹ NaCl Solution.	174
B.12	Experimental pOH data of 0.05 mol kg ⁻¹ Sodium Tetraborate in 0.4 mol kg ⁻¹ NaCl Solution.	176
C.1	Terms Contributing to the Final Smoothed pK ₂ ' as a Function of Ionic Strength and Temperature.	179
C.2	pK ₂ ' Values as a Function of Ionic Strength and Temperature, CG3 Equation.	181
C.3	Thermodynamic Values for the Dissociation of the Bisulphate Ion, CG3 Equation To 150°C.	183
C.4	Equation Coefficients For Dissociation Constant of the Bisulphate Ion.	184

C.5	Solution Concentrations Used in Determining The Dissociation Constant of the Bisulphate Ion.	188
C.6	Experimental Data of the Dissociation Constant of the Bisulphate Ion in 0.1 mol kg ⁻¹ KCl Solution.	189
C.7	Experimental Data of the Dissociation Constant of the Bisulphate Ion in 0.3 mol kg ⁻¹ KCl Solution.	191
C.8	Experimental Data of the Dissociation Constant of the Bisulphate Ion in 0.5 mol kg ⁻¹ KCl Solution.	193
D.1	Feldspar Hydrolysis Experimental Results.	196

PART I
INTRODUCTION

Chapter 1

INTRODUCTION

1.1 HYDROTHERMAL SOLUTIONS.

Hot aqueous fluids play an important role in many technological and geochemical processes.^{3,4,5} Examples include : corrosion and scaling in boilers, the cooling systems of nuclear reactors and in geothermal and conventional steam power plants; in materials synthesis, high temperature electrochemical processes and hydrothermal crystal growth; in the formation of hydrothermal ore deposits, mechanisms of mass transport and metasomatism in metamorphic rocks.

To understand the chemistry of such hydrothermal systems requires a complete and careful thermodynamic analysis of all the equilibria. However the application of solution thermodynamics at high temperatures has been impeded by the lack of data. This situation has arisen because of the difficulty of working with aqueous solutions at elevated temperatures.⁶ The solvent pressure and the corrosive nature of the fluids requires special design and fabrication of pressure vessels and not all the problems have been solved.⁴ Thus much effort has been directed to obtaining this data, either by experiment or by the use of various empirical methods of estimation.^{7,8}

1.2 THE IMPORTANCE OF ACIDITY MEASUREMENTS AT ELEVATED TEMPERATURES.

The hydrogen ion activity greatly affects the physico-chemical processes occurring in hydrothermal systems and the pH is in principle an experimentally measurable parameter. The pH directly influences or is indicative of the solute speciation and hence the chemistry occurring in many of the examples given above. These equilibria may be fully characterized by measuring the change in hydrogen ion activity as a function of temperature and composition. However few protolytic equilibria, such as ion hydrolysis and acid/base dissociation, have been thoroughly investigated so that knowledge of these high temperature aqueous solutions is severely limited.

In industrial plants stainless steels are mostly used for the containment of high temperature aqueous solutions. The corrosion failures which do occur can be directly attributed to a change in pH.⁹ Acidic solutions in boilers may be generated by contamination with hydrolysable chlorides such as MgCl_2 ⁹, while on the other hand concentrated alkaline solutions may form by evaporation of the dilute alkaline boiler water. The temperature and pH of these solutions determines the stoichiometry and the solubilities of the corrosion products, which are usually metal oxides, hydroxides or oxyhydroxides. The deposition of such metal complexes is the result of a series of hydrolytic reactions which are pH dependent.¹⁰ Thus the pH determines the stability of the various oxides/hydroxides and corresponding regions of passivity and corrosion are observed experimentally.^{9,11} To minimize the corrosion rate and to control the product composition and rate of mass transport, buffers such as sodium tetraborate are often used to maintain constant pH. However the pH conditions existing at high temperatures, even for the common buffers, are unknown and thus have to be approximated using low temperature data.

The acidity of hydrothermal solutions in geologic environments results from ion exchange equilibria with the host rocks, as well as from the many important homogeneous equilibria such as the self ionization of water (which is of fundamental importance in all aqueous systems) and the dissociation of naturally occurring species, e.g. the bisulphate ion and silicic acid. The subsurface fluid is experimentally found to be in virtual equilibrium with the host rocks. The pH in such solutions appears to be buffered by the acid hydrolysis of feldspar minerals to quartz and mica.^{12,13} These equilibria fix the pH, solute speciation, the extent of metal ion hydrolysis and the stoichiometries of the complexes formed. This is of interest in understanding the mechanisms of ore formation under hydrothermal conditions.

1.3 HIGH TEMPERATURE EMF MEASUREMENTS.

The extension of EMF measurements to obtain data at elevated temperatures is now well established. A number of recent exhaustive reviews^{4,14-16} thoroughly detail the many practical problems involved and extensively discuss the numerous electrochemical measurements that have been undertaken. No attempt is made to reproduce this material, except where directly relevant to this study.

To obtain thermodynamic and kinetic information using the EMF technique requires the measurement of the potential of an indicator (or "working") electrode against a reference electrode.

The hydrogen ion responsive electrode used for the vast majority of pH measurements at room temperature is the versatile glass electrode. However at elevated temperatures the use of the conventional glass electrode is severely restricted by its fragility and by the susceptibility of the glass membrane to chemical attack by the hot water solutions.¹⁷ Nevertheless there have been some studies to temperatures

of 150 °C, particularly by Kryukov¹⁴ and co-workers. This temperature appears to be the glass electrode's upper working limit. The hydrogen/hydrogen ion electrode is the primary reference for acidity measurements and this electrode has been used extensively in high temperature aqueous solutions.¹⁶ The major features which make it especially suitable are that it is the standard against which all other reference electrodes are measured, it is demonstrably reversible and hence suitable as a thermodynamic standard and lastly the components (H_2, H^+) are stable at elevated temperatures. The use of the hydrogen electrode is naturally limited to those systems stable under a hydrogen atmosphere.

The usual arrangement for obtaining meaningful pH measurements is to couple the hydrogen/hydrogen ion electrode to a reference electrode for which the standard electrode potentials (E^0) are known as a function of temperature. Many internal reference electrodes have been described^{14,16} and detailed investigation into the stability, response and measurement of standard electrode potentials is still a major feature of high temperature aqueous EMF studies. Unfortunately few of these electrodes function adequately at elevated temperatures. Errors may arise through the solubility, decomposition and hydrolysis of the electrode materials. For example, in the case of the silver/silver chloride electrode, which is one of the more serviceable high temperature reference electrodes, errors can arise from the appreciable solubility¹⁸ of silver chloride in chloride electrolytes and also from the apparent hydrolysis that occurs in basic media. Also when this electrode is coupled to a hydrogen/hydrogen ion electrode (the usual arrangement), uncertainties arise from the reduction of silver chloride with hydrogen, which occurs spontaneously at elevated temperatures. It may be impossible to adequately protect the surface of the silver

chloride. In addition, the poor agreement for E^0 values found by various workers makes it preferable to determine experimentally the E^0 of an electrode that is to be used for a specific purpose.¹⁴ This further complicates the experimental procedure.

An alternative approach would be to combine two hydrogen electrodes in a concentration cell. The potential of such a cell is determined by both of the activities and thus the derivation of the pH in one electrolyte is easily accomplished if the pH of the other solution is known.

1.4 PROPOSED RESEARCH.

1.4.1 Introduction.

In view of the problems associated with most reference electrodes and the apparent suitability of the hydrogen electrode, Macdonald, Butler and Owen¹ and Mesmer, Baes and Sweeton¹⁹ developed a concentration cell with transference, employing twin hydrogen electrodes, which allowed the direct measurement of the acidity in high temperature aqueous solutions. The cell is well suited for the study of the many important protolytic equilibria, which are difficult to study accurately using other experimental techniques. The work published^{14,16} suggests that these cells are capable of yielding accurate thermodynamic data.

The aim of this research was to construct a high temperature pH cell (based on Macdonald's design¹) and to use it to study the following important protolytic equilibria which are all of practical as well as fundamental value.

1.4.2 Ionization of Water.

The ionization of water is of prime importance in determining the acid-base properties of aqueous solutions. It is therefore of direct interest to have available accurate ionization constants as a function of temperature. In addition, the reliability and accuracy of the cell was confirmed by comparison with the considerable literature data.

1.4.3 Sodium Tetraborate Buffer.

The primary usefulness of the pH value is as an empirical or chemical index in aqueous solutions. However, there are few standard buffers adequately characterised and calibrated in sufficient detail at temperatures above 150 °C. The concentration cell was used to calibrate the sodium tetraborate (borax) buffer, at concentrations of 0.01 mol kg⁻¹ and 0.05 mol kg⁻¹, so that practical pH measurements at elevated temperatures could be more readily undertaken, without the limits imposed by the lack of suitable standards.

1.4.4 Second Dissociation of Sulphuric Acid.

Sulphuric acid is of great practical industrial importance and the bisulphate ion is an important ligand in hydrothermal systems. The complete thermodynamic treatment of the almost fully dissociated acid is unusually difficult.^{21,22} There is still disagreement²³ on the value of the second dissociation constant of sulphuric acid at 25 °C. It appears that the best value pK_2^0 lies between²⁴ 1.95 and 2.00 log units, and greater discrepancies exist at elevated temperatures. Thus the second dissociation constant of sulphuric acid was measured in view of the need for more reliable bisulphate dissociation constant data.

1.4.5 K-feldspar Hydrolysis.

Many natural hydrothermal fluids are buffered by natural silicate equilibria, such as the acid hydrolysis of K-feldspar to K-mica and quartz. The usual method²⁵ for obtaining equilibrium data from solubility studies is to rapidly quench a given sample to room temperature and measure the resulting pH. The equilibrium constant is calculated, assuming the absence of quenching reactions, from the measured pH. The concentration cell provided a means of measuring the pH in situ and at temperature. The feldspar hydrolysis equilibrium was chosen, since it is one of the least complicated and is relatively well understood.¹³

PART II

EXPERIMENTAL AND DATA ANALYSIS

Chapter 2

ELECTROCHEMICAL CELL, MATERIALS AND PROCEDURES

2.1 ELECTROCHEMICAL CELL.

2.1.1 Introduction.

To date, most electrochemical experiments have been conducted near ambient temperature where the environmental conditions are not severe and measurement precision is high. A number of experimental difficulties had to be overcome before meaningful measurements could be made at high temperatures and pressures.

2.1.2 Requirements For The Cell.

The major cell design requirements (as in most other high temperature aqueous studies) were as follows²⁶

1. The cell body had to be able to withstand the required temperature and pressure conditions.
2. The linings and fittings had to be such that solution contamination by dissolution of the autoclave walls was minimized.
3. Electrode seals had to be electrically insulating, as well as provide a pressure seal.

2.1.3 Cell Design.

The electrolyte concentration cell used in this study^{1,19} is shown diagrammatically in figure 2.1. It consisted of a heavy walled vessel

(316 stainless steel) with two concentric Teflon* compartments each containing a hydrogen electrode. The cell lid was bolted to the body and the vessel was compression sealed using a glass impregnated Teflon gasket. Similarly, pressure tight electrode seals were formed by compressing Teflon sheaths surrounding the electrodes.

Teflon was the preferred liner for temperatures up to 250 °C. Pure Teflon while chemically inert and easily machinable does soften and distort when not supported at temperatures above 200 °C. Glass impregnated Teflon and Teflon expand linearly^{27,28} by 7% and 15% respectively on heating from 25 to 200 °C. This volume increase is much greater than the approximate 1% volume increase of the stainless steel body²⁹ and consequently the seal material extruded through the gaps to release pressure. While this did initially improve the seal, eventual extrusion of the gasket material meant that the seals had a limited life and had to be replaced regularly. Teflon shrinks on cooling so that the seals were not self sealing.

The inner compartment was suspended from a threaded Teflon cap and solutions in both compartments were agitated with Teflon covered magnetic stirring bars. A liquid junction was formed through a plug of porous Teflon pressed into a hole at the bottom of the inner compartment.

An important feature of the cell was that the outer and inner compartments were connected via a small hole above the liquid surface in order to equalize the pressure in the cell compartments. This eliminated the major problem of having to estimate the hydrogen pressure (fugacity) in the presence of the high vapour pressure of the solvent and minimized transfer of solution through the porous plug. The hole was of small diameter (1mm) to reduce distillation from the outer to the inner

* Teflon-PTFE (polytetrafluoroethylene), Dupont Ltd.

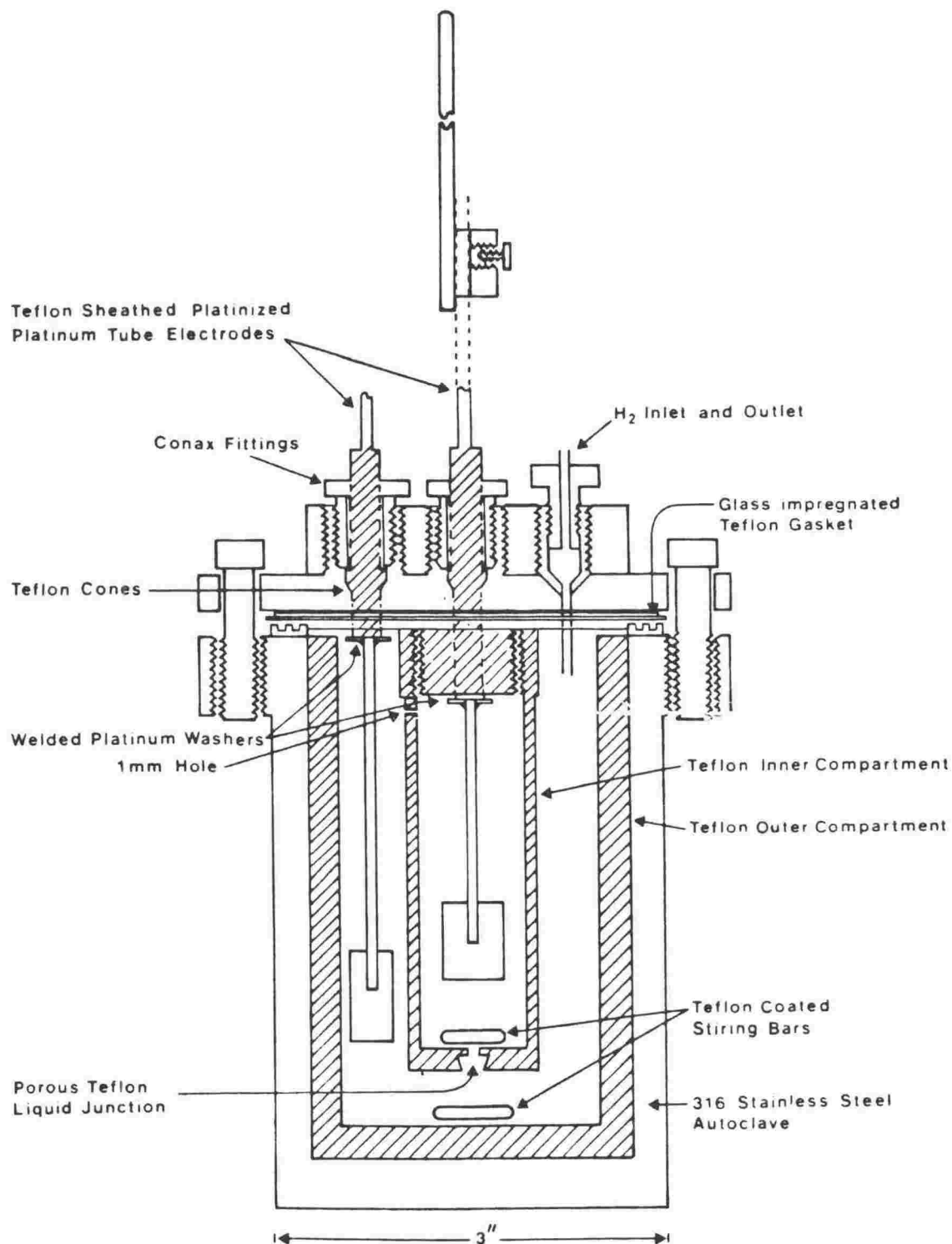


Figure 2.1: Electrolyte Concentration Cell.

compartment during heating up.

2.1.4 Electrodes.

The hydrogen electrodes consisted of pure platinum foil (99.9%, Degussa Co. Ltd.) attached to pure platinum tube (3mm OD, 1.5mm ID) supports. The tubes also served as thermocouple wells for internal monitoring of temperature and they were insulated from the autoclave body by "Conax" fittings containing Teflon cones and sheaths (figure 2.1). An initial problem of the tubes ejecting at elevated temperatures, was solved by bonding platinum washers to the tubes with gold solder, which effectively restricted their upward movement.

2.2 THERMOSTATING BATHS.

2.2.1 Temperature Control.

The autoclave was heated externally in an oil bath at temperatures up to 150 °C and in a salt bath at temperatures between 175 °C and 250 °C. The division between the oil and salt baths represented a convenient separation into "low" and "high" experimental temperature ranges.

The temperature in both baths was controlled by a proportional temperature controller (Thermo Electric "Slectrol" model 3813011110) with a chromel-alumel thermocouple sensor. The temperature within the autoclave was monitored with inconel sheathed chromel-alumel thermocouples (L.L. Wright Ltd.). The thermocouples were calibrated against a transfer standard platinum resistance thermometer* to ± 0.01 °C. The voltages were smoothed³⁰ with respect to temperature using a seven degree polynomial. The resulting standard deviations were always less than 0.1 °C. The thermocouples were calibrated directly in the oil bath while calibration in the salt bath was achieved by placing the

* calibrated by the Physics and Engineering Laboratory of the D.S.I.R.

thermocouples and the thermometer in a glass tube containing some MgO powder for increased thermal contact. The thermocouples were grounded to their metal sheathing but as the thermocouple wells were insulated from the autoclave body, all potential measurements were made floating.

2.2.2 Oil Bath.

The oil bath was of about 15 litres capacity and contained a heavy steam cylinder oil (Shell "Valvata" 460). The temperature controller operated two "Eutron" heaters in series dissipating in total 600 W. Above 100 °C a 1.2 kW heater was used as a boost to higher temperatures. Once the required temperature was reached, the heaters in series were used to maintain temperature control. The temperature within the autoclave remained constant to ± 0.2 °C at 75 °C and to ± 0.4 °C at 150 °C over the time required for the experimental measurements (1 to 2 hours).

2.2.3 Salt Bath.

For measurements between 175 °C and 250 °C, a thermostat bath of about 90 litres capacity containing a molten salt mixture was used. The arrangement of the bath and its fittings is described fully by Fellows.³¹ The autoclave was heated to 160 °C in the oil bath or more usually in a small non inductively wound a.c. furnace.³² In the feldspar hydrolysis experiments the a.c. furnace was used to heat the autoclave to 180 °C. The Slectrol temperature controller and a zero crossing switch power controller operated a 1.5 and a 2.2 kW heater respectively. Best temperature control was achieved by using the 2.2 kW heater to provide a constant source of background heat, while the 1.5 kW heater maintained the required temperature control. Both heaters were inconel sheathed (B.J. Cocksedge Ltd). The temperature within the autoclave remained constant to within ± 0.3 °C at 175 °C and to ± 0.6 °C at 250 °C over the time required for the experimental measurements.

2.2.4 Stirring.

The stirring bars contained within the cell compartments were activated by rotating a magnet beneath the cell. This was achieved in different ways in the oil and salt baths.

2.2.4.1 Oil Bath.

The simplest method was to submerge a shaded pole induction motor (with magnet attached) in the oil. The major problem of the motor "burning out" was solved by rewinding with high temperature enamel wire (1mm diameter). A reduction in voltage from 240 V to 6 V ensured electrical safety and less electrical stress on the insulation.

2.2.4.2 Salt Bath.

The electrical conductivity and the corrosive nature of the molten salt necessitated the use of a stainless steel enclosed magnet, gear driven from outside the bath. The stirring assembly required modifications and repairs throughout this work because of excessive bearing and gear wear. The final design, which operated routinely without malfunction is shown schematically in figure 2.2. It consisted of a shaft (with flexible coupling) attached to a pinion and thrust bearing. The pinion rotated a larger gear beneath which a magnet was attached. Use of graphite powder as a lubricant and a flow of cooling air were found to reduce significant wear.

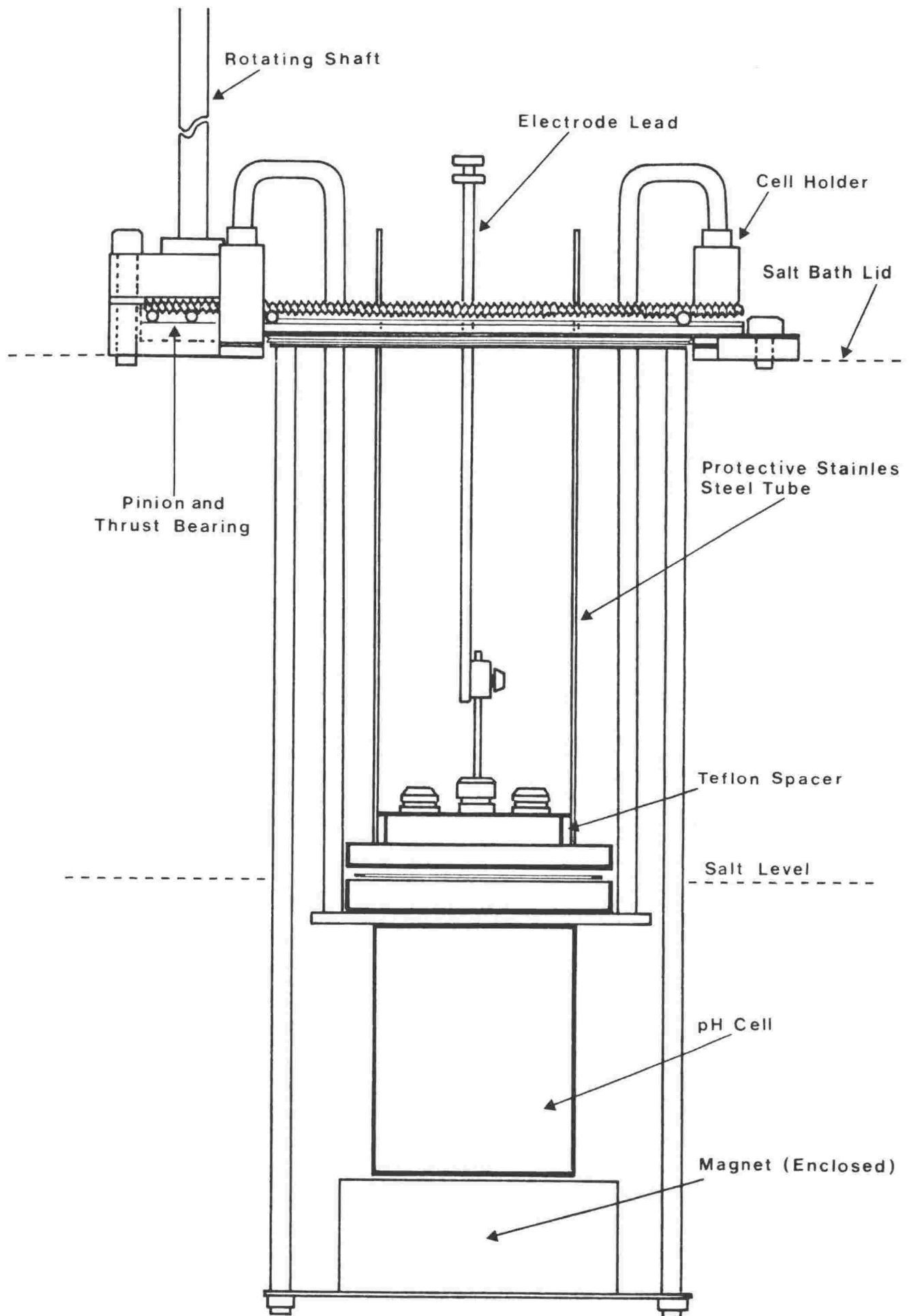


Figure 2.2: Salt Bath Stirring Assembly.

2.3 EXPERIMENTAL PREPARATION.

2.3.1 Electrodes.

The platinum electrodes were prepared as recommended by Ives and Janz.^{33,34} After cleaning in warm dilute aqua regia and cathodic electrolysis in dilute sulphuric acid, the electrodes were washed in distilled water and immediately plated using lead free 2% chloroplatinic acid in 2N hydrochloric acid, until coated with a light and even layer of platinum black. The electrodes were then washed and stored in distilled water until used.

2.3.2 Electrode Leads.

The high temperatures reached precluded the use of lead/tin solders for connecting the lead wires to the cell. A bronze block was fitted over and then locked onto the platinum tubes. The wires from the multimeter (see Section 2.4.1) were attached by clamping between two nuts on a threaded bronze rod which was brazed to the bronze block. (see Figures 2.1 and 2.2). The area in direct contact with the platinum was polished before each experimental run. A tube of stainless steel (filled with expanded mica to reduce temperature fluctuations) protected the leads from salt splash (see Figure 2.2).

2.3.3 Chemicals.

"Analar" potassium chloride and sodium chloride were dried at 150 °C for 4 hours and were used without further purification. K-feldspar*, "Merck"

* Supplied by A.J. Read, Chemistry Division, D.S.I.R. The K-feldspar (KAlSi_3O_8) was made by repeatedly fusing pure "natural" K,Na-feldspar with molten KCl at 900 °C.

quartz and optically pure K-mica⁺ were finely ground and dried before use. "Analar" sodium tetraborate decahydrate (borax) was recrystallized from distilled water. Because the transition temperature between the pentahydrate and decahydrate is 61 °C the recrystallization was carried out at less than 55 °C. The recrystallized product was stored³⁵ in a desiccator over a solution saturated with respect to sucrose and sodium chloride. This solution maintained constant humidity and protected the salt against decomposition. All acid and base solutions were prepared from sealed ampoules (Merck "Titrisol", BDH "CVS") which produced working solutions accurate to within 0.1% (manufacturers specifications).

All solutions were prepared with nitrogen purged, permanganate treated, double distilled water and were stored in polythene^{36,37} bottles under nitrogen to minimize atmospheric contamination.

The gas supplied to the hydrogen electrodes must be of adequate purity. Matheson prepurified (99.95%) hydrogen gas contains³⁸ about 500 ppm helium, trace amounts of hydrocarbons (<1 ppm) and less than 10 ppm oxygen. Helium is an inert impurity and does not impair the performance of the electrodes. However error could arise from the presence of oxygen which is reduced at the electrodes. The autoclave required a single charge of hydrogen. The advantage^{34,40} of this, in contrast to a flow of hydrogen was that all the residual oxygen would be removed by catalytic reaction on the surface of the platinized platinum electrodes. There was no evidence for the impaired functioning of the electrodes and initial experiments to test the reliability and accuracy of the cell gave good results (see Chapter 4). This confirmed that the hydrogen was of adequate purity and consequently the gas was used without any

⁺ Electron microprobe analysis (Wt. %) : SiO₂ 45.1, Al₂O₃ 32.8, FeO 3.6, MnO 0.1, MgO 0.7, Na₂O 0.4, K₂O 10.1, H₂O 4.0.

additional purification.

2.3.4 Porous Teflon Plug.

The performance of the concentration cell was critically dependent upon establishing a reliable interface through the porous teflon plug, which formed the liquid junction between the cell compartments. For good electrolytic contact the air in the pores of the Teflon must be replaced with KCl solution. The method used was to boil the plugs in concentrated KCl solution and then to cool. During boiling, air is expelled from the pores in the plug and replaced by KCl solution on cooling. The boiling/cooling procedure was repeated over 5 cycles taking care that KCl did not crystallize in the pores.

The Teflon plug was inserted* into the inner compartment and compressed to provide a sufficiently slow leak rate between the two compartments. Since teflon is non-wettable, some air would remain in the pore structure. On excessive compression the pore structure is likely to collapse and this, coupled with expansion and/or nucleation of gas in the pores, may account for the frequent interruption of flow through the liquid junction at elevated temperatures. Later work showed that the electrical resistance across the plug does increase with temperature.

Porous Teflon is particularly effective in nucleating gas bubbles.^{41,42} Thus another mechanism contributing to the loss of electrical continuity through the liquid junction, may have been the formation of a gas bubble in the inner compartment directly over the porous plug. This would effectively cause an infinite resistance making further measurements impossible. This explanation is supported by the

* The inner Teflon compartment was heated in boiling water to facilitate the insertion of the slightly oversized plug.

fact that some experimental runs were salvaged by a vigorous shake but generally this procedure was impractical as the electrical discontinuity once established, tended to reoccur. Modification of the connecting hole made little difference. However, an accidental Teflon burr centered in the hole appeared to be particularly effective in reducing the number of run failures.

Teflon of 10 μm pore size had to be compressed considerably before reproducible measurements could be obtained. Halving the pore size (to 5 μm) extended reproducible measurements to 225 $^{\circ}\text{C}$. The smaller pore size would be more effective in restricting any small flow of solution between the cell compartments and the greater rigidity of the Teflon may have enabled the plug to be compressed without total destruction of the pore structure. The 5 μm Teflon is however less deformable and thus the plugs were more difficult to insert and tended to leak* around the sides. These leaks were suppressed by wrapping Teflon tape around the plug's edge and heavily compressing around the plug's rim. The 5 μm pore sized Teflon performed satisfactorily except for experiments involving finely ground rock samples (see Chapter 7). The Teflon compartments were coated with a fine residual "mineral" layer at the end of each experiment. It is possible that the problem was being caused by the clogging of the pores with fine rock grains. For these experiments a 10 μm pore sized plug was enveloped in Teflon tape. A fine needle was used to puncture the tape from inside the inner compartment and the plug was moderately compressed, with the outer rim being compressed heavily as before. This procedure overcame the excessive compression/flow interruption problem associated with the 10 μm porous Teflon, and enabled reproducible measurements to be made for extended periods of time (>25hr) at 225 $^{\circ}\text{C}$.

* As observed on the bench and not inferred from drifting potentials.

In later experiments (see Chapter 5) the operation of the cell was extended to 250 °C by performing (before each experimental run) the boiling/cooling cycle on the inner compartment with plug inserted, followed by forcing (under positive pressure) saturated KCl solution through the plug.

After treatment and insertion of the plug the preparation procedure was continued as follows. The inner compartment was filled with KCl solution and visually checked (over 30 min.) for leaks around or through the Teflon plug. The plug was compressed (if required) and the compartment was placed in saturated KCl solution and evacuated, using a water pump, for 5-10 minutes. The rate of flow through the plug was related to the amount of compression and this was easily determined by measuring the electrical resistance across the porous plug with an a.c. bridge. The inner compartment was filled with and immersed in saturated KCl solution. Platinum foil electrodes were placed inside and beneath the compartment i.e. directly across the porous plug. Resistances of less than 1000 Ω generally implied insufficient compression and often resulted in irreproducible measurements while resistances greater than 2000 Ω often resulted in interruption of electrical continuity. The plug would be recompressed (if required) or alternatively the boiling/cooling/evacuation sequence would be repeated until the plug was sufficiently refilled with KCl solution, as indicated by a suitable resistance across the plug.

Although a purely empirical approach was used for preparing and inserting the porous Teflon plugs, the procedures described above were particularly effective in reducing the number of experimental failures due to drifting potentials or loss of electrical continuity.

2.4 EXPERIMENTAL TECHNIQUES.

2.4.1 Electrochemical Equipment.

All potential measurements were made with a 5.5 digit Dana 5100 digital multimeter with a maximum resolution $1\ \mu\text{V}$ on the 2 V range. To minimize the effects of noise and common mode signals, a two wire shielded cable

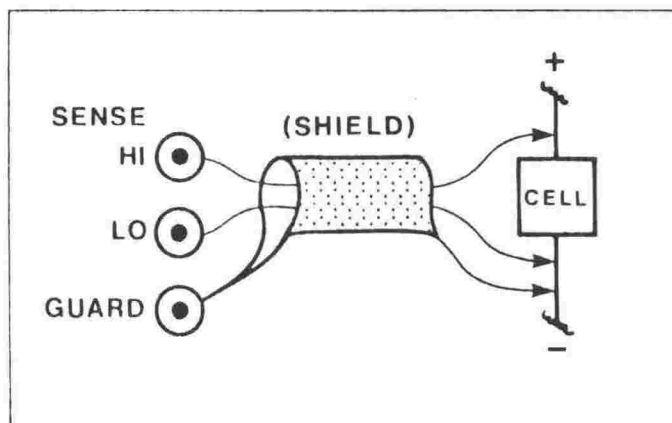


Figure 2.3: Voltage Measurement Connections.

was used for all voltage measurements. The configuration is shown in figure 2.3. The HI and LO inputs are floating, consequently the multimeter sees only the voltage difference between the inputs and not between the wires and ground. The function of the GUARD terminal was to eliminate the effect of ground loop currents and the shield provided a means of screening both wires from electrostatic interference. A.C. interference was further reduced by having the instrument's 3 pole active filter "on" for all potential measurements.

A Tinsley vernier potentiometer (Type 5590A) coupled with a calibrated* Weston standard cadmium cell and Manganin DC wire resistance box, were initially used to check the digital multimeter. This was done by manipulating the resistance box to obtain voltages between 0 and 1 V.

* Physics and Engineering Laboratory of the D.S.I.R.

Below 0.2 V the potentiometer and multimeter agreed to $\pm 10 \mu\text{V}$. Between 0.2 V to 0.5 V and 0.6 V to 1.0 V, the agreement was $\pm 60 \mu\text{V}$ and $\pm 90 \mu\text{V}$ respectively. The above equipment was also used to check the concentration cell for any thermal EMF¹⁹ due to possible slight differences in the composition of the electrode leads. The maximum EMF observed during measurements in which both compartments contained $0.01 \text{ mol kg}^{-1} \text{ HCl}$ in $1 \text{ mol kg}^{-1} \text{ KCl}$, was less than 0.1 mV up to 150°C .

2.4.2 Experimental Procedure.

The platinum electrodes were replated and the porous plug was prepared immediately before each experimental run.

Seals were checked by immersing the autoclave in water after pressurizing to 30 bar. The "Conax" fittings around the platinum electrodes were tightened until all leaks were eliminated. New seals tended to leak when first used at elevated temperatures irrespective of the amount of tightening.

The outer compartment and electrode and the inner compartment and electrode were each rinsed with their respective solutions. Solutions were not presaturated with hydrogen. The inner and outer compartments were filled with 18 and 80 cm^3 of solution respectively. This gave the same solution level in both cell compartments and ensured a zero hydrostatic pressure at the start of the experiment. In the feldspar hydrolysis experiments about 0.1 g of each of the minerals was placed in the outer compartment and both compartments were filled with the same acid solution. A calculation based on the density of saturated water vapour²⁰ and the volume of gas space in the autoclave showed that the maximum electrolyte concentration change resulting from evaporation of water into the gas phase, would be 0.8% between room temperature and 250°C . In practice the actual concentration change would be

considerably less than this because the volume increase of the Teflon liners and the effect of the hydrogen overpressure have been ignored in the above calculation. No correction was made for this effect and such corrections only become essential close to the solution-vapour critical temperature.

The autoclave was purged by cyclic compression/decompression with pure hydrogen. The procedure was repeated at least 5 times to remove all traces of oxygen from the system and the pressure was finally adjusted¹ to 6 bar.

The rate of heating in the oil and salt baths (in steps of 25 °C) was such that the temperature in the two compartments did not differ by more than 5 °C. This minimized¹ distillation from the outer to the inner compartment. Distillation was also minimized by maintaining an overpressure of hydrogen and having nearly equal ionic strengths in both cell compartments. For temperatures above 150 °C the autoclave was brought to temperature overnight. One problem encountered was the very slow thermal equilibration between the two cell compartments. The technique of slightly overshooting the required temperature and cooling sometimes helped but often resulted in loss of electrical continuity possibly caused by bubble nucleation over the porous plug.

2.4.3 Equilibrium and Reversibility.

It was assumed that the electrochemical cell had reached equilibrium at relatively constant temperature when the observed EMF values showed little variation (<0.3 mV) over a one hour period. At equilibrium, EMF changes tended to follow the thermal fluctuations. Since the Dana multimeter does not draw an appreciable current, the reversibility of the cell was often tested by momentarily "loading" the cell through a 1 M Ω resistor. The resulting potential changed back to the "equilibrium"

potential usually within 10 seconds. This indicated that the electrodes were behaving reversibly.

2.4.4 Time Required For a Complete Experiment.

Experimental preparation and cleaning up afterwards usually took about a day and a typical run lasted 10-12 hours. Although the procedure for preparing the porous plugs was relatively straightforward it usually took 1-2 days to complete, because of the difficulty of inserting a "leak free" plug without completely cutting off the electrolytic contact. The cell seals were easily replaced except that extreme care had to be taken when inserting the platinum electrodes into the Teflon sheaths. The platinum tubes were easily bent and the ease of insertion had to be balanced against an inability of sealing the cell without excessive tightening of the Conax fittings, which results in rapid destruction of the Teflon sheaths. Experiments at each required solution concentration were repeated until 2 to 4 (mostly 3) reproducible runs were obtained. After successful completion at the lower temperatures the above procedure was repeated for the higher temperature range. Data from all experiments with the same nominal solution concentrations were combined and analysed together. Since experiments were not necessarily performed consecutively and as there was usually a gap of some months between the end of the low temperature measurements and the start of the high temperature measurements, the reproducibility of the methods and procedures adopted could be reliably assessed (see Chapter 4).

2.4.5 Problems.

Experimental failures were associated with three major problems : mechanical failure of the stirring apparatus, drifting potentials and loss of electrical continuity. The mechanical problems were eventually solved towards the end of this research. Lack of stirring resulted in the potentials becoming offset by tens of millivolts so that the runs had to be abandoned. Drifting potentials usually indicated seal failure. This problem was easily solved in following experiments by replacing the Teflon seals. However, recurring drifting potentials were associated with the failure of the porous plug which then had to be recompressed or replaced. The most persistent problem was the interruption of electrical continuity at temperatures above 150 °C. The only effective solution was to prepare and insert a new porous plug. Overall about 1 in 4 experimental runs ended in failure, except that only a third of the feldspar hydrolysis experiments were successfully completed. Thus the time taken to complete this research was considerably extended.

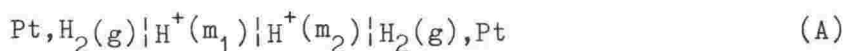
Chapter 3

DATA REDUCTION AND ANALYSIS

3.1 THERMODYNAMIC RELATIONSHIPS.

3.1.1 Potentiometric Determination of Acidity.

The electrolyte concentration cell with transference, used in this study can be represented by



Solution (2) was a known reference solution (generally in the outer compartment) while solution (1) was the solution to be measured. The Nernst equation gives the change in EMF (E) of this cell

$$E = \frac{RT}{F} \ln \frac{(a_{\text{H}^+})_2}{(a_{\text{H}^+})_1} + E_J \quad (3.1)$$

where E_J is the liquid junction potential. Rearranging (3.1) and recognizing that the relative activity* is given by

$$a_i = \gamma_i \frac{m_i}{m_i^0} \quad (3.2)$$

where γ_i and m_i represent the activity coefficient and molal (mol kg^{-1}) concentration respectively, gives the following expression for $F[(m_{\text{H}^+})_1]$

$$F[(m_{\text{H}^+})_1] \equiv \ln(m_{\text{H}^+})_1 - \ln(m_{\text{H}^+})_2 + \frac{E-E_J}{RT/F} + \ln \frac{(\gamma_{\text{H}^+})_1}{(\gamma_{\text{H}^+})_2} = 0 \quad (3.3)$$

* The individual ion activities and the corresponding activity coefficients cannot be determined experimentally and are thus defined conventionally.

The above equations permit an experimental measure of the acidity of an unknown solution, in terms of the hydrogen ion concentration or pH, to be obtained easily. Throughout this work pH was defined as

$$\text{pH} = -\log a_{\text{H}^+} \quad (3.4)$$

Experimental pH measurements were used to calculate equilibrium data such as the ionization constant of water and the dissociation constant of the bisulphate ion. For example, The equilibrium constant (K) for the process



was formulated as follows

$$\text{pK}'_2 = \text{pH} + \log \frac{m_{\text{HSO}_4^-}}{m_{\text{SO}_4^{2-}}} + \log \frac{\gamma_{\text{HSO}_4^-}}{\gamma_{\text{SO}_4^{2-}}} \quad (3.6)$$

The amounts of HSO_4^- and SO_4^{2-} present were calculated, assuming the first dissociation to be complete³⁹, from the known stoichiometric concentration of sulphuric acid and the measured pH.

For the measurements involving alkaline solutions, a_{H^+} was replaced by K'_W/a_{OH^-} . For example, if compartment 2 contained hydroxide solution then the expression for the ionization constant of water (K'_W) becomes

$$\text{pK}'_W = \frac{-F(E-E_J)}{2.303RT} - \log[(m_{\text{H}^+})_1(m_{\text{OH}^-})_2] - \log \frac{\gamma_{\text{H}^+}\gamma_{\text{OH}^-}}{a_{\text{H}_2\text{O}}} \quad (3.7)$$

All the equilibrium constants, quotients and pH's were calculated assuming no ion pairing between the already dissociated ions in the various electrolyte media. The term "apparent" usually signifies this aspect and it has been assumed throughout this work. This is an

idealized situation but some cancellation in the concentrations of the ion pairs between the the cell compartments would occur. Furthermore the technique of extrapolating the equilibrium quotients, which have been corrected for Debye-Hückel interactions (indicated by a prime), to infinite dilution also reduces these effects (Sections 3.1.3, 3.3).

3.1.2 Liquid Junction Potentials.

The potential of the junction (E_J), which makes an unavoidable contribution to the EMF of cell (A), must be taken into account before accurate thermodynamic data can be derived. The junction potential is given⁴⁰ by

$$E_J = \frac{-RT}{F} \int_1^2 \sum \frac{t_i}{z_i} d \ln \alpha_i \quad (3.8)$$

where the integration is between the limits corresponding to the two solutions (1 and 2) forming the liquid junction. The transport number, t_i , of an ion i (of charge z) is defined as the fraction of the current carried by that ion and in terms of equivalent conductance λ_i this becomes

$$t_i = \frac{z_i \lambda_i m_i}{|z_i| \sum |z_i| \lambda_i m_i} \quad (3.9)$$

Equation (3.8) is not rigorously thermodynamic since neither the potential of a liquid junction nor the individual ion activities can be measured; hence the junction potentials cannot be evaluated without restrictive assumptions. The simplest approximation, and the one most often used⁴⁰, is to treat the junction as a continuous series of mixtures. In this model, the solution at any point in the interface may be regarded as a mixture, varying linearly with distance through the

* Eq. 3.9 defines t_i as the number of moles of ion i transported per unit time of charge transport, it is positive for cations and negative for anions.

junction, of the two extreme solutions 1 and 2. If the activities of the ions in these two end solutions are set equal to their concentrations and the equivalent conductances are assumed to be independent of composition, equation (3.8) can now be integrated directly. The result is the Henderson equation.^{34,43}

$$E_J = \frac{RT}{F} \frac{\sum (z_i / |z_i|) \lambda_i [(m_i)_2 - (m_i)_1]}{\sum |z_i| \lambda_i [(m_i)_2 - (m_i)_1]} \ln \frac{\sum |z_i| \lambda_i (m_i)_1}{\sum |z_i| \lambda_i (m_i)_2} \quad (3.10)$$

This equation is independent of the geometry of the junction and consequently the liquid junction potential is independent of the way in which the junction is formed. The junction was always between solutions containing the same principal electrolyte at nearly equal, relatively high concentrations (0.1-1 mol kg⁻¹). In this case the logarithmic factor in equation (3.10) is near unity and can be linearized⁴⁴ giving the approximation

$$E_J = -\sum D_i [(m_i)_2 - (m_i)_1] \quad (3.11)$$

where

$$D_i = \frac{RT}{F} \frac{|z_i| \lambda_i}{z_i \sum |z_i| \overline{m_i} \lambda_i} \quad (3.12)$$

A high concentration of supporting electrolyte effectively suppresses the major portion of the liquid junction potential, allowing the small residual component (<3 mV) to be reliably estimated using equation (3.11).

There is a widely recognized dilemma with the calculation of liquid junction potentials. The summation of equation (3.11) cannot be evaluated exactly, without a complete knowledge of the ionic species present. However, all the ionic species present cannot be deduced from

a potentiometric measurement without a knowledge of the summation. Since there is no simple algebraic solution, a root finding algorithm was employed to solve equation (3.3). The species in the reference solution (compartment 2) were assumed to be known exactly. A value for the unknown hydrogen ion concentration in compartment 1 was chosen as an approximate root. This sets the concentrations of the other hydrolysis products and a liquid junction potential could be calculated using equation (3.11). If $(m_{H^+})_1$ is an approximate root then by Newton's method⁴⁵

$$[(m_{H^+})_1]_{X+1} = [(m_{H^+})_1]_X - \frac{F[(m_{H^+})_1]}{F'[(m_{H^+})_1]} \quad (3.13)$$

is a better approximation. The above basic formula was used to generate the next approximation and the iterative procedure was halted when two successive approximations for $(m_{H^+})_1$ were within 10^{-6} .

3.1.3 Activity Coefficients.

The method used to evaluate thermodynamic equilibrium data consisted of measuring the EMF of cell (A) over a range of electrolyte molalities followed by a short graphical extrapolation of equations and data in ionic strength (I) to infinite dilution. Hence it was necessary to evaluate the activity coefficients of ionic species over an extended range of temperature and ionic strength.

The establishment of reference pH values (equation 3.4) for the borate buffer solutions clearly requires a scale of single ion activity. Although scales of single ion activity must have an arbitrary basis, it is usual to endow the single ion activity with the behaviour characteristic of the mean activity coefficient. Between ionic strengths of 0.01 and 0.1 mean activity coefficients can be expressed by the

"extended Debye-Hückel equation" with adjustable ion size parameter a . Consequently, activity coefficients of ions (i) are often calculated by

$$\log \gamma_i = \frac{-Az_i^2 I^{\frac{1}{2}}}{1 + BaI^{\frac{1}{2}}} \quad (3.14)$$

with estimated values of a . The constants A and B are functions of the temperature, dielectric constant and the density of water, and they were evaluated from equations given by Helgeson.⁴⁶ The ionic strength (I) is defined here as

$$I = \frac{1}{2} \sum z_i^2 m_i \quad (3.15)$$

The Debye-Hückel limiting equation does not take into account such factors as short range ion-ion interactions and ion-solvent interactions, which have an important influence on the activity in more concentrated solutions ($I > 0.1$). These defects are often rectified by adding terms (generally linear) in ionic strength. For example, an equation such as

$$\log \gamma_i = \frac{-Az_i^2 I^{\frac{1}{2}}}{1 + BaI^{\frac{1}{2}}} + CI \quad (3.16)$$

which has one higher term and where C is usually an adjustable parameter. If the equilibrium quotients which have been corrected for Debye-Hückel interactions using equation 3.14, are plotted against I , a linear plot should be obtained. The thermodynamic equilibrium constants are now easily evaluated by extrapolation to infinite dilution. The linearity of such plots has been well established in room temperature studies⁴⁷ indicating that equation 3.16 is a good approximation with C constant. Similarly the Debye-Hückel equation with one linear CI term

was found to be entirely applicable⁴⁸ in expressing the mean ionic activity coefficients of dilute electrolytes up to 275 °C.

The formation of ion pairs would be expected to occur with the various ions in the electrolytic media used in this study. This will effect the slope of the plots but not the extrapolated values (unless the concentrations of the ion pairs is very great). As the solution becomes more dilute, fewer ion pairs form and thus the correction becomes zero at infinite dilution.⁴⁹

The method increasingly used in the literature is an ion interaction/virial coefficient treatment developed by Pitzer and collaborators.^{21,50-52} The virial coefficients, which are empirical functions of the ionic strength, are found by fitting available experimental data. One major criticism of such series expansion equations is their lack of an exact physical interpretation and alternative approaches^{7,53} which explicitly take into account ion association, solvation and long and short range interactions, may be fundamentally more appropriate. Nevertheless, the virial equations appear to yield good results, even for concentrated solutions and complex systems, over a wide temperature range.

The ratio of the activity coefficients in equation 3.3 was calculated using equation 3.14. This correction was relatively minor because of the nearly equal, relatively high ionic strengths in both cell compartments.

There is an agreed convention for the single chloride ion activity coefficient (referred to as the Bates-Guggenheim Convention⁵⁴) used by the National Bureau of Standards (NBS, USA) in setting up the reference pH scale. A Debye-Hückel equation is used where the coefficient $B\alpha$ is replaced by 1.5.

$$\log \gamma_i = \frac{-A I^{\frac{1}{2}}}{1 + 1.5 I^{\frac{1}{2}}} \quad (3.17)$$

This equation is applicable at ionic strengths of 0.1 or less. In this work, measurements of the hydroxide ion concentration in sodium tetraborate/sodium chloride solutions were used to derive pH values from the relation

$$\text{pH} = \log m_{\text{OH}^-} + \log \gamma_{\text{OH}^-} + \text{pK}_W \quad (3.18)$$

For this calculation, values of γ_{OH^-} have been assumed to be equal to γ_{Cl^-} . Recently Liu and Lindsay⁵⁵ have calculated mean molal activity coefficients for sodium chloride from osmotic coefficient measurements* over the full range of NaCl concentrations up to saturation at temperatures from 75 to 300 °C. Their values were substituted for the chloride ion activity coefficients, assuming that $\gamma_{\text{Cl}^-} = \gamma_{\text{Na}^+}$. The pH values so calculated were compared to those calculated using the Bates-Guggenheim convention (equation 3.1⁷~~4~~). The pH values at the ionic strength of the buffer were obtained by extrapolation to ionic strengths of 0.02 and 0.1 for 0.01 and 0.05 mol kg⁻¹ sodium tetraborate solutions respectively. It is important to note that there is a difference between the reference borate buffer pH scale determined here and that set up by the NBS.^{54,56} In the NBS approach, reference pH values are evaluated by direct measurement of the function $\text{p}(a_{\text{H}^+} \gamma_{\text{Cl}^-}) - \log m_{\text{Cl}^-}$ in suitable electrochemical cells (without liquid junction). The measurements are extrapolated to zero chloride concentration (to remove

* Osmotic coefficients are a sensitive measure of the non ideality of the water in the solutions and are closely related to the activity coefficients of the solute.⁵⁷

the effect of the added chloride) and combined with a conventional single ion activity coefficient of the chloride ion (at a given ionic strength (I)). This allows pH values, as defined notionally by equation (3.4), to be obtained.

The reproducibility and precision of the pH cell was confirmed by measuring the ionization constant of water. The activity coefficient term in equation (3.7) was equated to an analytical expression⁵⁸, used by Macdonald¹ and Mesmer¹⁹, so that direct comparison with their results could be made.

$$\log \frac{\gamma_{H^+} \gamma_{OH^-}}{a_{H_2O}} = \frac{-2SI^{\frac{1}{2}}}{1 + AI^{\frac{1}{2}}} + BI + CI^{\frac{3}{2}} \quad (3.19)$$

The various coefficients have the following values

$$S = 1.814 \times 10^6 / (\epsilon T)^{\frac{3}{2}} \quad (3.20)$$

$$A = 50.308 (\epsilon T)^{\frac{1}{2}} \quad (3.21)$$

$$B = 0.266 + 5.2 \times 10^{-4} t \quad (3.22)$$

$$C = -0.035 - 4.88 \times 10^{-4} t \quad (3.23)$$

Here \mathcal{Q} is equal to 3.6, and ϵ is the dielectric constant⁵⁹ for water. Previous work^{1,19} showed that equation (3.19) is applicable up to 125 °C but breaks down at higher temperatures. Sweeton⁶⁰ et al. have recently extended measurements of the ionization product of water

$$Q'_W = m_{H^+} m_{OH^-} \quad (3.24)$$

down to ionic strengths of 0.02 using a flowing concentration cell with liquid junction. Using an arbitrary smoothing equation*, with over 15 parameters, they extrapolated Q'_W to give K^O_W at infinite dilution. The pK^O_W values obtained in this work were within the uncertainties of the flowing cell results. Thus reliable pK'_W values above 125 °C, calculated using the relatively simple activity coefficient expression of equation 3.19, could still be obtained by linear extrapolation to zero ionic strength.

Values of $\gamma_{H^+}\gamma_{SO_4^{2-}}/\gamma_{HSO_4^-}$, which were required to derive the equilibrium constants for the dissociation of the bisulphate ion, were computed from the Debye-Hückel equation.

The mean activity coefficient of an electrolyte dissociating into j kinds of ions, is defined⁵⁷ as

$$\log \gamma_{\pm} = \frac{1}{n} \sum_i^j n_i \log \gamma_i \quad (3.25)$$

where the dissociation of one molecule of electrolyte produces a total number of ions n of which n_i are of the i kind. Hence for the electrolyte (1) H_2SO_4 which completely dissociates into $2H^+$ and SO_4^{2-}

$$\log \gamma_{\pm}^3(1) = \sum_i^2 n_i \log \gamma_i \quad (3.26)$$

and similarly for the hypothetical electrolyte (2) $HHSO_4$

$$\log \gamma_{\pm}^2(2) = \sum_i^2 n_i \log \gamma_i \quad (3.27)$$

It follows that

$$\log \frac{\gamma_{H^+}\gamma_{SO_4^{2-}}}{\gamma_{HSO_4^-}} = \log \frac{\gamma_{H^+}\gamma_{SO_4^{2-}}}{\gamma_{H^+}\gamma_{SO_4^{2-}}} = \log \frac{\gamma_{\pm}^3(1)}{\gamma_{\pm}^2(2)} \quad (3.28)$$

$\gamma_{HSO_4^-}$

* i.e. a semi-empirical equation with sufficient parameters added to give a good fit to the data.

and substituting (for $\log \gamma_i$) the extended Debye-Hückel equation (3.14) gives

$$-\log \frac{\gamma_{H^+} \gamma_{SO_4^{2-}}}{\gamma_{HSO_4^-}} = \frac{4AI^{\frac{1}{2}}}{1 + BaI^{\frac{1}{2}}} \quad (3.29)$$

Linear extrapolation of pK_2' against I to infinite dilution gives pK_2^0 . Because the exact theoretical significance of the ion size parameter a is still unclear and the assumptions made in the theory are not valid for the concentration ranges of interest, the term Ba is often determined empirically.^{22,61,62} For example, by successive substitution to obtain the best horizontal line in a plot of pK_2' against I . Naumov⁶³ et al. recommend a value of a between 0.3 to 0.6 nm for 1-1 and 1-2 electrolytes. Preliminary calculations (at 150 °C) showed that increasing the ion size from 0.3 to 0.5 nm decreased pK_2' by about 0.2 and 0.4 log units. in 0.1 and 0.5 mol kg⁻¹ KCl respectively. However, values extrapolated to infinite dilution were within 0.05* of each other. In the absence of any firm experimental values it was not possible to decide on the most appropriate value of a . Robinson and Stokes⁵⁷ recommend a value of 0.363 nm for KCl solutions and this value was also used by Macdonald.¹ Consequently, the parameter a^0 was held constant at 0.363 nm and B was calculated at each required temperature. This corresponds to Ba values of 1.2 and 1.4 at 75 and 250 °C respectively.

Pitzer²¹ et al. have recently calculated the thermodynamic properties of sulphuric acid at ambient temperatures. The use of their relatively complex equations was unwarranted in view of the uncertainties in the present data, but perhaps more seriously, the

* The estimated experimental uncertainties were of the order of 0.05 log units, see Section 6.4, page 105.

interaction coefficients of the ion pairs (K^+Cl^- , $K^+SO_4^{2-}$ and $K^+HSO_4^-$) are not known over the temperature range considered in this study.

3.1.4 Standard State.

The "hypothetical one molal" standard state⁶⁴ was used for all solute species. The standard state was chosen so that the mean molal ionic activity coefficient approached unity as the concentration of the solute was reduced to zero, at every temperature and pressure.

$$\gamma_{\pm} \rightarrow 1.0 \quad \text{as} \quad I \rightarrow 0.0 \quad (3.30)$$

Similarly the individual ion activity coefficients were defined to approach unity at infinite dilution.

3.2 DEPENDENCE OF EQUILIBRIUM DATA ON TEMPERATURE.

3.2.1 Introduction.

The analysis of the temperature dependence of equilibrium data ~~on~~ and the derivation of associated thermodynamic quantities has been well reviewed^{65,66} recently, so only a summary relevant to this study is included here.

The van't Hoff equation relates the dependence of $\ln K$ on temperature at temperature T to ΔH at that temperature. However, ΔH may depend on temperature. Thermodynamics does not define what form this dependence takes and therefore the problem was to choose, from the observed dependence of K on T , the most appropriate equation from which all the thermodynamic quantities could be calculated.

3.2.2 Valentiner Equation.

The Valentiner⁶⁷ equation, which was one of the first proposed for analysing the dependence of $\ln K$ on T , was successfully used to fit a wide range of equilibrium data in this study. The dependence of $\ln K$ on T is described by a three term equation with one term proportional to T^{-1} and another proportional to $\ln T$.

$$\ln K = \frac{a_1}{T} + a_2 + a_3 \ln T \quad (3.31)$$

The Valentiner equation can accommodate situations where the plot of $\ln K$ against T passes through a minimum or a maximum. At such points $\Delta H=0$. The values of K are indeterminate when T is zero or infinity and the equation uses as one boundary value the temperature $T=1$ K. At this temperature (which is well outside the experimental temperature range) $\ln K=a_1+a_2$ and $\Delta H=R(a_3-a_1)$. Equation 3.31 is readily differentiated to yield

$$\Delta H = R(a_3 T - a_1) \quad (3.32)$$

where

$$\Delta C_p = a_3 R \quad (3.33)$$

Hence

$$\Delta S = R(a_2 + a_3(\ln T + 1)) \quad (3.34)$$

3.2.3 Clark and Glew Equation.

Occasionally the Valentiner equation could not account for all the features (see section 3.3, page 41) found in a particular data set. Rather than arbitrarily adding further combinations of temperature terms to account for deviations from linearity, an alternative approach was used, where an expression was formulated for the dependence of ΔH on temperature. The values of ΔH and ΔC_p at any experimental temperature, T , are expressed as a deviation from their values at some reference temperature, θ , by a Taylor's series expansion (arbitrarily terminated at the first derivative of ΔC_p). Thus

$$\Delta C_{p,T} = \Delta C_{p,\theta} + \left(\frac{d\Delta C_p}{dT} \right)_\theta (T-\theta) \quad (3.35)$$

and (noting that $dH/dT = C_p$)

$$\Delta H_T = \Delta H_\theta + \Delta C_{p,\theta}(T-\theta) + \frac{1}{2} \left(\frac{d\Delta C_p}{dT} \right)_\theta (T-\theta)^2 \quad (3.36)$$

Combining the above equations with the standard expressions and using the temperature transformation $x=(T-\theta)/\theta$, together with the expansion of logarithmic terms gives the Clark and Glew equation.^{2,68}

$$R \ln K_T = R \ln K_\theta + \frac{\Delta H_\theta}{\theta} t_1 + \Delta C_{p,\theta} t_2 + \frac{\theta}{2} \left(\frac{d\Delta C_p}{dT} \right)_\theta t_3 \quad (3.37)$$

where

$$t_i = x^i \sum_{n=1}^{\infty} \frac{n}{n+(i-1)} (-x)^{n-1} \quad (3.38)$$

The t_i temperature variable terms between 25 and 250 °C are given in Table B.2. The method is quite general and can be extended when

required to include higher terms than the first derivative of ΔC_p . It has the further advantage of carrying out the definite integration in a well defined temperature range θ to T , thus avoiding integrations from zero to temperature T . The Taylor's expansion requires that the significance of adding each new temperature variable must be tested. If only three terms are used the Valentiner equation is recovered. However, the reference temperature is θ and not 1 K. In the present study data that could not be adequately described by the Valentiner equation required no more than four temperature variable terms in the Clark and Glew equation.

3.3 STATISTICAL TREATMENT OF DATA.

For each solution several values of cell potential (E) were obtained at intervals of approximately 25 °C. The actual temperatures of the solutions, at which measurements were made, usually differed from one experimental run to another, by more than the error in the temperature measurement. The potentials were "normalized" (see section 3.4.2, page 46) by calculating an equilibrium constant (or pH) using the known relationship (e.g. equations 3.1 and 3.6) between E and the stoichiometric solution concentrations. The first stage of analysis consisted of combining the equally weighted data from all the solutions of nominally the same composition, and then smoothing with respect to temperature, using the Valentiner equation and then if required, the Clark-Glew equation. These equations express the independent parameter as a linear function of the fitting parameters and so were amenable to analysis using the least squares technique. All calculations were carried out on the IBM 4341 using the statistical analysis package SAS.⁶⁹

Three major criteria were used in judging the adequacy of the fits.

1. The standard deviation of the fit (s_f) provided a guide to the quality of the data and the success of the equation in accounting for the dependence of $\ln K$ on T . The standard deviation was also compared with the estimated precision of the experimental values.
2. A plot of the residuals (e.g. $\ln K[\text{calculated}] - \ln K[\text{observed}]$) against temperature was inspected for any systematic trends which would indicate that the smoothing equation was unsatisfactory.
3. Reasonableness of the derived thermodynamic parameters when compared to other properties of the system or with values calculated for similar chemical changes.

The Valentiner equation gave sinusoidal residual plots when used for fitting some data sets. In these cases the four term Clark-Glew equation generated the expected random scatter in the residual plots.

SAS calculates a considerable amount of other statistical information the most useful of which was the standard error. Standard errors were calculated for the equation coefficients, as well as (at selected temperatures) of the smoothed $\ln K$ values and of the derived thermodynamic quantities. Thus the 99% confidence intervals were easily calculated by multiplying the standard error by the appropriate 't' distribution value, assuming that the measurements were part of a Gaussian distribution.

One important feature of the Clark-Glew equation is that each thermodynamic parameter at temperature, θ , is related to one parameter obtained from the least squares analysis and if θ is near the experimental temperature range, the standard errors on these quantities are less than on those based on the Valentiner equation whose effective reference temperature is at $T=1$ K.

The second stage of the analysis involved linear extrapolation of the three or four smoothed equilibrium constants against $1/T$ (at constant

temperature) to obtain pK^0 at $I=0$ at each temperature. The values at infinite dilution were then fitted with the same equation that was used for the initial temperature smoothing. This is in effect a fit of the already smoothed data and consequently "perfect" fits resulted and the standard errors were grossly underestimated. An alternative multilinear analysis⁷⁰ was used, where all the data was simultaneously smoothed and extrapolated to zero ionic strength. For example, assuming a linear relationship, the Valentiner equation becomes

$$\ln K = \frac{(a_1 + b_1 I)}{T} + a_2 + b_2 I + (a_3 + b_3 I) \ln T \quad (3.39)$$

Thus if the measurements were made at 25 °C intervals between 75 and 225 °C, seven three term equations were replaced by one six term equation. Setting the ionic strength to zero gives the equation for the infinite dilution values. This analysis gave identical results as the two stage procedure except that reliable error estimates could now be obtained. All equations at zero ionic strength, given in the appendices, were derived using this multilinear approach.

3.4 ASSIGNMENT OF UNCERTAINTIES.

In this section various sources of error are identified and the magnitude of the resulting uncertainties estimated. Specific numerical estimates are given in the relevant "error" sections of Part III.

3.4.1 Systematic Errors.

The fundamental physical properties measured were potential differences, an electrochemical cell potential and a thermocouple potential. The temperature was calculated from the thermocouple voltage, via calibration. These results together with the known composition of

the reference solution were used to evaluate the hydrogen ion activities of the solution in the other cell compartment. For example, if the "unknown" was a sulphuric acid solution of stoichiometric concentration, m , then an equilibrium constant (the primary result) may be calculated from equation 3.6. Thus the error in the primary result involved uncertainties in measurement of cell potential and temperature, solution make-up and in estimation of the liquid junction potentials and activity coefficients.

The Dana multimeter has a resolution of $1\ \mu\text{V}$, and under controlled conditions was found to be accurate to better than $\pm 0.01\ \text{mV}$ up to $0.2\ \text{V}$ and $\pm 0.06\ \text{mV}$ up to $0.5\ \text{V}$. (section 2.4.1, page 22). However, potential readings tended towards an equilibrium value and/or fluctuated with minor temperature variations, so that they were never sufficiently stable to be able to be measured with the above accuracy. These fluctuations were much greater than the resolution and stability of the multimeter. For reasonable precision in the primary data a precision in E of $\pm 0.1\ \text{mV}$ is necessary. The potentials were recorded after they had become constant to within $0.1\ \text{mV}$ for at least 15 minutes and thus the uncertainty in the final result, from systematic error, is smaller than that due to random error.

The thermocouples were calibrated³⁰ to $\pm 0.01\ ^\circ\text{C}$ against a standard platinum resistance thermometer which has a certified calibration error of less than $0.001\ ^\circ\text{C}$. The temperatures in both compartments, which usually differed by less than $0.1\ ^\circ\text{C}$, were averaged to give the cell temperature at an estimated error of $\pm 0.3\ ^\circ\text{C}$.

All solutions were made up by weight to $\pm 0.001\ \text{g}$. A known weight of stock acid or base solution and dried potassium or sodium chloride was diluted to give an acid or base concentration of about $0.01\ \text{mol kg}^{-1}$ and a supporting electrolyte concentration between 0.1 and $1\ \text{mol kg}^{-1}$. The

uncertainty of 0.1% in the ampoule concentration combined with weighing errors gives a 0.25% uncertainty in the final acid or base concentration and less than 0.1% for the supporting electrolyte. Sodium tetraborate decahydrate (borax) was weighed directly to give solution concentrations of 0.01 and 0.05 mol kg⁻¹ with uncertainties less than 0.01%.

Liquid junction potentials for cell (A) were estimated using the Henderson equation (3.11). An uncertainty in the calculation was introduced by the lack of data for molar conductivities at elevated temperatures. Quist and Marshall⁷¹ have estimated the limiting molar conductivities for a number of single ions at temperatures up to 400 °C, and their values were used throughout. No data exists for the limiting ionic conductivities of the borate hydrolysis species and so these were equated to the conductivity of the chloride ion. It was difficult to assign an exact uncertainty in the calculated liquid junction potentials. The validity of the Henderson equation, which is a restricted representation of effects at liquid junctions (especially at high temperatures) is in some doubt^{14,34,72} and it was unlikely that the junction formed actually corresponded to the assumptions underlying the derivation of the equation. Rock⁷³ found that at room temperature the potentials of cells with symmetrical junctions, after adjustment using the Henderson equation, agreed well with values of potentials of cells without liquid junction. In the present work a similar situation occurs where the same supporting electrolyte was at near equal, high concentration in both compartments. However no experiments have yet been performed to test the validity of the Henderson equation at elevated temperatures. In this study the calculated liquid junction potentials were usually less than 3mV and this generally represented a minor correction to the measured potential. A conservative estimate of 10% error in the liquid junction potential was assumed.

Similarly, imperfections in the Debye-Hückel theory and the uncertainties of the value of the parameter β allows the activity coefficient to be calculated⁶³ with an estimated uncertainty of $\pm 2\%$.

All the above systematic errors were combined as follows.⁷⁴ Given that

$$y = F(x, z, \dots, w) \quad (3.40)$$

with estimates of uncertainty $\Delta x, \Delta y, \dots, \Delta z$ then the corresponding uncertainty in y is

$$\Delta y = \left| \frac{\partial y}{\partial x} \right| \Delta x + \left| \frac{\partial y}{\partial z} \right| \Delta z + \dots + \left| \frac{\partial y}{\partial w} \right| \Delta w \quad (3.41)$$

This will overestimate the size of Δy and can be considered as an estimate of the maximum possible uncertainty.

3.4.2 Random Errors.

Random errors, which contribute to the imprecision of a result, are produced by the unpredictable and unknown variations in the experimental situation.

For a replicate set of experiments the scatter of the observed data points about the fitted curve of cell potential against temperature can give an indication of the precision and quality of the results obtained (section 3.3, page 41).

For each ionic strength enough solution was prepared for four experimental runs. More solution was made up (as required) if there were any run failures. At a later date the sequence was repeated for the high temperature range. All solutions were at nominally the same ionic strength but minor variations in make-up of acid or base solutions could give rise to significant differences in the measured cell

potential (e.g. 5mV) at equivalent temperatures. Thus in most cases a simple plot of potential against temperature was not indicative of the imprecision of a set of results. For example, in determining the dissociation constant of the bisulphate ion the easiest way to adjust to a common set of measurement conditions was to calculate an equilibrium constant which is then independent of the reference acid solution and sulphuric acid concentration. Where a comparison could be made, the residual deviation plot of the primary result (e.g. pK,pH) against temperature exactly mirrored that of potential against temperature, indicating that the imprecision of the former was directly related to that of the latter. Given the solution concentrations, it was relatively easy to "back-calculate" a cell potential from the primary result. Thus in all the "error" sections of Part III an indication is given of the magnitude and imprecision of the measured cell potentials.

3.4.3 Derived Functions.

Differentiation of the Valentiner equation with respect to temperature gives an equation for ΔH and a further differentiation yields ΔC_p . Differentiation always results in loss of precision therefore ΔH and ΔS will be less precisely known than pK and ΔC_p will have the highest uncertainty. Even for the most precise data over the normal experimental temperature range (0-60 °C), it is not possible to attach significance to changes of less than approximately 80 Jmol⁻¹ in ΔH and 8 Jmol⁻¹K⁻¹ in ΔC_p .⁷⁵ Timini⁷⁶ used the Clark-Glew equation to show that over that same temperature range even small errors* can lead to large uncertainties in ΔC_p . In comparison with calorimetric data Timini concluded that the dissociation constant method was not as yet capable

* For example an error of ± 0.00025 pK units, which is greater accuracy than the most accurate experimental pK work.

of furnishing reliable ΔC_p values. However more reliable values could be obtained with measurements at 5 K intervals and over a temperature range of at least 100 K.

Thus in this work, the numerical values obtained from the derived functions were not significant in themselves but the order of magnitude and trends with temperature were useful in understanding the chemical systems under study.

PART III

RESULTS AND DISCUSSIONS

This part is divided into four chapters. Each chapter contains the presentation of the final results and an evaluative discussion corresponding to an experimental system studied. All raw data, primary results and other data such as coefficients of equations are presented in the appendices.

Chapter 4

IONIZATION CONSTANT OF WATER

4.1 INTRODUCTION.

The ionization reaction of water has been and continues to be extensively studied. The earlier low temperature work, mostly below the boiling point of water, has been reviewed by Harned and Owen⁷⁷ up to 1957 and by Clever⁷⁸ up to 1968. The relatively recent studies, which have extended the measurements of the ionization constant of water to temperatures greater than 100 °C at saturation vapour pressure (SVP), are of particular interest as good agreement with the present data may be expected and would lead to a reliable set of values over a wide range of temperature.

4.2 RESULTS.

The smoothed values for pK'_W in 0.1-1 mol kg⁻¹ KCl solution are listed in Table 4.1 and plotted as a function of ionic strength in Figure 4.1. The pK_W^O values were found by extrapolating to zero ionic strength the lines of best fit to the data at ionic strengths up to and including $I=1.0$. The experimental values and plots of pK'_W are given in Tables A.3 to A.7 and in Figures A.1 to A.4 of Appendix A. Equation coefficients are listed in Table A.2 and Table A.1 contains a complete presentation of the primary results which combine to give the values listed in Table 4.1. The values for pK_W^O and associated thermodynamic parameters are listed in Table 4.2. The values at 25 °C are below the experimental temperature range and were calculated using the equations given in Table A.2.

TABLE 4.1

pK'_W Values a Function of Ionic Strength and Temperature.

$t/^{\circ}C$	Ionic Strength ($I/mol\ kg^{-1}$)			
	0.1	0.3	0.5	1.0
75	12.721 ± 0.011	12.717 ± 0.020	12.703 ± 0.019	12.648 ± 0.025
100	12.247 ± 0.005	12.246 ± 0.011	12.222 ± 0.011	12.192 ± 0.014
125	11.887 ± 0.005	11.880 ± 0.011	11.848 ± 0.011	11.824 ± 0.014
150	11.616 ± 0.005	11.597 ± 0.011	11.560 ± 0.011	11.529 ± 0.014
175	11.416 ± 0.005	11.382 ± 0.008	11.342 ± 0.011	11.291 ± 0.014
200	11.275 ± 0.008	11.221 ± 0.011	11.179 ± 0.014	11.100 ± 0.014
225	11.182 ± 0.011	11.106 ± 0.017	11.063 ± 0.025	10.949 ± 0.019
n	51	39	37	36
s_f	0.012	0.016	0.017	0.021

The primary values listed above and in the following chapters are not rounded so that full precision to the final result is maintained.

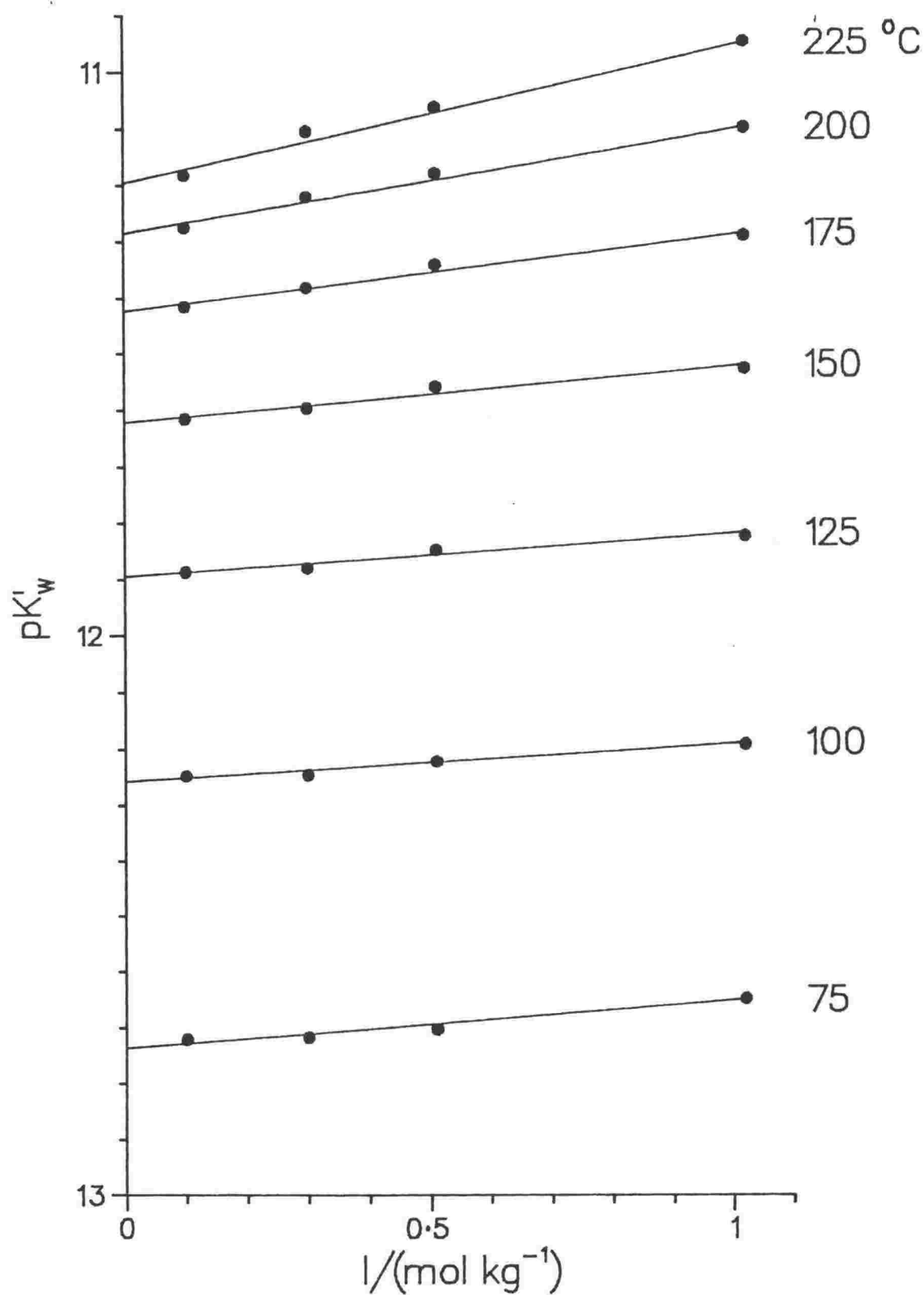


Figure 4.1: The Variation of pK'_w with Ionic Strength at Various Temperatures.

TABLE 4.2

Thermodynamic Values for the Ionization of Water.

t/°C	$-\log K_W^0$	ΔG^0 (kJ mol ⁻¹)	ΔH^0 (kJ mol ⁻¹)	ΔS^0 (J K ⁻¹ mol ⁻¹)
25*	14.2 ± 0.1	80.9 ± 0.3	63 ± 2	-59 ± 6
75	12.74 ± 0.02	84.89 ± 0.09	51 ± 1	-98 ± 3
100	12.258 ± 0.007	87.57 ± 0.05	44.4 ± 0.8	-116 ± 2
125	11.894 ± 0.007	90.66 ± 0.06	38.2 ± 0.5	-132 ± 1
150	11.622 ± 0.007	94.15 ± 0.06	31.9 ± 0.4	-147 ± 1
175	11.424 ± 0.007	98.01 ± 0.06	25.6 ± 0.7	-162 ± 2
200	11.286 ± 0.008	102.23 ± 0.07	19 ± 1	-175 ± 2
225	11.20 ± 0.01	106.8 ± 0.1	13 ± 2	-188 ± 3

$$\Delta C_p^0 = -252 \pm 17 \text{ J K}^{-1} \text{ mol}^{-1}$$

$$n = 163, s_f = 0.017$$

* extrapolated

4.3 ERRORS.

The errors given in Table 4.1 and 4.2 are the 99% confidence intervals derived⁷⁹ from the least squares analysis. In Table 4.3 the estimated errors are given at 75 and 225 °C. The way in which these errors were calculated is described in Section 3.4, page 43. For example, at I=0.1 and at 75 °C the various contributions to the final error are summarized in Table 4.4. The random errors in Table 4.1 are less than the estimated errors given in Table 4.3. At 75 °C and at I=0.1 the activity coefficient contributes a small error to the total, while at 225 °C this error becomes more significant (see Table A.1) and contributes about half the total error. The overall experimental error is of the

order of 0.02 log units. The potentials and errors (in millivolts) corresponding to the pK'_W and the 99% confidence intervals given in Table 4.1, are listed in Table 4.5.

TABLE 4.3

Estimated Errors in pK'_W as a Function of Ionic Strength at 75° and 225°C

I/mol kg ⁻¹	75°C	225°C
0.1	12.721 ± 0.023	11.182 ± 0.019
0.3	12.717 ± 0.020	11.106 ± 0.018
0.5	12.703 ± 0.019	11.063 ± 0.019
1.0	12.648 ± 0.018	10.949 ± 0.019

Table 4.5 shows the size of the random errors in relation to the measured potentials. The potentials range in value from 578 mV to 668 mV. In the worst case at I=0.5 and 225 °C the error of 2.5 mV is only 0.39% of the total potential. These calculated errors are of the same magnitude or less, than the liquid junction potential corrections (see Tables 4.4 and A.1).

TABLE 4.4

Contributions to the Final Error in pK'_W at $I=0.1$ and at 75° and 225°C .

Temperature	75°C	0.0073
Concentrations	$m_{\text{H}^+}, m_{\text{OH}^-}=0.01$	0.0022
Potential	-0.58129 V	0.0015
Junction Potential	4.81 mV	0.0070
Activity Coefficient	0.236	0.0050
Total Error		0.023 log units
Temperature	225°C	0.0041
Concentrations	$m_{\text{H}^+}, m_{\text{OH}^-}=0.01$	0.0022
Potential	-0.66750 V	0.0010
Junction Potential	3.37 mV	0.0034
Activity Coefficient	0.395	0.0080
Total Error		0.019 log units

TABLE 4.5

Potentials (mV) and Calculated Errors in pK'_W as a Function of Ionic strength at 75° and 225°C .

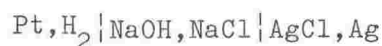
Ionic Strength ($I/\text{mol kg}^{-1}$)

$t/^\circ\text{C}$	0.1	0.3	0.5	1.0
75	-581.29 ± 0.76	-580.15 ± 1.28	-579.22 ± 1.31	-577.81 ± 1.76
225	-667.50 ± 1.10	-651.79 ± 1.73	-644.79 ± 2.50	-632.52 ± 1.92

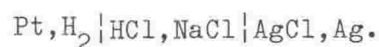
4.4 PREVIOUS WORK.

4.4.1 Studies That Employed the Silver/Silver Chloride Electrode.

Perkovets and Kryukov⁸⁰ derived pK_W^0 values at temperatures between 100 and 150 °C from EMF measurements employing the cell



where E^0 values for the silver/silver chloride electrode were obtained from Greeley⁸¹ et al. Bezboruah⁸² et al. in a low temperature study (up to 85 °C) employed a similar cell but used the E^0 values taken from the data of Bates and Bower.⁸³ Dobson and Thirsk⁶⁶ reported K_W^0 values between 100 and 200 °C from simultaneous measurements of potentials on the "Harned" cell above and the cell



This obviated the need to use literature standard electrode potential data and required no correction for the partial pressure of hydrogen.

4.4.2 Conductivity Methods.

Non EMF methods, particularly conductivity measurements, have been used mainly at very high pressures or in the supercritical region, to calculate ionization constants of water. At SVP, values of K_W^0 have been reported by Bignold⁸⁴ et al. from conductivity measurements on pure water up to 271 °C and by Fisher and Barnes⁸⁵ from conductivity measurements on ammonium acetate/acetic acid mixtures up to 350 °C. Fisher⁸⁶ has since reassessed his earlier results.

4.4.3 Hydrogen Electrode Concentration Cell Studies.

Macdonald, Butler and Owen¹(MBO) and Mesmer, Baes and Sweeton¹⁹(MBS) used concentration cells of similar design to those those used in this study to measure K_W^0 to 200 °C and Q_W' in 1 mol kg⁻¹ KCl to 300 °C respectively. Busey and Mesmer⁸⁷ also used the cell to measure Q_W' in 1 and 3 mol kg⁻¹ NaCl solution. In later work Sweeton, Mesmer and Baes⁶⁰(SMB) measured Q_W' as a function of ionic strength (in KCl media) to 300 °C in a hydrogen electrode flowing concentration cell. In a critical review⁸⁸ this later work has been accepted as the most reliable and accurate that has appeared in the literature. The results have recently been used as the baseline values (0-300°C) for the new formulation of the ionic constant of water issued by the International Association for the Properties of Steam (IAPS).⁸⁹

4.5 DISCUSSION AND COMPARISON WITH OTHER WORK.

4.5.1 Introduction.

The differences between previously published work and this study are small and thus the agreement is best shown as a deviations plot in Figure 4.2. The literature results are summarized in Table 4.6. Unless otherwise stated, these results are compared with the values of pK_W^0 obtained by extrapolation of the data over the full range of ionic strength up to $I=1.0$.

4.5.2 Studies Employing the Silver/Silver Chloride Electrode.

The agreement between those studies employing silver/silver chloride electrodes and this work and indeed other literature results, is not good and generally outside the estimated uncertainties. This supports the view that the silver/silver chloride electrode functions improperly at high pH and under a hydrogen atmosphere. Dobson and Thirsk

encountered unstable cell potentials. The scatter of their values with respect to this work is very marked, deviating by 0.09, -0.1 and 0.02 log units at 100 150 and 200°C respectively. Perkovets and Kryukov appear to have obtained more stable potentials and their pK_W^0 values are consistently higher by about 0.03 units.

TABLE 4.6

Literature Results for the Temperature Dependence of the Ionization Constant of Water.

t/°C	25	75	100	125	150	175	200	225
Bignold, Brewer and Hearn ⁸⁴	14.00	12.714	12.283	11.958	11.720	11.555	11.451	11.398
Bezboruah et al. ⁸²	14.02	12.771	-	-	-	-	-	-
Dobson and Thirsk ¹⁴	-	-	12.17	11.98	11.72	11.43	11.27	-
Fisher ⁸⁶ recalculated	13.99	12.705	12.258	11.907	11.635	11.436	11.300	11.225
Macdonald, Butler and Owen ¹	13.98	12.69	12.24	11.89	11.62	11.42	11.27	-
Marshall and Franck ⁸⁹	13.99	12.712	12.265	11.912	11.638	11.432	11.289	11.208
Perkovets and Kryukov ⁸⁰	13.99	-	12.29	11.92	11.66	-	-	-
Sweeton, Mesmer and Baes ⁶⁰	13.99	12.709	12.264	11.914	11.642	11.441	11.302	11.222
This Work (From I=0.5)	14.1*	12.727	12.256	11.899	11.631	11.436	11.299	11.210
This Work (From I=1)	14.2*	12.737	12.258	11.894	11.622	11.424	11.286	11.196

* extrapolated

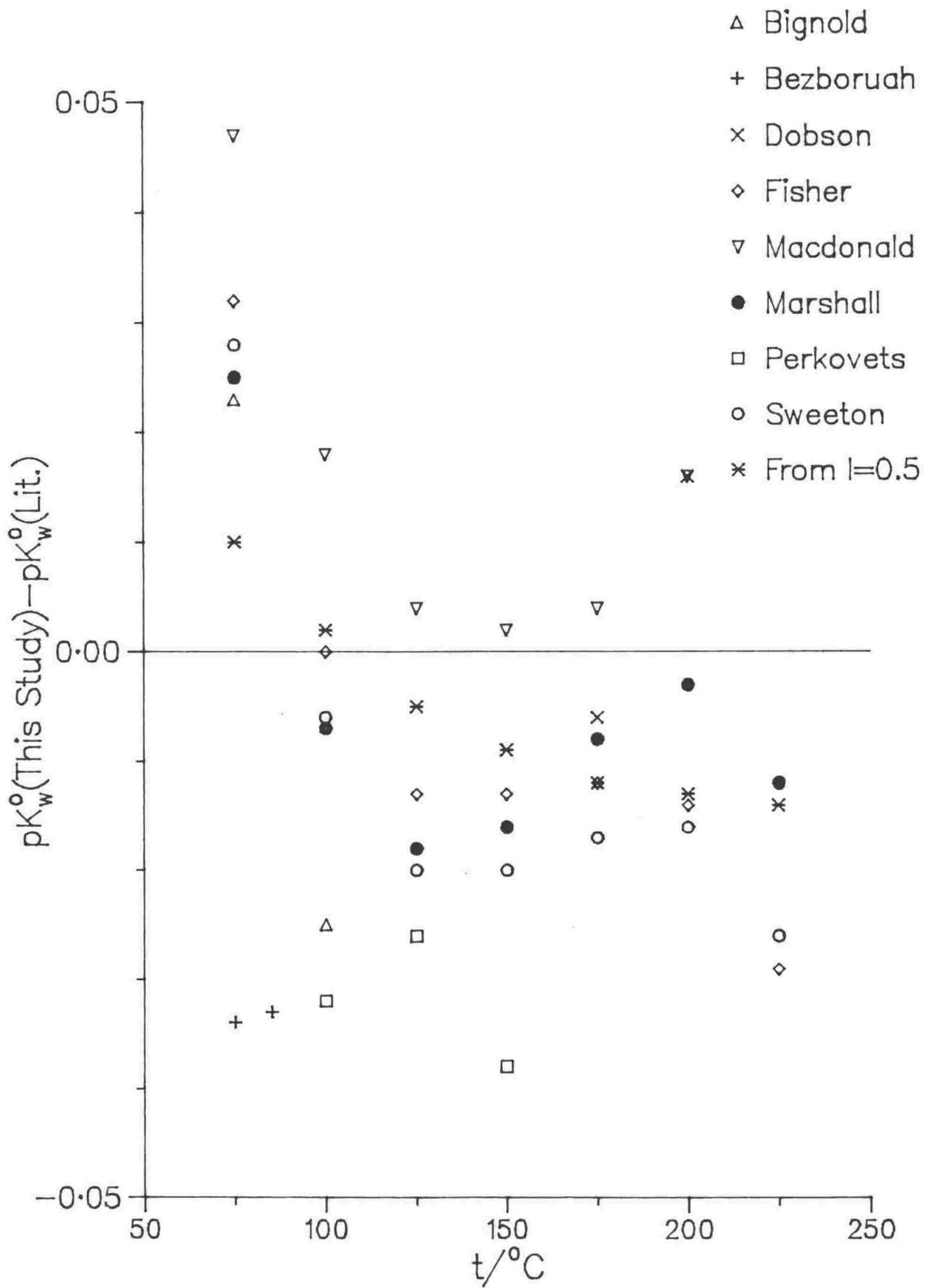


Figure 4.2: The Deviation Between the pK_w^0 Values Found in This Study and Previously Published Work.

4.5.3 Conductivity Measurements.

Bignold Brewer and Hearn calculated ionization constants from the limiting molar conductivity of water at various temperatures. Their results agree at 75 and 100 °C but thereafter progressively deviate to higher pK_W^0 's, reaching a maximum difference of 0.2 log units at 225 °C. Although the specific conductivity of water measurements of Bignold et al. are probably the most precise that have appeared in the literature, their derivation of ionization constants is severely limited by the lack of accurate limiting molar conductivity data for hydrogen and hydroxide ions. Fisher's results, based on conductance measurements of the hydrolysis of ammonium acetate, agree well with this work. Between 100 and 200 °C the deviations are less than 0.02 units. At 75 and 225 °C their values are 0.03 log units lower and higher respectively.

4.5.4 Macdonald, Butler and Owen's Study.

MBO's study is important in that the concentration cell used in this work was based directly on their design and the same methods were used for analysing the results. MBO's pK_W^0 values are all consistently lower but the deviations are well within the probable uncertainties of both studies (of about 0.02 units), except at 75°C, where the values differ by 0.05 units. There are however differences in the pK_W' values determined at higher ionic strengths. If the activity expression used (Eq. 3.19) correctly represents the ionic strength dependence of the term $\gamma_{H^+}\gamma_{OH^-}/a_{H_2O}$, then plots of pK_W' against I would be expected to be linear with almost zero slope. Equation 3.19 has been found⁵⁸ to be satisfactory to <1% in 0-3 mol kg⁻¹ KCl solution at temperatures to 60°C. The acceptability of this equation up to 125°C was demonstrated by the linear and horizontal pK_W' v. I curves obtained by MBO. At higher temperatures the ionization constants deviated to more negative values,

particularly in 1 mol kg⁻¹ KCl solution. In Figure 4.1 it is seen that the slopes progressively deviate to lower pK'_W values, as found by MBO, but the points from I=0.1 to 1 remain reasonably co-linear up to 225 °C. Extrapolation from I=0.5 gives pK_W^O values which were lower by 0.01 and 0.002 units at 75 and 100 °C and progressively higher by 0.005 to 0.014 log units between 125 and 225°C. These deviations are well within the estimated experimental error and thus there was no justification for taking the extrapolation from I=0.5, although the results appear to be in better accord with the "best" previously published values (Figure 4.2). MBO attributed this deviation to the formation of KOH ion pairs, and it is likely that this is the mechanism causing progressive deviation from zero slope. However, the good linearity of the plots allows any ion pairing effects to be accurately extrapolated out. Except at 75°C, the pK_W^O 's found in this work and in MBO's study are all lower than the other literature results. There is no obvious reason for this discrepancy except that dilute hydroxide solutions are susceptible to carbon dioxide contamination which is known⁸² to lower pK'_W . However the overall deviations are small and generally within 0.02 log units. The 75°C point is the exception in that it is significantly higher than all the other literature results. One possible explanation is that equilibrium was being reached very slowly at the lower temperatures and thus non equilibrium potentials were recorded. The random error of this point (Table 4.2) is double that calculated for all the other ionization constants between 100 and 225°C.

4.5.5 Sweeton, Mesmer and Baes's Flowing Cell Results.

The most complete pK'_W results as yet presented are those reported by SMB using the hydrogen electrode flowing concentration cell. Their values listed in Table 4.6 and used in the deviations plot, are biased by the

inclusion of lower temperature literature data, the high temperature conductivity data of Bignold et al. and results from their earlier study of Q'_W in 1 mol kg⁻¹ KCl solution using a hydrogen electrode "static" pH cell. Bignolds data deviates considerably at temperatures greater than 100 °C and it is not clear whether only the low temperature results (50-100°C) or all the data were included. Nevertheless the agreement between this work and SMB is reasonable. Except at 75 °C their data is consistently higher than in this study. The deviations are less than 0.02 units except at 75 and 225 °C where the deviations from this study are 0.028 and -0.026 units respectively. The errors in their study are estimated at about 0.02 units. The agreement between MBO and SMB is a lot worse with differences greater than 0.02 units between 75 and 200 °C.

Although the apparent agreement at infinite dilution is good, an exact comparison with SMB's results is difficult as their final values were obtained by simultaneously fitting their own results with selected literature data. A table given in their paper "summarizes" the experimental values obtained at different ionic strengths. It is clear that these results are smoothed (possibly for ease of presentation) to give $\log Q'_W$ values at 50 °C intervals, as their measurements were made at 50 °C increments from 50 to 250 °C. These results (presumably the raw data and not the summarized values) were then smoothed using an empirical equation, obtained by combining semi-empirical equations describing heat capacity, activity coefficient and pressure coefficient behaviour, with enough terms added to give a good fit of the data. The result is an unwieldy 15 parameter equation of limited use and labourious to use. SMB estimated the probable experimental uncertainties and give statistical errors (3 σ) for the derived thermodynamic quantities. However the number of results used and the overall standard

deviation of the fit are not given. There is no graphical representation of the raw primary data and the table discussed above is inadequate to fully describe their experimental results. Thus it is difficult to assess, from the information provided, the overall reliability of their results and whether all the 15 parameters were needed to describe the data within the precision of the pK'_W values. Thus SMB's results cannot be compared directly to the results found in this study.

4.5.6 Mesmer and Co-workers, Static Cell Studies.

The ionization products in 1 mol kg^{-1} KCl solution found by MBO, MBS and this work are listed in Table 4.7. SMB's smoothed flowing cell results are also included. MBO did not give any analytical expressions for the

TABLE 4.7

pQ'_W in 1 mol kg^{-1} KCl Solution, Various Studies.

t / °C	75	100	150	200	225
Busey Mesmer ⁸⁷ (NaCl)	-	11.887	11.136	10.612	-
Busey Mesmer ⁹⁰ (fitted)	11.366	11.872	11.121	10.608	10.418
Macdonald, Butler Owen and Owen ¹	12.42	11.92	11.14	10.58	-
Mesmer, Baes and Sweeton ¹⁹	12.401	11.903	11.157	10.648	10.458
Sweeton, Mesmer and Baes ⁶⁰	12.404	11.916	11.181	10.680	10.490
This Study	12.373	11.888	11.150	10.620	10.403

temperature dependence of the ionization constants at various ionic strengths. The data listed were obtained from the graphical representations given by MBO and recalculated to give ionization products. Busey and Mesmer⁸⁷ measured the ionic product of water in 1 and 3 mol kg⁻¹ NaCl solution at 50°C intervals up to 300°C and in a later paper Busey and Mesmer⁹⁰ presented a complete tabulation of the thermodynamic quantities for Q'_W in NaCl media to 300°C from infinite dilution to $I=5$. Having only the data at 1 and 3 mol kg⁻¹ NaCl, they used SMB's flowing cell results in KCl media to fix the infinite dilution and pressure dependent behaviour. The values from this computation are listed in the second line of Table 4.7.

There is good agreement with MBS and MBO and the results found in this study. In contrast, SMB's flowing cell results are all higher and progressively deviate by -0.03 units at 75°C to -0.09 units at 225°C. SMB's flowing cell results included the earlier static cell measurements and the conclusion reached is that the flowing cell measurements would have deviated even more were it not for the biasing effect of the earlier static cell results. Thus SMB's results at 1 mol kg⁻¹ KCl appear to be in error at the higher temperatures. The good agreement with SMB's results at infinite dilution suggests that their results are reliable at ionic strengths of 0.1 or less. The $\log Q'_W$ vs. I curves fitted by SMB are of moderate slope up to $I=0.1$ at which point there is a sharp increase in slope towards infinite dilution. Thus, even if the ionic products at ionic strengths of 0.5 and 1 are in error, reliable values at $I < 0.1$ ensure that the extrapolation to zero ionic strength using an equation with 15 adjustable parameters, is good.

The comparison of Busey and Mesmer's study and the earlier determinations of the ionic product in KCl media is important in

calculating the extent of association of NaOH as compared to KOH. There is good correspondence between their "experimental" values and this work in 1 mol kg⁻¹ KCl solution. The effect of using the KCl infinite dilution parameters, for smoothing the experimental results at 1 and 3 mol kg⁻¹ NaCl, is to further lower the ionization products. Thus the apparent difference between the KCl flowing cell results and the smoothed NaCl results is that much greater. It is highly likely that this is a product of the smoothing procedures adopted by Mesmer and coworkers, rather than a real effect.

4.5.7 IAPS Equation.

Recently Marshall and Franck⁸⁹ detailed the development of the new IAPS equation for the ionic constant of water. The authors believe that the equation presented describes pK_W^O within 0.01 units up to 200 °C and to within 0.02 units up to 374 °C at SVP. SMB's results were exclusively used in evaluating this equation along the liquid-vapour saturation curve from 0-300 °C. The pK_W^O values given by the equation naturally agree well with SMB's results. Above 125°C the IAPS pK_W^O values are lower than SMB's results and progressively deviate to -0.014 units at 225 °C. The IAPS formulation agrees to 0.02 units of the pK_W^O values found in this study.

4.5.8 Conclusion.

The results presented show that the static pH cell was capable of yielding ionization constants in good agreement with previously published work. The pK_W^O at 75°C appears to be high but the uncertainty at this point still encompasses the literature values. The self consistency of the results gives confidence in the reliability of the cell and in the methods and procedures adopted, as described in Chapter

2. The discrepancies with SMB's results with respect to this work and MBO's data are difficult to explain. The hydrogen electrode flowing cell is more sophisticated and complicated apparatus than the static cell and the differences could simply be due to inadequate corrections applied to the initial results (e.g. extrapolation to infinite flow rate). A later study by Busey and Mesmer of the ionization reaction in 1 mol kg⁻¹ NaCl using the static pH cell, gave values relatively similar to those found for 1 mol kg⁻¹ KCl solution in this study. It is likely that the extent of association of NaOH does not differ significantly from KOH up to 225°C at unit ionic strength. In addition SMB's choice of complex smoothing equations, the inclusion of literature data and the omission of an adequate representation of their primary results further obscures the real situation. From the above discussion it is evident that further study of the ionization reaction of water at higher temperatures and ionic strengths is required. Unfortunately, at the time this work was undertaken experimental problems prevented measurements above 225°C.

4.6 THERMODYNAMIC PARAMETERS.

Differentiation of the Valentiner equation gave a constant ΔC_p^0 of -252 ± 17 J K⁻¹ mol⁻¹. The thermodynamic parameters follow the usual trends with temperature (discussed more fully in Chapter 6) of decreasing ΔH^0 and increasing negative ΔS^0 . The strong ordering of H₂O molecules around the ions at elevated temperatures is reflected in the large negative entropy change for the ionization reaction. Thus the Gibbs energy change becomes more positive even though ΔH^0 is decreasing, because of the large contribution of the negative $T\Delta S^0$ term. At 276.6 °C $\Delta H^0=0$ and $\log K_W^0$ is at a maximum of -11.13. Considering the shallow nature of the curve at the turning point, this is in good agreement with the extrapolated values of 280 °C and -11.09 as determined by MBO.

In a recent calorimetric study up to 150 °C Olofsson and Olofsson⁹¹ presented empirical equations describing ΔC_p^0 , ΔH^0 and K_W^0 as a function of temperature at 101.325 kPa. These equations were well suited for extrapolation purposes and the results agreed well up to 225 °C with SMB's results recalculated to 101.325 kPa. Discrepancies at the highest temperatures were thought to arise from errors in SMB's EMF measurements. It is interesting to note that at 200 °C SMB's pK_W^0 is 0.02 units higher, rising to 0.3 units at 300 °C. This further supports the view that SMB pK_W' 's are too high at temperatures of 200 °C and above. Olofsson and Olofsson found the temperature maximum to occur at 269 °C, which perhaps fortuitously, is in good agreement with the value derived from equation 3.31.

A comparison between the thermodynamic parameters derived by SMB, Olofsson and Olofsson and those derived from this work is shown in Table 4.8. It is evident that the simple assumption of a constant ΔC_p^0 does not lead to very significant differences between the thermodynamic parameters found in this work and those of the other studies, where a more realistic quadratic type function was used to express the temperature dependence of the heat capacity.⁹² The values at 25 °C differ slightly but the agreement is still reasonable considering the extrapolation involved. Thus the derived functions found in this study, although of limited use for extrapolation purposes are likely to give reliable interpolated results between 75 and 225 °C.

TABLE 4.8

Comparison of the Thermodynamic Parameters for the Ionization of Water at 25, 75 and 225°C.

Reference	ΔG^0 (kJ mol ⁻¹)	ΔH^0 (kJ mol ⁻¹)	ΔS^0 (J K ⁻¹ mol ⁻¹)
t=25 °C			
This Work*	80.9 ± 0.3	63 ± 2	-59 ± 6
Olofsson & Olofsson	79.87	55.82	-80.7
Sweeton Mesmer Baes	79.87 ± 0.04	55.81 ± 0.10	-80.7 ± 0.4
t=75 °C			
This Work	84.89 ± 0.09	51 ± 1	-98 ± 3
Olofsson & Olofsson	84.71	46.48	-109.8
Sweeton Mesmer Baes	84.71 ± 0.05	46.29 ± 0.24	-110.3 ± 0.8
t=225 °C			
This Work	106.8 ± 0.1	13 ± 2	-188 ± 3
Olofsson & Olofsson*, ⁺	106.9	13.5	-187
Sweeton Mesmer Baes	107.02 ± 0.11	8.5 ± 1.5	-198 ± 3

* extrapolated

⁺ pressure of 101.325 kPa; the correction at 225 °C is less than 0.02 log units.

4.7 RECOMMENDED VALUES FOR THE IONIZATION CONSTANT OF WATER.

Olofsson and Hepler⁸⁸ selected SMB's study as the "best" available because of the good correspondence with the calorimetry-based results between 0 and 150 °C and also with the values based on extrapolation to 300 °C. The agreement at the lower temperatures is no doubt partly due to the inclusion by SMB of the best low temperature literature results.

Later work by Olofsson and Olofsson⁹¹ suggests that SMB's results may be in error at the highest temperatures. Marshall and Franck gave no reason for using SMB's results in evaluating the IAPS equation other than they believed the measurements to be the most accurate. SMB's results to 300 °C are reasonably consistent with the studies at higher temperatures and pressures. Their results agree very well with Fisher's measurements, which were obtained by a non EMF technique. This gives some weight to the overall reliability of their final tabulated values. Nevertheless, there is good correspondence between the ionization constants derived in most of the different studies. Thus the results of this work, which are listed in Table 4.2, are equally valid in representing, within the experimental uncertainties of 0.02 log units, the ionization products between 75 and 225 °C. Over the temperature range 0-300°C the IAPS equation is likely to give the best description of the ionization constant of water. Further work is required before all the inconsistencies and discrepancies above 250 °C are fully explained.

Chapter 5

CALIBRATION OF SODIUM TETRABORATE BUFFERS

5.1 INTRODUCTION.

Solutions of 0.01 mol kg^{-1} and 0.05 mol kg^{-1} sodium tetraborate (borax : $\text{Na}_2\text{B}_4\text{O}_7 \cdot 10\text{H}_2\text{O}$) are well established as primary and secondary standard buffers. These buffers have been calibrated at temperatures between 0 and 95°C on a conventional scale by Bates⁵⁴ and co-workers and the derived pH values have been accepted internationally by IUPAC (ref. 93 and references therein). There is however a real need for calibrated pH standards at temperatures greater than 100°C so that experiments that require a known pH, such as corrosion or geochemical solubility studies, can be more readily undertaken.

In a recent study Manning⁴¹ (employing silver/silver chloride and hydrogen electrodes and using methods similar to that used by Bates) calibrated potassium tetraoxalate, potassium hydrogen tartrate and potassium hydrogen phthalate buffers at various temperatures between 100 and 200°C . Manning's study specifically excluded borax because of the excessive reduction of AgCl by hydrogen which occurs at high pH. Borax solutions are thermally stable, which makes them suitable for high temperature standards and are not reduced under a hydrogen atmosphere. Thus the high temperature hydrogen electrode pH concentration cell was well suited for the direct calibration of the borax buffers.

5.2 PREVIOUS WORK.

There have been relatively few studies attempting the high temperature calibration of borax buffers. The earliest high temperature (up to 250 °C) pH calibration study was that undertaken by Le Peintre⁹⁴ in 1960. Le Peintre employed a hydrogen electrode concentration cell to measure the pH of hydrochloric acid solutions as well as of the tartrate, phosphate, acetate and 0.01 mol kg⁻¹ borate buffers. However Le Peintre stated that the reliability of his results was limited by the leakage of solution between the cell compartments. Chaudon⁹⁵ used a hydrogen electrode concentration cell, of similar design to that employed by Le Peintre, to measure the pH values of boric acid/lithium hydroxide solutions up to 300 °C. The results given by Chaudon are not directly comparable to the values derived in this work. However in an introductory section Chaudon listed the pH values of 0.01 mol kg⁻¹ sodium tetraborate solution between temperatures of 25 and 300 °C. It is not clear where these values originated from or how they were derived. Further discussion of these results will be given in Section 5.5. Kryukov⁹⁶ et al. calibrated, between 25 and 150 °C, the 0.01 mol kg⁻¹ borax as well as the tetraoxalate and phthalate buffers using a concentration cell with transport employing hydrogen electrodes or glass and hydrogen electrodes. Perkovets and Kryukov⁹⁷ measured the pH values of these same buffers in NaCl media up to 150 °C but used hydrogen and silver/silver chloride electrodes without liquid junction.

The only other study above 150 °C is that by Mesmer Baes and Sweeton^{98,99} (MBS) who studied boric acid hydrolysis using the pH cell in conjunction with a titration technique. From their results Seward¹⁰⁰ calculated the pH of borate solutions varying in boron concentration from 0.1 to 0.6 mol kg⁻¹ up to 350 °C and determined the first ionization constant of silicic acid from quartz solubility in such

solutions. This previous data is discussed below in detail, in conjunction with the present work.

Sodium tetraborate at a concentration of 0.05 mol kg^{-1} has been designated by IUPAC⁹³ as an operational standard and the pH values up to 95°C have been assigned by comparison with the pH values of the primary standard 0.05 mol kg^{-1} potassium hydrogen phthalate in cells with liquid junction. The liquid junction potential is not corrected for and is thus incorporated into the operational pH measurement. The effect this may have on the derived pH values is shown for 0.01 mol kg^{-1} sodium tetraborate solution which has been calibrated as a primary reference standard (i.e. on a conventional scale in cells without transference) as well as an operational reference standard. The operational pH values at 80 , 90 and 95°C are higher than the primary reference values by 0.03 , 0.05 and 0.06 units respectively. As the 0.05 mol kg^{-1} sodium tetraborate solution does not match the 0.05 mol kg^{-1} potassium hydrogen phthalate as well as the 0.01 mol kg^{-1} sodium tetraborate in terms of composition and ionic strength, it is likely that the liquid junction potential at 0.05 mol kg^{-1} forms a more significant component of the assigned pH's. Thus the values derived in this work cannot be directly compared to the operational pH values of the borax solutions. There appears to be no other direct determinations of pH between temperatures of 75 to 250°C of the 0.05 mol kg^{-1} sodium tetraborate solution.

5.3 RESULTS.

The pOH values were smoothed using the four term Clark-Glew equation at a reference temperature (θ) of 423.15 K (Section 3.2.3, page 39). Although the Valentiner equation gave fits with comparable standard deviations, the resulting residual deviation plots, especially for the 0.05 mol kg^{-1} sodium tetraborate solutions, showed definite sinusoidal

character, indicating unsatisfactory fits of the data (Sections 3.2 and 3.3, pages 38 and 41). The pOH values for 0.01 and 0.05 mol kg⁻¹ borax solutions as a function of ionic strength are listed in Table 5.1 and 5.2. These values were calculated using the Bates-Guggenheim convention ($B\alpha=1.5$) in the calculation of the chloride ion activity coefficient. The ionic strength was calculated assuming that each mole of Na₂B₄O₇ furnished 2Na⁺ and 2OH⁻ ions. Sodium chloride was added to bring the ionic strength up to the required value.

Table 5.3 gives the same range of pOH values calculated using the NaCl activity coefficient data given by Liu and Lindsay.⁵⁵ These values are plotted as a function of ionic strength in Figures 5.1 and 5.2. The pOH values calculated using the NaCl activity coefficient data were derived from the $-\log m_{\text{OH}^-}$ values given in Table B.3 of Appendix B. These hydroxide concentrations were calculated from the smoothed pOH values found using the Bates-Guggenheim convention.

The infinite dilution pOH values and the values at the ionic strength of the buffer, assuming both the Bates-Guggenheim convention and NaCl activity coefficient data, are listed in Table 5.4 and 5.5 for 0.01 and 0.05 mol kg⁻¹ sodium tetraborate solutions respectively. These were found from the simultaneous straight line extrapolation of all the data to zero ionic strength. The primary experimental results are listed and plotted in Appendix B.

TABLE 5.1

pOH Values of 0.01 mol kg⁻¹ Sodium Tetraborate Solution as a Function of Ionic Strength at Various Temperatures.

t/°C	I = 0.11	0.32	0.52
75	3.865 ± 0.003	3.930 ± 0.005	3.992 ± 0.005
100	3.485 ± 0.002	3.559 ± 0.004	3.614 ± 0.003
125	3.182 ± 0.002	3.262 ± 0.004	3.314 ± 0.003
150	2.944 ± 0.001	3.029 ± 0.003	3.079 ± 0.003
175	2.759 ± 0.001	2.848 ± 0.003	2.897 ± 0.003
200	2.620 ± 0.002	2.713 ± 0.004	2.760 ± 0.003
225	2.519 ± 0.002	2.616 ± 0.003	2.661 ± 0.003
250	2.451 ± 0.003	2.554 ± 0.005	2.595 ± 0.004
n	73	72	72
s _f	0.003	0.006	0.006

TABLE 5.2

pOH Values of 0.05 mol kg⁻¹ Sodium Tetraborate Solution as a Function of Ionic Strength and Temperature.

t/°C	I = 0.10	0.31	0.51
75	3.730 ± 0.002	3.856 ± 0.002	3.917 ± 0.002
100	3.363 ± 0.002	3.495 ± 0.002	3.554 ± 0.002
125	3.051 ± 0.002	3.190 ± 0.002	3.251 ± 0.002
150	2.790 ± 0.001	2.936 ± 0.002	3.000 ± 0.001
175	2.575 ± 0.002	2.728 ± 0.002	2.797 ± 0.001
200	2.403 ± 0.002	2.563 ± 0.002	2.635 ± 0.002
225	2.271 ± 0.002	2.437 ± 0.002	2.510 ± 0.001
250	2.174 ± 0.003	2.345 ± 0.002	2.418 ± 0.003
n	71	69	68
s _f	0.003	0.003	0.003

TABLE 5.3

pOH Values Using NaCl Activity Coefficients, as a Function of Ionic Strength at Various Temperatures.

0.01 mol kg⁻¹ Sodium Tetraborate

t/°C, I=0.11	0.32	0.52
75	3.864	3.921
100	3.482	3.549
125	3.180	3.254
150	2.943	3.023
175	2.761	2.847
200	2.624	2.717
225	2.526	2.627
250	2.462	2.572

0.05 mol kg⁻¹ Sodium Tetraborate

t/°C, I=0.10	0.31	0.51
75	3.730	3.847
100	3.362	3.485
125	3.050	3.181
150	2.790	2.930
175	2.578	2.727
200	2.409	2.567
225	2.280	2.446
250	2.187	2.361

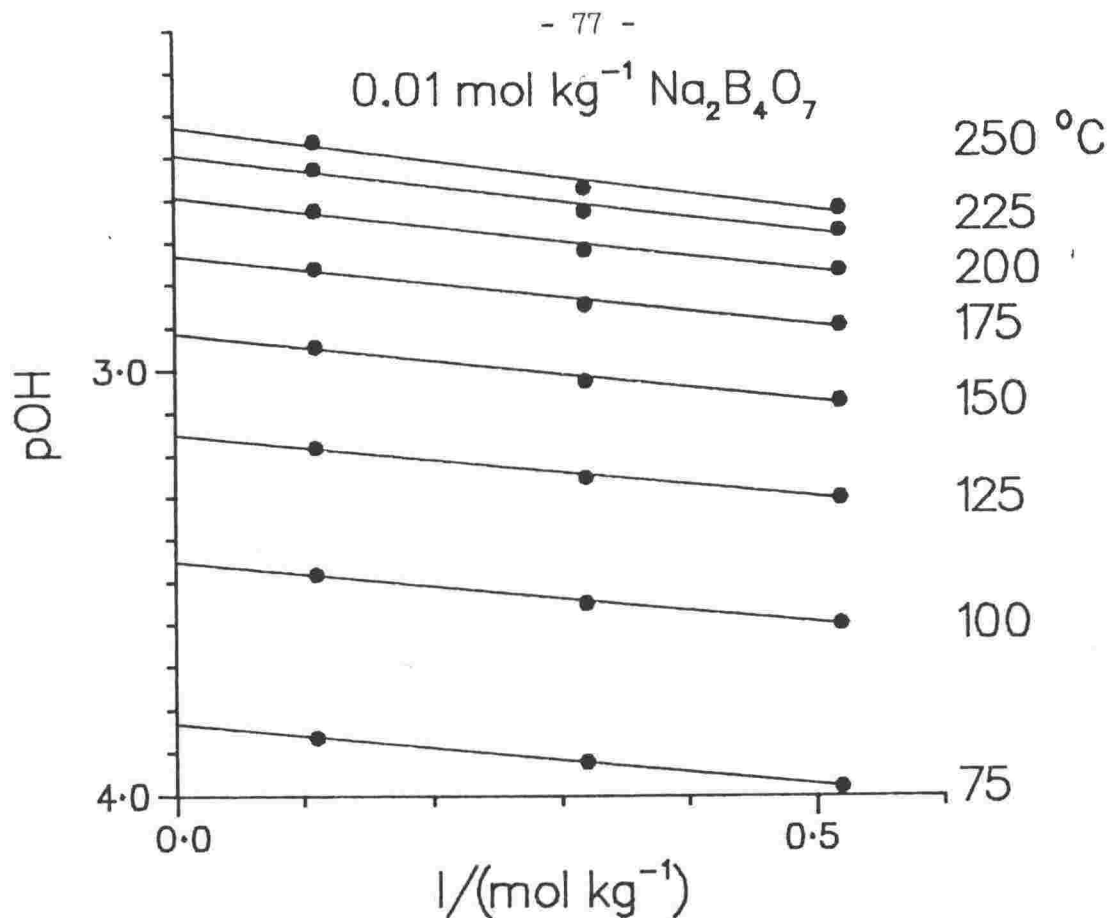


Figure 5.1: The Variation of pOH of 0.01 mol kg^{-1} Sodium Tetraborate Solution with Ionic Strength at Various Temperatures.

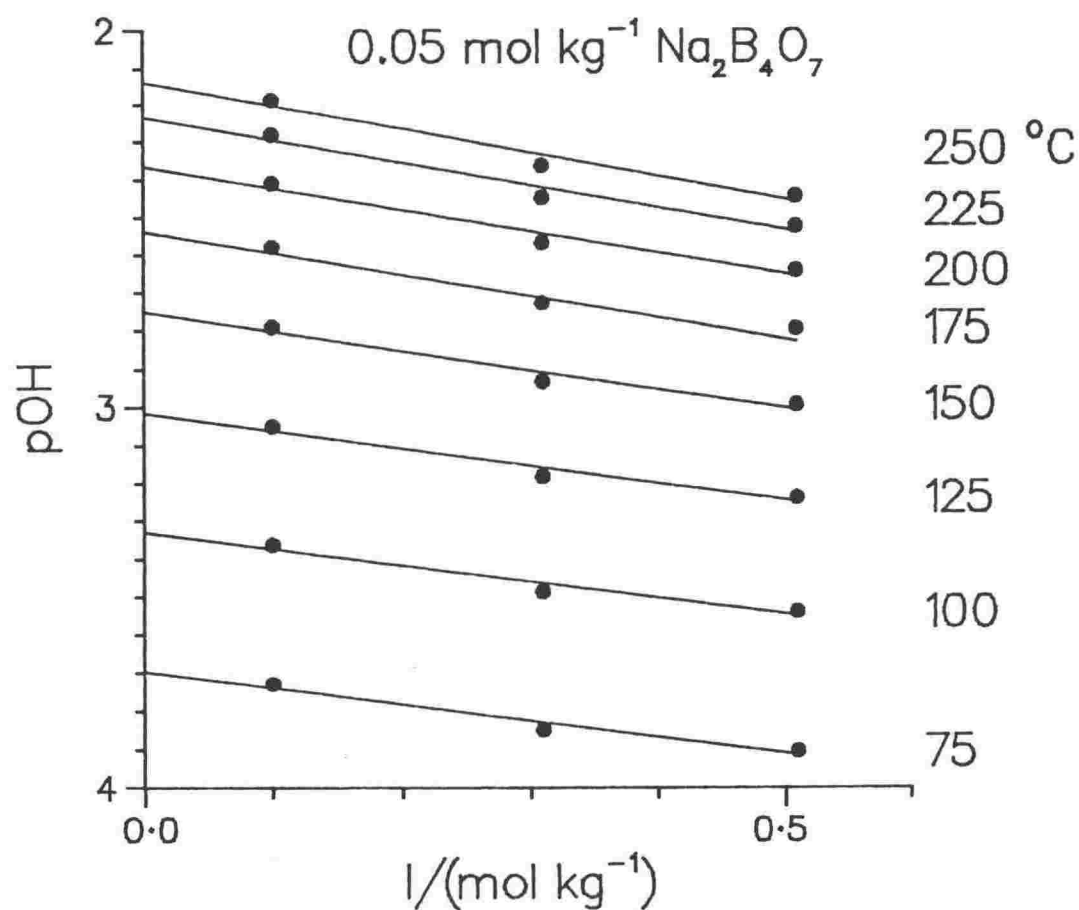


Figure 5.2: The Variation of pOH of 0.05 mol kg^{-1} Sodium Tetraborate Solution with Ionic Strength at Various Temperatures.

TABLE 5.4

Extrapolated pOH Values Calculated Using the Bates-Guggenheim Convention.

Sodium Tetraborate				
0.01 mol kg ⁻¹			0.05 mol kg ⁻¹	
t/°C	I = 0	0.02	0	0.1
25*	4.9 ± 0.1	4.9 ± 0.1	4.6 ± 0.2	4.7 ± 0.1
75	3.831 ± 0.011	3.837 ± 0.010	3.695 ± 0.018	3.740 ± 0.014
100	3.453 ± 0.007	3.459 ± 0.007	3.327 ± 0.013	3.374 ± 0.010
125	3.151 ± 0.007	3.157 ± 0.007	3.013 ± 0.013	3.062 ± 0.010
150	2.912 ± 0.006	2.919 ± 0.006	2.750 ± 0.011	2.801 ± 0.008
175	2.727 ± 0.006	2.734 ± 0.006	2.533 ± 0.012	2.587 ± 0.009
200	2.588 ± 0.007	2.595 ± 0.006	2.359 ± 0.012	2.416 ± 0.009
225	2.489 ± 0.006	2.496 ± 0.006	2.226 ± 0.012	2.285 ± 0.009
250	2.425 ± 0.011	2.432 ± 0.010	2.129 ± 0.019	2.190 ± 0.014
n = 216, s _f = 0.010			n = 207, s _f = 0.019	

*extrapolated

TABLE 5.5

Extrapolated pOH Values Calculated Using The NaCl Activity Coefficient Data.

Sodium Tetraborate				
0.01 mol kg ⁻¹			0.05 mol kg ⁻¹	
t/°C	I = 0	0.02	0	0.1
25*	4.9	4.9	4.6	4.7
75	3.833	3.838	3.697	3.739
100	3.453	3.459	3.329	3.372
125	3.152	3.157	3.016	3.062
150	2.914	2.920	2.753	2.803
175	2.731	2.737	2.537	2.592
200	2.593	2.600	2.365	2.423
225	2.494	2.502	2.233	2.294
250	2.429	2.437	2.139	2.201

*extrapolated

5.3.1 Activity Coefficients.

The pOH's listed are conventional in that the values involve a single ion activity. In this study the chloride ion activity coefficient was assumed to be equal to that of the hydroxide ion because of the lack of suitable estimates for the latter and so that a direct comparison could be made with pOH values derived by Seward. The activity coefficients were calculated using the Bates-Guggenheim convention or equated to the NaCl activity coefficients experimentally determined by Liu and Lindsay. The Bates-Guggenheim convention is applicable at ionic strengths of 0.1 or less and thus the NaCl activity coefficients were considered less

arbitrary and more appropriate in representing activity coefficient behaviour at elevated temperatures and at the relatively high ionic strengths used in this study. However the differences between the two sets of results is small. The maximum difference in the pOH at 250 °C and at $I=0.5$ is only 0.03 units and the extrapolated values are almost the same (Tables 5.4 and 5.5).

5.4 ERRORS.

The errors given in Tables 5.1, 5.2 and 5.4 are the 99% confidence intervals derived from the least squares analysis. The errors of the values calculated using the NaCl coefficient data in Tables 5.3 and 5.5 are comparable to those errors listed in Tables 5.1, 5.2, and 5.4 since both sets of data were derived from the same measured hydroxide ion concentration.

The potentials and errors corresponding to the values listed in Tables 5.1 and 5.2 are shown in Table 5.6. The measured potentials range from 5 to 120 mV with calculated errors, corresponding to the confidence intervals, between 0.1 and 0.5 mV. The decreasing magnitude of the potentials with temperature results in the final pOH values becoming more sensitive to uncertainties in the limiting molar conductivities of the ions which are used in calculating the liquid junction potentials. This is particularly so for 0.05 mol kg^{-1} sodium tetraborate solutions where a significant portion of the uncertainty in the liquid junction potential arises from the unknown variation with temperature of the molar conductances of the borate species. The conductivities of these species were equated to the molar conductivity of the chloride ion. For this assumption (see Section 5.5.5) a large uncertainty of 10% was used in calculating the estimated error.

The various contributions to the calculated experimental error at $I=0.11$ in 0.01 mol kg^{-1} sodium tetraborate solution are shown in Table 5.7, while Table 5.8 gives the calculated experimental error for both solutions at various ionic strengths at 75 and 250 °C. The estimated error is thus of the order of 0.02 and 0.05 log units for the 0.01 and 0.05 mol kg^{-1} sodium tetraborate solutions respectively. The small random errors of 0.001-0.005 log units shown in Tables 5.1 and 5.2 reflect the good internal consistency of the results. The larger error on the extrapolated values in Table 5.4, particularly for the 0.05 mol kg^{-1} sodium tetraborate solution, gives an indication of the non linearity of the pOH values as a function of ionic strength (Figures 5.1 and 5.2).

TABLE 5.6

Potentials (mV) and Calculated Errors of the Sodium Tetraborate Solutions as a Function of Ionic Strength at 75° and 250°C.

0.01 mol kg^{-1} Sodium Tetraborate

$t/^{\circ}\text{C}$	$I = 0.11$	0.32	0.52
75	-115.92 ± 0.21	-120.04 ± 0.35	-123.46 ± 0.35
250	-22.99 ± 0.30	-26.56 ± 0.51	-26.66 ± 0.41

0.05 mol kg^{-1} Sodium Tetraborate

$t/^{\circ}\text{C}$	$I = 0.10$	0.31	0.51
75	-105.30 ± 0.14	-114.84 ± 0.14	-118.04 ± 0.14
250	5.19 ± 0.19	-4.89 ± 0.20	-8.26 ± 0.31

TABLE 5.7

Contributions to the Final Error in pOH of 0.01 mol kg⁻¹ Sodium Tetraborate at I=0.11 and at 75°C.

0.01 mol kg⁻¹ Sodium Tetraborate

Temperature	75 °C	± 0.3 °C	0.001
Potential	-115.92 mV	± 0.1 mV	0.001
Junction Potential	4.28 mV	± 17%	0.011
Reference m _{OH⁻}	0.01	± 0.25%	0.001
Activity Coefficient	0.125	± 2%	0.002
Total Error			----- 0.016 log units

TABLE 5.8

Estimated Errors in pOH as a Function of Ionic Strength at 75° and 250°C.

0.01 mol kg⁻¹ Sodium Tetraborate

t/°C	I = 0.11	0.32	0.52
75	3.865 ± 0.016	3.930 ± 0.011	3.992 ± 0.011
250	2.451 ± 0.014	2.554 ± 0.011	2.595 ± 0.011

0.05 mol kg⁻¹ Sodium Tetraborate

t/°C	I = 0.10	0.31	0.51
75	3.730 ± 0.065	3.856 ± 0.027	3.917 ± 0.020
250	2.174 ± 0.055	2.345 ± 0.024	2.418 ± 0.019

5.5 DISCUSSION AND COMPARISON WITH OTHER WORK.

The previously published results and the results of this work are listed in Table 5.9 and smoothed curves are plotted in Figures 5.3 and 5.4. The results for this study were obtained by combining the pK_W^O results (extrapolated from $I=1.0$) found earlier and the pOH values at the ionic strength of the buffer listed in Table 5.5 (i.e. the pOH values derived using the NaCl activity coefficient data). The error (listed in Table 5.9) is a combination of the random error in both the pK_W^O and pOH values. The IAPS pK_W^O value at 250 °C (11.191) was used to convert the pOH to the corresponding pH because this temperature is outside the temperature range of the experimentally determined pK_W^O 's. Similarly in Table 5.9 Seward's recalculated pOH values have been converted to the corresponding pH values using the ionization constants of water found in this study, except at 250 °C where the IAPS value was used. Thus the errors in the pK_W values, which contribute a major portion of the uncertainty in the calculated pH's, are also incorporated in Seward's results. Equations for the smoothed pH values are given in Table B.4.

5.5.1 0.01 mol kg⁻¹ Sodium Tetraborate Solution.

The pH values given by Chaudon and those values recalculated by Seward from MBS's results are consistent with this work where a minimum in pH was found to occur between 175 and 200 °C. This trend is inconsistent with the other studies. Le Peintre's pH values progressively decrease to 250 °C and Kryukov et al., and Perkovets and Kryukov's results are linear over their experimental temperature range of 100-150 °C. Although this does not exclude a minimum occurring at higher temperatures, the linear trend observed in the latter two studies appears to be in better accord with Le Peintre's results. However the effect of the environmental conditions (high pH and hydrogen atmosphere), which are

TABLE 5.9

Literature Results for the Temperature Dependence of the pH of Sodium Tetraborate Buffers.

t /°C =	25	75	100	125	150	175	200	225	250
0.01 mol kg ⁻¹ Sodium Tetraborate									
Bates ⁵⁴	9.18	8.90	8.82*	-	-	-	-	-	-
Chaudon ⁹⁵	9.18	-	8.85	-	8.73	-	8.72	-	8.80
Kryukov ⁹⁶ <u>et al.</u>	9.16	-	8.81	8.73	8.66	-	-		
Le Peintre ⁹⁴	9.22 ⁺	-	8.22 [#]	8.75	8.65	8.60	8.56	8.53	8.50
Perkovets and Kryukov ⁹⁷	9.18	-	8.84	8.77	8.68	-	-	-	-
Seward's recalculations ¹⁰⁰		8.954	8.855	8.797	8.767	8.754	8.754	8.765	8.831
This Work		8.899	8.799	8.737	8.701	8.687	8.686	8.694	8.754
	±	0.024	0.014	0.014	0.013	0.014	0.014	0.019	0.030
0.05 mol kg ⁻¹ Sodium Tetraborate									
Seward's recalculations		8.971	8.859	8.797	8.773	8.774	8.793	8.821	8.902
This Work		8.998	8.886	8.833	8.819	8.830	8.865	8.902	8.990
	±	0.028	0.017	0.017	0.015	0.016	0.017	0.022	0.034

* extrapolated

⁺ at 20 °C

[#] an interpolated pH value of 8.83 was derived using Le Peintre's results. Thus the value of 8.22 is most likely a misprint for 8.82.

particularly severe for both glass and silver/silver chloride electrodes, are unknown at the elevated temperatures and this may account for their results.

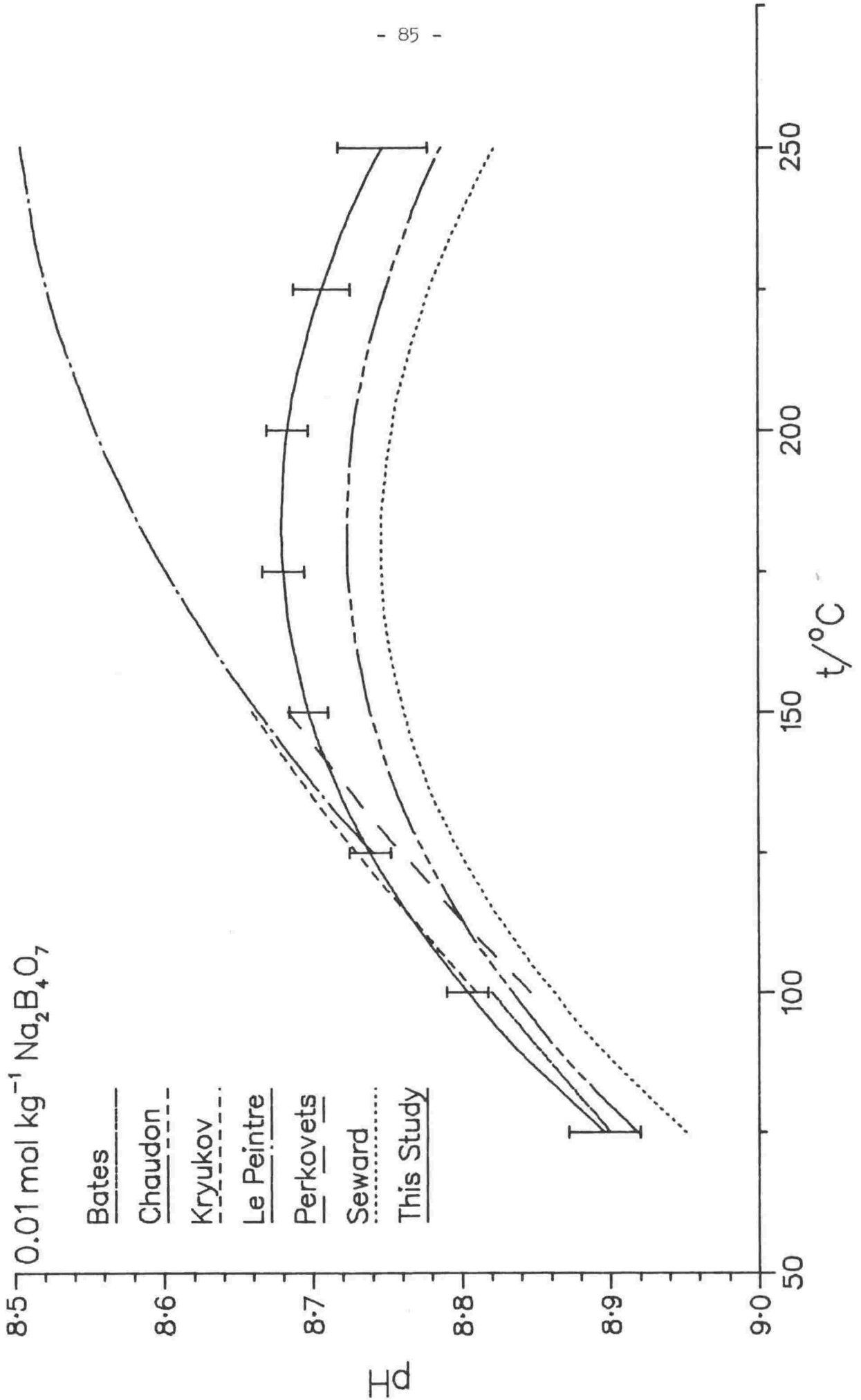


Figure 5.3: Literature Results for the Variation in pH of 0.01 mol kg⁻¹ Sodium Tetraborate Solution with Temperature.

5.5.1.1 Between 75 and 150 °C

The results agree well with the other work at temperatures up to 150 °C. The values determined by Perkovets and Kryukov and Bates in cells without liquid junction, are offset to higher pH's with respect to the other studies (excluding Seward's recalculations). This deviation may have been caused by malfunction of the silver/silver chloride electrodes. However, the smallness of the shift (<0.03 units) and the lack of other studies precludes any definite conclusion. Le Peintre's results agree well with this work at temperatures less than 125 °C. His value of 8.22 at 100 °C is inconsistent with all the other literature values and may simply be a misprint*, although this cannot be checked as no experimental results or smoothing equations are given in their paper.

Chaudon's pH values are all higher than the values derived in this work. The agreement between the two sets of results becomes better with decreasing temperature. As previously indicated there is some confusion as to how the values listed by Chaudon were derived. If the same procedures were followed as described in the section on pH measurements of the boric acid/lithium hydroxide solutions, then it is likely that the reference solution was 0.01 mol kg^{-1} hydrochloric acid. It appears that the pH values of the reference solution were taken from Greeley^{81,101,102} et al., who determined the thermodynamic properties of hydrochloric acid with a cell containing hydrogen and silver/silver chloride electrodes. Thus these values may be suspect due to the malfunction of the silver/silver chloride electrode under a hydrogen atmosphere and in the presence of chloride media. There was no inert electrolyte added to either of the cell solutions and the compartments were connected via a salt bridge containing saturated (at 25 °C) KCl

* Most likely for 8.82.

solution. This would have minimized the liquid junction potential but was probably not as effective as forming the liquid junction between the same principal electrolyte. Thus, it is considered that more reliable results were derived in this study, by extrapolating the pH values against ionic strength to the ionic strength of the buffer.

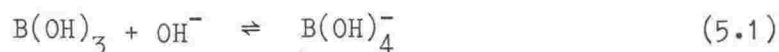
5.5.1.2 Between 150 and 250 °C

Le Peintre's pH values decrease to a pH of 8.5 at 250 °C. These results are not considered reliable above 150 °C because of the problems he experienced in suppressing leakage between the cell compartments. Moreover this trend was not observed by Chaudon who employed a cell based on Le Peintre's design. Le Peintre estimated the error in his data to be between 0.02 and 0.05 units at 200 °C, however the maximum error was set at 0.1 units because of the experimental difficulties. This error is quite large considering that the change in pH, indicated by the results of this work, is only of the order of 0.2 units between temperatures of 75 and 250 °C. Chaudon's values are uniformly higher by about 0.04 pH units between temperatures of 150 and 200 °C. This may have been caused by diffusion of the bridge solution into the cell compartments. However the lack of a detailed experimental section and analysis of (in particular) these results, makes any further comparison impossible.

As the only other values above 150 °C are those of MBS as recalculated by Seward, their experimental and data reduction methods will be briefly detailed so that a better comparison can be made with the results found in this study.

5.5.2 Mesmer, Baes and Sweeton's Study.

MBS used the static hydrogen electrode pH cell to study the hydrolysis of dilute boric acid as a function of KCl concentration from 0.13 to 1.0 mol kg⁻¹ at 50 degree intervals from 50 to 290 °C. The concentration of boric acid was about 0.02 mol kg⁻¹, so that the interference from polyborates could be considered negligible and the initial boric acid to KOH ratio was set at 2:1. The first dissociation quotient of the reaction



was calculated from the known stoichiometric concentration of boron and the initial and the measured hydroxide ion concentrations. Extrapolation to zero ionic strength gave the thermodynamic parameters for B(OH)_4^- at infinite dilution.

To investigate polyborate species formation, titration experiments were conducted at boron concentrations up to 0.6 mol kg⁻¹ in 1 mol kg⁻¹ KCl solution and at 50, 100 and 200°C. A ligand number, defined as the average number of bound hydroxides per boron atom, was calculated from the known stoichiometries. An extensive linear least squares analysis was then undertaken where numerous schemes of possible species that could be formed were tested until there was a satisfactory agreement between the calculated and experimentally determined ligand numbers. The formation of three polyborates : $\text{B}_2(\text{OH})_7^-$, $\text{B}_3(\text{OH})_{10}^-$ and $\text{B}_4(\text{OH})_{14}^{2-}$ (as well as the mononuclear species) best accounts for MBS's results. The concentrations of all three polyborates decrease with temperature and the dimer is formed in minor amounts at low temperatures. The divalent polyborate was found to be least significant and was only needed to explain the data at 50 °C. Thermodynamic parameters were derived for all the species in 1 mol kg⁻¹ KCl.

Preliminary results were reported by MBS at the 32nd International Water Conference (1971)⁹⁸ where expressions, incorporating an ionic strength function for the temperature dependence of the equilibrium quotients, were presented. The same ionic strength dependence, which was experimentally determined only for the first equilibrium quotient, was assumed for all the equilibria even though the polyborate equilibrium quotients were measured in 1 mol kg⁻¹ KCl. MBS subsequently published⁹⁹ a full account of their work; however, the ionic strength functions were eliminated⁺ from the equilibrium expressions for the polyborate species.

Seward¹⁰⁰ used the equilibrium expressions as originally reported by MBS (i.e. those incorporating the ionic strength functions) to calculate, at ionic strengths of $B_T/2^*$, the hydroxide ion concentrations of borax solutions, at boron concentrations up to 0.6 mol kg⁻¹ and to 350 °C. The method used was a Newton-Raphson iterative solution of two equations involving a mass and charge balance of all the species reported by MBS. The pOH's were found by adding the activity coefficients of the chloride ion (as determined by Liu and Lindsay) to the calculated hydroxide ion concentration at the ionic strength of the buffer.

5.5.3 Comparison with Mesmer, Baes and Sweeton's Results, as Calculated by Seward.

The pH's of the 0.05 mol kg⁻¹ sodium tetraborate solution derived in this work are higher by about 0.1 to 0.2 pH units between temperatures of 75 and 250 °C than those derived for the 0.01 mol kg⁻¹ solution. In

⁺ The ionic strength was set to unity.

^{*} B_T is the total boron concentration and thus a 0.01 mol kg⁻¹ sodium tetraborate solution has an ionic strength of 0.02.

contrast, the pH's of 0.04 and 0.2 mol kg⁻¹ borate solutions calculated by Seward differ insignificantly (<0.02 pH units) between temperatures of 75 and 175 °C. At 250 °C the pH of the 0.2 mol kg⁻¹ solution is about 0.1 pH units higher than that of 0.04 mol kg⁻¹ solution.

Seward's calculations show that for 0.01 mol kg⁻¹ sodium tetraborate ($B_T=0.04$), MBS's pH's are all higher than the literature results. At 75 and 250 °C MBS's values are higher by 0.06 and 0.08 units respectively than found in this study. However the general shape of the curves and the pH minimum at about 188 °C are in very good agreement. The agreement with 0.05 mol kg⁻¹ borax solution is reasonable up to 125 °C. Seward's values then progressively deviate to lower pH's reaching a maximum difference of 0.1 units at 250 °C as shown in Figure 5.4. Thus these results show that at a boron concentration of 0.04 mol kg⁻¹, greater hydrolysis of boric acid occurs, while at 0.2 mol kg⁻¹ boron less occurs than is indicated by Seward's calculation of MBS's results.

Neither MBS's work nor Seward's calculations took into account the formation of KOH ion pairs or ion pairing between potassium and borate ions. Borax dissolves to give the borate species and hydroxide ions in equilibrium amounts. If the lower pH's (i.e higher pOH's) of the 0.01 mol kg⁻¹ sodium tetraborate solutions found in this study are a result of the increased tendency for sodium to ion pair over potassium, then it would be expected that slightly lower pH's would be observed in 0.05 mol kg⁻¹ sodium tetraborate. The pH's found are in fact higher than those calculated by Seward.

For this study the reference compartment contained NaCl and NaOH in approximately the same concentrations as in the borax solutions. The formation of NaOH ion pairs, and hence the reduction in concentration of the hydroxide ions, would be expected to occur to similar extents in both cell compartments. Thus formation of the NaOH ion pairs would not

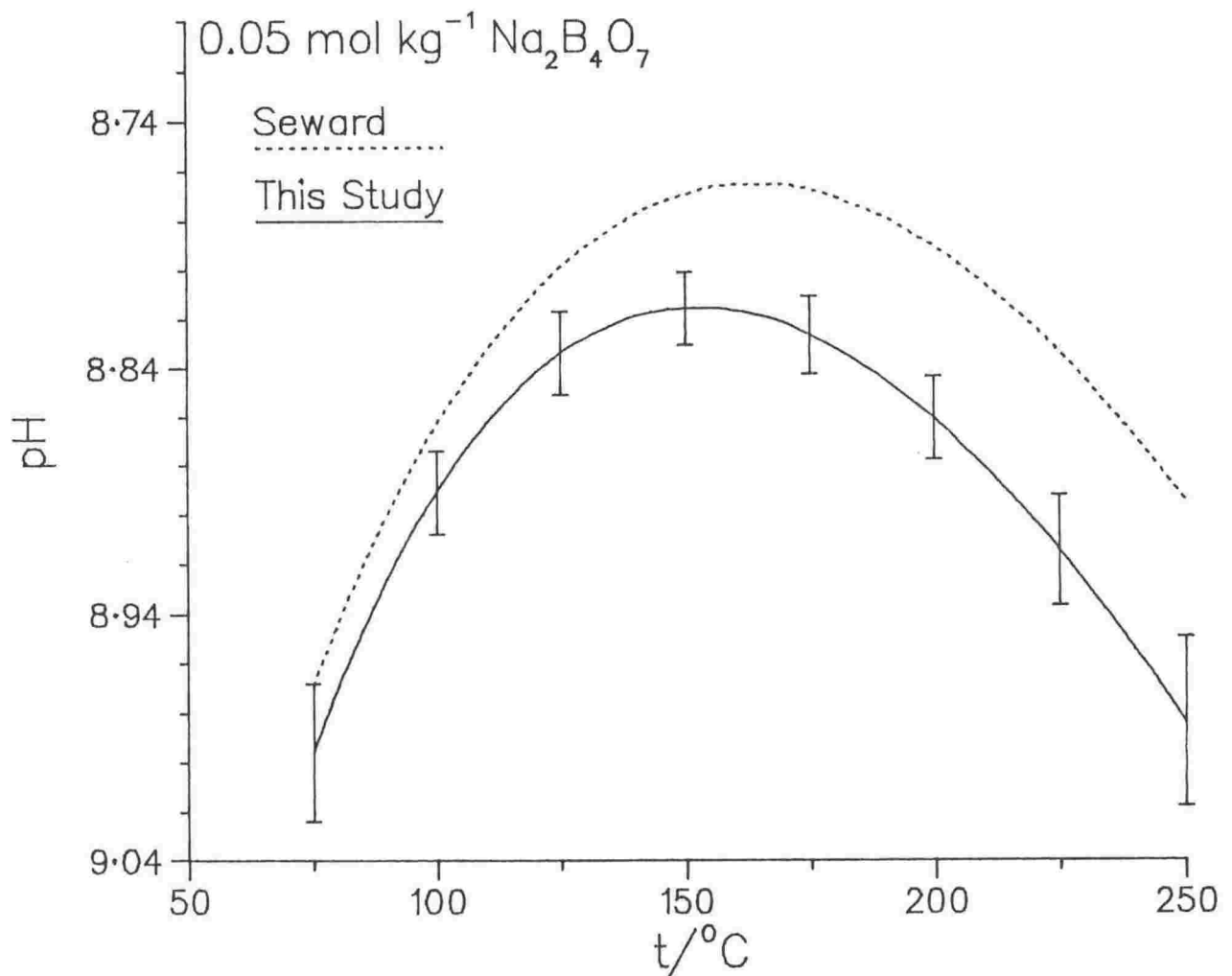


Figure 5.4: The Variation in pH of 0.05 mol kg⁻¹ Sodium Tetraborate as Found in This Study and From Swards Calculations.

introduce significant error in the final calculated pOH's. The formation of ion pairs between sodium and borate species would be expected to show up in the plots of pOH as a function of ionic strength as deviations from linearity and also as changes in slope with increasing temperature. In figures 5.1 and 5.2 it is evident that there is almost no change in slope as the temperature is increased from 75 to 250 °C in both 0.01 and 0.05 mol kg⁻¹ borax solutions. Similarly there is good linearity up to 0.5 mol kg⁻¹ NaCl at all temperatures, allowing accurate extrapolation to infinite dilution. These results support the

view that ion pairing between sodium and the relatively large borate and polyborate species does not occur to any appreciable extent. Similar behaviour with potassium-borate species would be expected. Thus the differences between these and MBS's results are not easily explained through a difference in the tendency of potassium and sodium ions to form ion pairs.

The extent of polyborate formation in 0.01 mol kg^{-1} sodium tetraborate solution would be small, particularly at the higher temperatures. Thus the almost uniform shift of Seward's values over the whole temperature range suggests that MBS's determination of the first equilibrium quotient is in doubt. However this explanation is untenable because the first equilibrium quotients derived in this study agree well with MBS's results (see Section 5.5.4). The greater discrepancies in pH between the two studies for the 0.05 mol kg^{-1} sodium tetraborate solution, may indicate that the polyborate equilibrium quotients are in error.

The data found in this study were obtained with minimal numerical manipulation when compared to the computations of MBS and subsequent back calculation by Seward to find pOH's. No doubt, part of the discrepancy arises because of the extensive numerical processing involved. Discrepancies would also arise because of MBS's assumption that the same ionic strength dependence holds for the polyborate equilibrium quotients as found for the first dissociation equilibrium quotient. In this study the good internal consistency of the results, the linearity of pOH against ionic strength and the good correspondence with lower temperature literature results gives some confidence that the final pH's obtained are indeed reliable.

5.5.4 Boric Acid Dissociation.

It is interesting to compare values of the first equilibrium constant of boric acid (K_b) calculated in this study with the values derived by Chaudon and MBS. In the former two studies, where the boron concentration was about 0.04 and 0.09 mol kg⁻¹ respectively, no account was taken of the formation of the polyborate species. MBS's experiments were conducted at a boron concentration of 0.02 mol kg⁻¹ so that the interference from polyborates could be considered negligible. Chaudon derived his values from pH measurements of boric acid and lithium hydroxide solutions (1000 ppm and 3 ppm respectively) at ionic strengths of 0.1 and 0.015. Values of ^{the first dissociation constant of Boric acid} pH were generated from an analytical equation given by Chaudon and were then converted to the equilibrium constants of the neutralization reaction (5.1) by combining with the pK_W^O values derived in this study, except at 250 °C where the IAPS value was used. The equilibrium quotients derived in this work (Table B.3) are linear and almost horizontal curves against ionic strength, as shown in Figure 5.5. MBS's results are also linear up to ionic strengths of 0.5. Thus the infinite dilution values were evaluated by linear extrapolation of the Q_b 's to zero ionic strength. The small dependence of the equilibrium quotient on ionic strength, which was also found by MBS, is attributable to the activity ratio $\gamma_{B(OH)_4^-}/\gamma_{OH^-}$ being near unity.

MBS estimated the error in $\log K_b$ to about 0.01 log units between temperatures of 50 and 290 °C. Chaudon did not state the precision of his results. The error is likely to be of the same magnitude as in this work, about 0.02 to 0.05 log units between temperatures of 75 and 250 °C.

If the first equilibrium reaction predominates at higher temperatures then it would be expected that the K_b values derived at different boron concentrations would converge with increasing

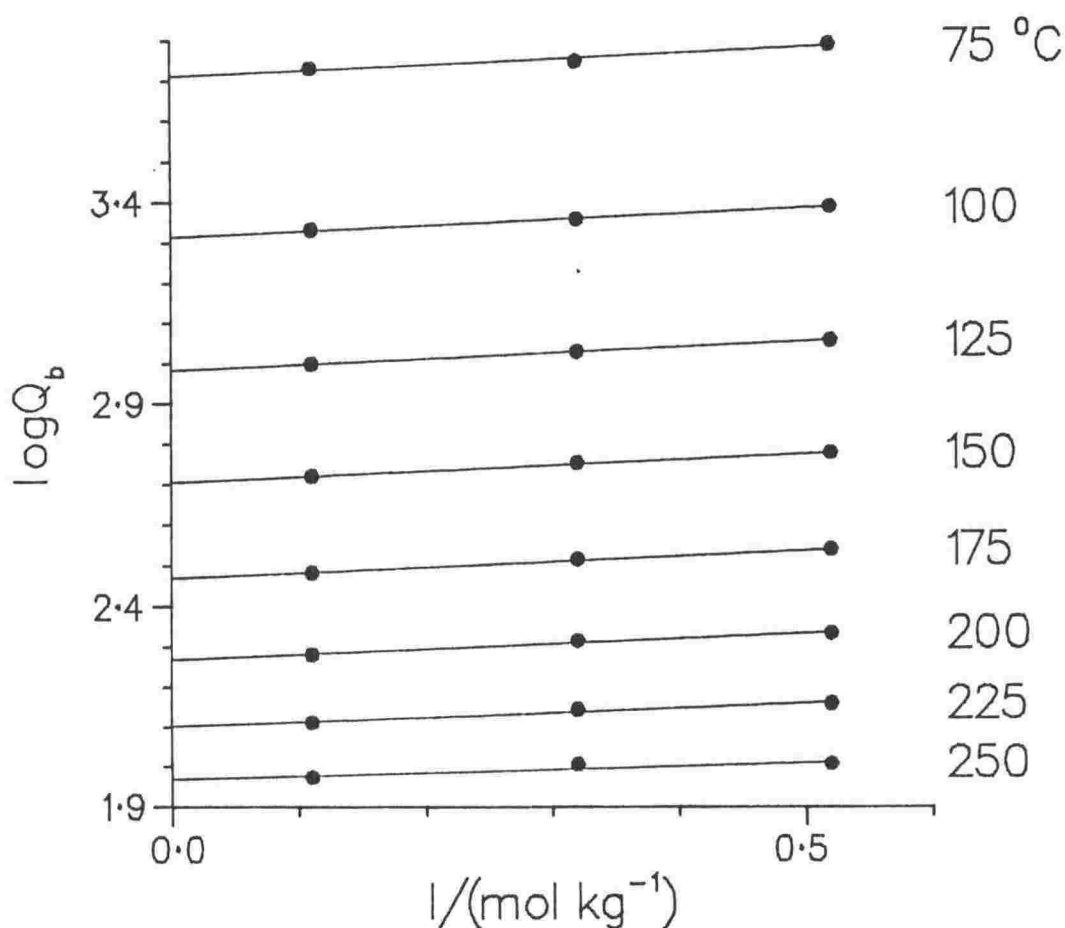


Figure 5.5: The Ionic Strength Dependence of $\log Q_b$ in 0.01 mol kg^{-1} Sodium Tetraborate Solution at Various Temperatures.

temperature, because of the decreasing polymerization. This trend is observed as shown in Table 5.10. The $\log K_b^0$ values derived in this work agree to 0.01 log units with MBS's results over the temperature range studied and also, at temperatures between 200 and 250 °C, with Chaudon's values. MBS found evidence for polyborate formation at boron concentrations greater than 0.03 mol kg^{-1} . However, these results suggest that the extent of polyborate formation is insignificant at a boron concentration of 0.04 mol kg^{-1} . Included in Table 5.10 are the $\log K_b^0$ values derived for the 0.05 mol kg^{-1} sodium tetraborate. It is expected that there would be significant polymer formation at this boron concentration (0.2 mol kg^{-1}) and the $\log K_b^0$ values are lower than those

TABLE 5.10

Temperature Dependence of the First Equilibrium Constant of Boric Acid.

		$\log K_b^0$							
$t / ^\circ\text{C} =$		75	100	125	150	175	200	225	250
MBS									
0.02 mol kg ⁻¹		3.71	3.31	2.98	2.70	2.46	2.27	2.11	1.98
This Work									
0.04 mol kg ⁻¹		3.71	3.32	2.99	2.71	2.47	2.27	2.10	1.97
This Work									
0.20 mol kg ⁻¹		3.59	3.21	2.88	2.60	2.36	2.15	1.98	1.84
Chaudon									
0.09 mol kg ⁻¹		3.95	3.49	3.11	2.78	2.51	2.28	2.09	1.97

derived for the 0.01 mol kg⁻¹ sodium tetraborate solution. From these and MBS's results it appears that as the concentrations of the polyborate species increase with increasing boron concentration, the derived $\log K_b^0$ values become lower. However at temperatures less than 200 °C Chaudon's results are inconsistent with this trend. At 75 °C Chaudon's $\log K_b^0$ value is about 0.25 log units higher than that derived by MBS and in this study. The experimental error at 75 °C is estimated to about 0.02 log units. Since the boron concentration used by Chaudon was about 0.09 mol kg⁻¹, it would be more reasonable to expect his $\log K_b^0$ values to lie between the values derived for the sodium tetraborate solutions at boron concentrations of 0.04 and 0.2 mol kg⁻¹. The reasons for the discrepancy at the lower temperatures is not clear. The good agreement of the $\log K_b^0$ values between temperatures of 200 and 250 °C, in contrast to the pH values of the 0.01 mol kg⁻¹ sodium tetraborate solution, places further doubt on the reliability of Chaudon's results.

5.5.5 Assumptions Made in Deriving the pOH Values.

There were two major assumptions made in deriving the pOH values in this study. Firstly that only monovalent hydrolysis species were formed and secondly that the limiting molar conductivities of these species could be equated to the molar conductivity of the chloride ion. The first assumption is reasonable as MBS only needed to invoke the divalent species to obtain the best fit of the data at 50 °C. This species was found to form in minor amounts and was not uniquely defined. Thus the ionic strength remains virtually constant throughout the whole temperature range. The second assumption was necessary because of the lack of molar conductivity data for the borate species (or of like ions) over the temperature range studied.

An estimate of the molar conductivity of the $\text{B}(\text{OH})_4^-$ ion at 25 °C may be derived by assuming that this ion is a member of the homologous series : ClO_4^- , MnO_4^- , ReO_4^- and IO_4^- . The conductances of these species^{57,103} appear to increase linearly with decreasing covalent radius of the central atom. Extrapolating to the covalent radius of the boron atom gives a value of $75 \text{ S cm}^2 \text{ mol}^{-1}$ for the conductivity of the orthoborate ion. This value compares favourably with the conductivity of the chloride ion which is $76 \text{ S cm}^2 \text{ mol}^{-1}$ at 25 °C. Data given by Robinson and Stokes⁵⁷ suggests that the conductivities of the polyborate species may be of the order of 40 to $60 \text{ S cm}^2 \text{ mol}^{-1}$ at 25 °C. The orthoborate ion is the predominant species in solution and the conductivity of this ion (at 25 °C) appears to be similar in magnitude to that of the chloride ion. Thus a 10% error was considered to be a reasonable estimate of the uncertainty in the assumption that the conductivity of the borate species could be equated to the conductivity of the chloride ion.

The extent of hydrolysis decreases with increasing temperature. At 75 °C where the concentration of the polyborate species is expected to be high, the measured potentials were of the order of 100-120 mV (see Table 5.6 and B.4) and the calculated liquid junction potentials varied from 0.1 to 4 mV. Thus not knowing the exact molar conductivity of the borate and polyborate species will make very little difference to the calculated pOH.

TABLE 5.11

Changes in pOH Caused by a 10% Variation in the Calculated Molar Conductivity of the Chloride Ion at 250°C.

$$\lambda^0 / (\text{S cm}^2 \text{ mol}^{-1})$$

Borax Concentration (mol kg ⁻¹), I=0.1	430	478	525
0.01	2.459	2.451	2.444
0.05	2.226	2.174	2.127

At higher temperatures the pOH is substantially controlled by the first equilibrium reaction. Table 5.11 gives the change in pOH caused by a 10% variation in the calculated molar conductivities of the borate ion (i.e. chloride ion) at 250 °C and at an ionic strength of 0.1, where the liquid junction potentials are not effectively suppressed. The total effect in 0.01 mol kg⁻¹ sodium tetraborate is small and thus the uncertainty in the molar conductivity cannot account for the discrepancy between Seward's recalculations and this work. The situation in the 0.05 mol kg⁻¹ sodium tetraborate experiments at I=0.1 was different in

that the solutions did not contain NaCl (whereas the reference compartment contained about 0.1 mol kg^{-1} NaCl, 0.01 mol kg^{-1} NaOH) and the measured potentials at 250°C were the same order of magnitude as the calculated liquid junction potentials. Thus a 10% variation in the molar conductivity, results in a pH change of about 0.05 units. A pOH value of 2.190 ± 0.014 at $I=0.1$ and 250°C was derived (Table 5.4) from a simultaneous fit and extrapolation of all the data between ionic strengths of 0.1 to 0.5. This compares with a value of 2.174 ± 0.003 (Table 5.2) found from a fit of the data at $I=0.1$. Thus the value at 0.1 is reasonably consistent, assuming a linear relationship, with the pOH's found at the higher ionic strengths. The minimum uncertainty in pOH at 250°C of the 0.05 mol kg^{-1} borax solution is thus likely to be at least 0.05 units. Furthermore it is likely that the molar conductivity of the chloride ion is higher than that of any of the borate species. Thus the pH values derived using more reliable molar conductivity data would be lower and hence closer to Seward's calculated values.

MBS made the same assumption in equating the borate conductivities to those of the chloride ion. This results in little error in 0.01 mol kg^{-1} sodium tetraborate solutions. At higher boron concentrations their experiments were conducted in 1 mol kg^{-1} KCl where the liquid junction potential was adequately suppressed. Nevertheless a major part of the discrepancy between these and MBS's results for the 0.05 mol kg^{-1} sodium tetraborate solution, particularly at the higher temperatures, may be assigned to the unknown variation with temperature of the molar conductivities of the borate species.

5.6 RECOMMENDED pH VALUES FOR THE SODIUM TETRABORATE BUFFERS.

5.6.1 0.01 mol kg⁻¹ Sodium Tetraborate Solution.

5.6.1.1 Between 75 and 150 °C.

The data of Bates (up to 95 °C), Kryukov et al., and Le Peintre* are consistent and in good agreement with the results of this study up to temperatures of 125 °C. Above 125 °C the rate of change with temperature of the pH values derived in this work, of the values given by Chaudon and also of those values calculated by Seward from MBS's results, is less than in the other studies, where there is an apparent linear decrease in pH. Although the absolute differences are small (<0.04 pH units) up to 150 °C, the pH values in this study are considered more reliable because of the susceptibility to chemical attack of the glass and the silver/silver chloride electrodes which were employed in the other studies.

5.6.1.2 Between 150 and 250 °C.

Le peintre's and Chaudon's studies are the only other direct experimental determinations of pH above 150 °C. The results of this work, Chaudon's values and Seward's recalculations place the pH values derived by Le Peintre in some doubt. Experimental problems experienced by Le Peintre may account for the discrepancy. There is good agreement with Chaudon's results except that the values were presented in passing without any detailed explanation or analysis. The agreement with Seward's values is reasonable considering the assumptions involved in deriving the pH's from MBS's results. Thus the pH's of 0.01 mol kg⁻¹ sodium tetraborate solution determined in this study, between temperatures of 75 and 250 °C, are considered to be the most reliable that have yet been reported.

* Assuming the 100 °C pH value is 8.82.

5.6.2 0.05 mol kg⁻¹ Sodium Tetraborate Solution.

The only direct determination of pH between 75 and 250 °C is that reported in this work. Thus the lack of other experimental studies makes a valid assessment of the reliability of these values difficult. The pH's are consistent with those calculated by Seward from MBS's results. Although the uncertainty in the liquid junction potential at the highest temperatures gives rise to an uncertainty of 0.05-0.08 pH units, it is considered that the experimentally determined values are preferred because of the assumptions involved in Seward's calculations.

Chapter 6

SECOND DISSOCIATION CONSTANT OF SULPHURIC ACID

6.1 INTRODUCTION.

Experimentally, the determination of the second dissociation constant of sulphuric acid at temperatures between 75 and 225 °C was found to be unusually difficult. The reproducibility in initial experiments appeared to be very poor. It was soon apparent that a stable potential was being reached only very slowly, after some 2-3 hours at 75 °C. Presaturation of the solutions with hydrogen had no observable effect but the rate of attainment of equilibrium was found to be critically dependent on having well prepared platinum electrodes (Section 2.3.1, page 17). The present results are in reasonable agreement with previous work up to 150 °C, however a deviation from linearity was observed at higher temperatures. This trend has not been observed in previous studies.

6.2 PREVIOUS WORK.

There have been numerous²¹⁻²⁴ investigations of the second dissociation constant of sulphuric acid at 25 °C. However considering the importance of this electrolyte there have been relatively few studies at elevated temperatures. Hamer¹⁰⁴ employed a cell with hydrogen and silver/silver chloride electrodes, containing sodium sulphate and bisulphate solutions, to measure ionization constants between temperatures of 0 and 60 °C. Davies¹⁰⁵ et al. used this same cell with solutions of

~~sulphuric acid to evaluate ionization constants between 25 and 50 °C~~

Both these studies have been extensively reanalysed.¹⁰⁶ Young, Singleterry and Klotz²² have recently described their earlier⁷⁷ spectrophotometric measurements up to 55 °C using the indicator methyl orange. Lietzke, Stoughton and Young⁶¹ evaluated the equilibrium constant from the solubility of AgSO_4 in sulphuric acid solutions up to 225 °C and similarly Marshall and Jones⁶² from the solubility of calcium sulphate in sulphuric acid up to 350 °C. Ryzhenko¹⁰⁷ calculated dissociation constants from conductivity measurements on potassium bisulphate solutions at 100, 156 and 218 °C. Quist, Marshall and Jolley¹⁰⁸ and Quist and Marshall¹⁰⁹ determined the second dissociation constants at 100 and 200 °C from the electrical conductance of sulphuric acid and potassium bisulphate solutions respectively. Pavlyuk, Smolyakov and Kryukov¹¹⁰ determined equilibrium constants between 25 and 175 °C using a spectrophotometric method with 2,6-dinitrophenol as indicator. Schöön and Wannholt¹¹¹ used a glass electrode with an external calomel electrode (kept at 23 °C) to measure dissociation quotients as a function of ionic strength up to 150 °C. Their study is of limited use as there were no experimental or smoothed data given, nor any line fitting equations. The method used to derive pK_2^0 's from the graphical representation given by Schöön and Wannholt is described below in Section 6.5.1.

6.3 RESULTS.

The data up to 150 °C was smoothed satisfactorily using the three term Clark-Glew equation (CG3) at a reference temperature of 373.15 K. Over the whole temperature range considerably better fits were obtained using the four term Clark-Glew (CG4)* equation at a reference temperature of

* The CG3 equation is formulated (Section 3.2.3, page 40) assuming a ΔC_p which is constant with temperature, while assuming a linear dependence

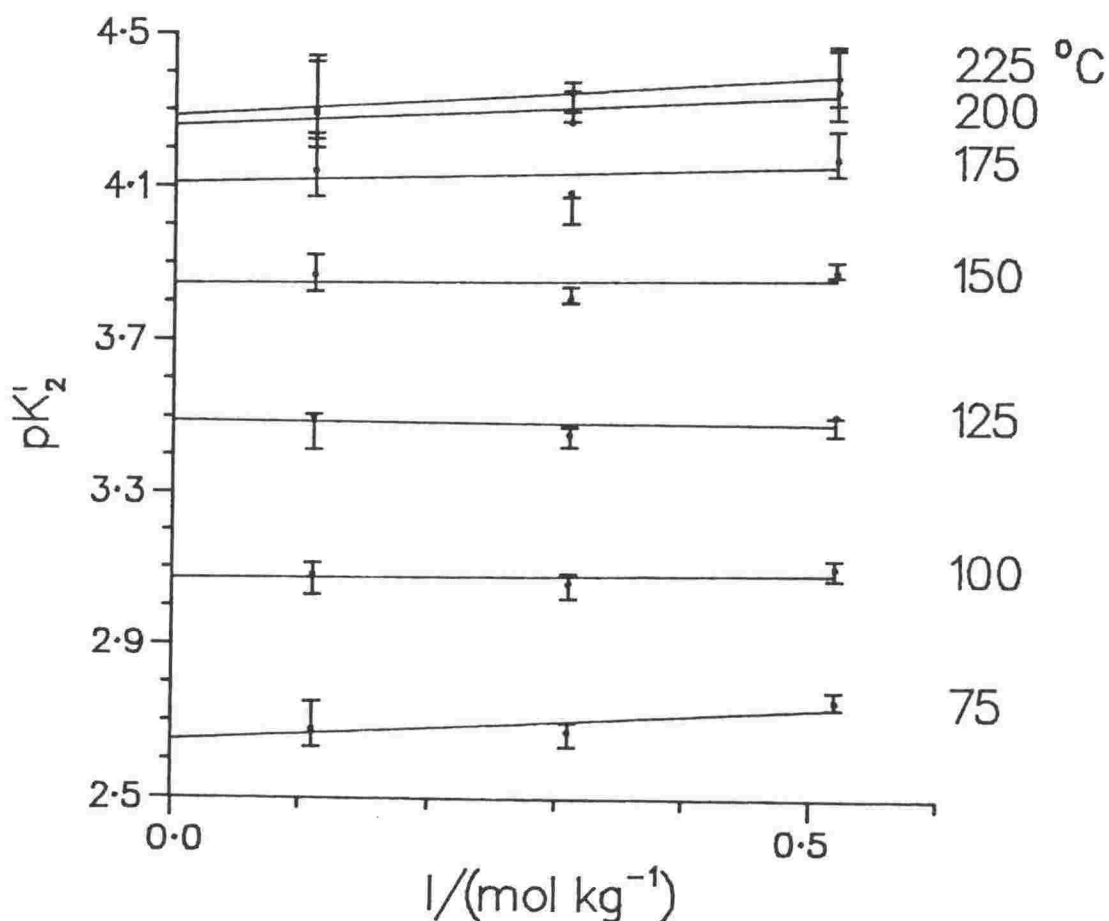


Figure 6.1: The Variation of pK'_2 as a Function of Ionic Strength at Various Temperatures, CG4 Equation to 225°C.

423.15 K. The smoothed dissociation constants as a function of ionic strength found using the CG4 equation up to 225 °C are plotted in Figure 6.1 and the numerical values are listed in Table 6.1. The error bars drawn in Figure 6.1 give the maximal deviation (i.e. the spread) of the dissociation constants about the fitted values at each ionic strength and temperature. The infinite dilution values and derived thermodynamic parameters found from the simultaneous linear extrapolation of all the

with temperature results in the CG4 equation. The CG3 and Valentiner equation are equivalent in that double differentiation of the latter equation with respect to temperature gives a ΔC_p independent of temperature.

TABLE 6.1

pK'_2 Values as a Function of Ionic Strength and Temperature, CG4 Equation.

	$t/^{\circ}\text{C}$ I = 0.11	0.31	0.52
75	2.678 ± 0.038	2.673 ± 0.028	2.753 ± 0.050
100	3.083 ± 0.027	3.063 ± 0.021	3.104 ± 0.034
125	3.501 ± 0.026	3.457 ± 0.019	3.507 ± 0.033
150	3.869 ± 0.024	3.809 ± 0.017	3.883 ± 0.026
175	4.143 ± 0.028	4.089 ± 0.020	4.178 ± 0.024
200	4.294 ± 0.026	4.275 ± 0.019	4.356 ± 0.022
225	4.305 ± 0.048	4.353 ± 0.028	4.393 ± 0.033
n	74	63	62
s_f	0.050	0.033	0.046

data to zero ionic strength are listed in Table 6.2. The CG3 and CG4 equations reproduce the experimental data within the estimated uncertainties to temperatures of 150°C . Thus the smoothed results derived using the CG3 equation are presented in Appendix C, Figure C.1 and Tables C.2 and C.3. The various terms contributing to the calculated dissociation constants are listed in Table C.1 and the experimental data in 0.1, 0.3 and 0.5 mol kg^{-1} KCl are also listed and plotted in Appendix C.

For all ionic strengths scatter in the experimental EMF data and hence in the derived dissociation constants, is marked at temperatures above 150°C . Solutions were not presaturated with hydrogen gas, with the exception in experiments at $I=0.11$ up to 150°C . Thus a very slight change in concentration, due to a small amount of water loss, may

TABLE 6.2

Thermodynamic Values for the Dissociation of the Bisulphate Ion, CG4
Equation To 225°C.

t/°C	pK ₂ ⁰	ΔG ⁰ (kJ mol ⁻¹)	ΔC _p ⁰ (J K ⁻¹ mol ⁻¹)	ΔH ⁰ (kJ mol ⁻¹)	ΔS ⁰ (J K ⁻¹ mol ⁻¹)
75	2.65 ± 0.05	17.7 ± 0.3	-451 ± 304	-38 ± 8	-159 ± 23
100	3.07 ± 0.03	22.0 ± 0.2	-199 ± 198	-46 ± 3	-181 ± 8
125	3.49 ± 0.03	26.6 ± 0.3	53 ± 100	-48 ± 3	-186 ± 7
150	3.85 ± 0.03	31.2 ± 0.2	305 ± 67	-43 ± 3	-175 ± 8
175	4.11 ± 0.03	35.3 ± 0.3	557 ± 151	-32 ± 3	-151 ± 6
200	4.26 ± 0.03	38.6 ± 0.3	810 ± 255	-15 ± 6	-114 ± 12
225	4.29 ± 0.05	40.9 ± 0.5	1062 ± 362	8 ± 13	-66 ± 27

n = 199, s_f = 0.049

account for the increased scatter and the higher standard deviation of the fit at I=0.11, when compared to the fits at higher ionic strength. The standard deviations of the fits over the whole temperature range are high because of the biasing effect of the scattered points above 150 °C.

6.4 ERRORS.

The errors given in Tables 6.1 and 6.2 are the 99% confidence intervals derived from the least squares analysis. The calculated potentials and errors corresponding to the smoothed values listed in Tables 6.1 and C.2 are listed in Table 6.3. The errors at 75 and 225 °C derived by combining all the estimated systematic errors are listed in Table 6.4. The magnitudes of these various contributions to the error at I=0.11 and at 225 °C are listed in Table 6.5.

TABLE 6.3

Calculated Potentials (mV) and Errors in pK'_2 as a Function of Ionic Strength at 75°, 150° and 225°C.

t/°C I =			
0.11			
0.31			
0.52			
CG3 Equation			
75	-7.140 ± 0.231	-10.340 ± 0.159	-11.004 ± 0.162
150	-1.083 ± 0.102	-3.078 ± 0.112	-3.552 ± 0.112
CG4 Equation			
75	-7.157 ± 0.314	-10.312 ± 0.262	-10.937 ± 0.480
225	-0.690 ± 0.114	-1.982 ± 0.119	-2.590 ± 0.117

TABLE 6.4

Estimated Errors in pK'_2 as a Function of Ionic Strength at 75°, 150°, and 225°C.

t/°C I =			
0.11			
0.31			
0.52			
CG3 Equation			
75	2.680 ± 0.040	2.670 ± 0.033	2.746 ± 0.032
150	3.911 ± 0.037	3.823 ± 0.038	3.892 ± 0.038
CG4 Equation			
75	2.678 ± 0.039	2.673 ± 0.033	2.753 ± 0.032
225	4.305 ± 0.077	4.353 ± 0.053	4.393 ± 0.048

TABLE 6.5

Contributions to the Final Error in pK_2' at $I=0.11$ and at 225°C .

Temperature	225 $^\circ\text{C}$	± 0.3 $^\circ\text{C}$	<0.001
Potential	-0.69 mV	± 0.1 mV	0.001
Junction Potential	0.55 mV	$\pm 10\%$	0.020
m_{H^+} (reference)	0.01	$\pm 0.25\%$	0.001
$m_{\text{H}_2\text{SO}_4}$	0.01	$\pm 0.25\%$	0.038
Activity Coefficient	0.813	$\pm 2\%$	0.016
Total Error			----- 0.077 log units

A large contribution to the total error in pK_2' is the uncertainty in the sulphuric acid concentration. This is because the concentrations of sulphate and bisulphate ions are calculated from the very small difference between the measured hydrogen ion concentration (Section 3.1.1, page 28) and that expected with no hydrolysis. Thus analytical errors in the sulphuric acid concentration as well as errors in the EMF (which gives the measured hydrogen ion concentration) will be magnified to large errors in the dissociation constants.¹¹³ However as the difference gets larger, for example with increasing ionic strength or with decreasing temperature, the errors decrease.

The value of the equilibrium constant depends critically upon the expression chosen for the product of the ionic activity coefficients. At 225°C the activity coefficient quotient ranges in value from about 0.5 to 1.3 between ionic strengths of 0.1 and 0.5. The errors involved in estimating the activity coefficient are not removed by the extrapolation to infinite dilution.¹¹³ Thus because this correction is so large when compared to the equilibrium quotient, a relatively small percentage change in the activity coefficient quotient gives rise to a

correspondingly large shift in the final extrapolated dissociation constants. This also accounts for a major part of the relatively large discrepancies^{24,112} in pK_2^0 of about 0.05 log units, between the literature results at 25°C (see Section 6.5.1 for further discussion). The 2% error in the activity coefficient quotient assumed in this work is only a conservative estimate and depending on the choice of the ion size parameter, could be high as high as 4%.

The measured potentials ranged in magnitude from 0.7 to 11 mV (Table 6.3) and the liquid junction potential (Table C.1) from 0.5 to 2 mV. In the water and borax systems the liquid junction correction was generally minor in comparison with the measured EMF and thus a large uncertainty in using the Henderson equation to estimate liquid junction potential had little effect on the precision of the final result. This is not the case in the present situation, particularly at the higher temperatures, where the measured potentials are of the same magnitude as the estimated liquid junction potentials. Furthermore large errors in the limiting molar conductivities, particularly at lower ionic strengths where the liquid junction potential is not sufficiently suppressed and forms a significant component of the measured potential, rapidly propagate to give large errors in the final dissociation constants. This is especially true in the case of the bisulphate ion*, for which there is a large uncertainty in the molar conductivity values. Nevertheless all the data is internally consistent and the experimental results given in the appendices may be easily recalculated if and when better estimates of molar conductivities and activity coefficient quotients become available.

* The dissociation of HSO_4^- severely limits the precision with which the conductance of this ion can be determined at temperatures < 300°C.

6.5 DISCUSSION.

6.5.1 Comparison with Other Work.

The results found in this work are compared with previous studies in Table 6.6 and in Figure 6.2. The dissociation constants found in the various studies show considerable divergences at elevated temperatures. These discrepancies are also a feature of room temperature data published by different workers. The major difficulty in obtaining

TABLE 6.6

Literature Results for the Temperature Dependence of the Dissociation Constant of the Bisulphate Ion, pK_2^0 .

t/°C	25	75	100	125	150	175	200	225
Lietzke Stoughton Young - Solubilities ⁶¹	1.891	2.699	3.010	3.334	3.688	4.087	4.489	4.941
Lietzke Stoughton Young - Fitted	1.987	2.636	2.987	3.352	3.728	4.113	4.506	4.905
Marshall Jones ⁶²	1.988	2.539	2.855	3.189	3.534	3.887	4.246	4.608
Pavlyuk Smolyakov ¹¹⁰ Kryukov	1.993	2.661	3.020	3.391	3.772	4.161	-	-
Quist Marshall ¹⁰⁹	-	-	3.18	-	-	-	4.60	-
Quist Marshall ¹⁰⁸ Jolley	-	-	3.08	-	-	-	4.03	-
Ryzhenko ¹⁰⁷	-	-	3.04	-	3.80	-	4.58	-
Schöön Wannholt ¹¹¹	2.00	2.70	3.08	3.44	3.79	-	-	-
This Work (up to 150 °C)	1.9*	2.653	3.066	3.480	3.893	4.3*	4.7*	5.1*
This Work (up to 225 °C)	2.1*	2.649	3.073	3.489	3.846	4.111	4.262	4.286

* extrapolated

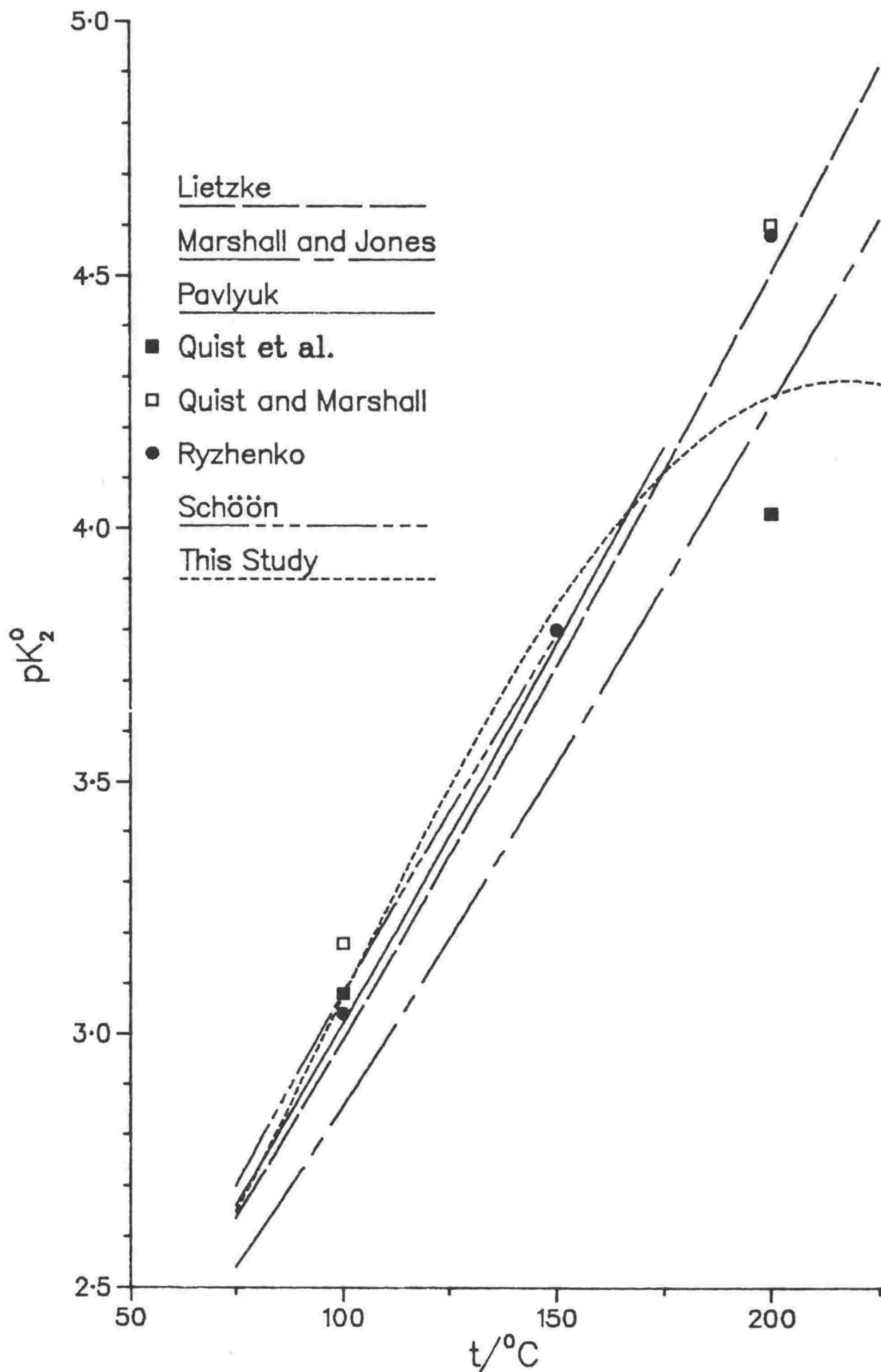


Figure 6.2: Literature Results for the Variation of the Dissociation Constant of the Bisulphate Ion with Temperature.

unequivocal thermodynamic ionization constants (where these are about 3 log units) appears to be due to the uncertainty in estimating the hydrogen ion molality from EMF measurements.^{106,113-115} This uncertainty, which is not removed by extrapolation to zero ionic strength, arises from the choice of the $B\theta$ parameter required to estimate the activity coefficients. Hamer¹¹⁶ reanalysed his earlier results¹⁰⁴ and concluded that pK_2^0 values derived using cell (I)



depended upon the choice of the ion-size parameter, while unexpectedly, those derived with sulphuric acid and sodium chloride solutions did not. However Covington^{106,114} et al. have recently shown that for all EMF methods, regardless of the cell solution used, the pK_2^0 values depend on the value chosen for the ion-size parameter in the Debye-Hückel formula. Furthermore new measurements by Covington¹⁰⁶ et al. using cell (I), which were in substantial agreement with their earlier¹¹⁴ determination using cell (II),



did not substantiate Hamer's original results. Since the activity term is different in the Nernst equation for each cell, it is not expected that concordant values of the ionization constant will be obtained for a given choice of the ion-size parameter. Covington¹⁰⁶ et al. using data obtained with Cell I at 25 °C, derived a pK_2^0 value of 1.95 ± 0.02 , where the uncertainty arises from the range of reasonable choices for the ion-size parameter. Their earlier analysis¹¹⁴ of previously published work showed that the pK_2^0 values calculated from EMF measurements at 25 °C could only be fixed between 1.94 and 2.01 because of the combined uncertainties of the choice of the ion-size parameter

and the extrapolation of results. Spectrophotometric methods are not superior to EMF methods in this regard because specific salt effects on the indicator cause uncertainties of similar magnitude to those arising in the analysis of EMF data.

The other difficulty in obtaining concordant pK_2^0 values may be due to the formation^{117,118} of metal-sulphate (MSO_4^-) ion pairs when ions like Na^+ , K^+ , Ag^+ and Ca^{2+} are present in solution. In a critical analysis of room temperature calorimetric data Cabani and Gianni¹¹² concluded that differences in the published data raised doubts about the importance of species such as $NaSO_4^-$. They suggested the need for more experimental information to establish whether such species are formed in solution. The possible formation of ion pairs is discussed below in Section 6.5.3.

Two sets of Lietzke's data are listed, values obtained from solubilities and values obtained from a temperature fit of that data. The authors did not estimate any errors but the deviation of 0.04 to 0.09 units between the two sets of results gives some indication of the uncertainty of their data. The latter set is the one that is plotted in Figure 6.2. Marshall and Jones's dissociation constants, which are also derived from solubility studies, were about 20% lower than Lietzke Stoughton and Young's results. Marshall and Jones estimated their error (3σ) to be no greater than about 0.05 log units and they could not adequately account for the large discrepancy. The conductivity results of Quist and Marshall and Quist, Marshall and Jolley are probably the least reliable as in both studies difficulties were encountered in determining the limiting molar conductivities of the SO_4^{2-} and HSO_4^- ions, which are needed to calculate the dissociation constants, due to the dissociation of the bisulphate ion. The errors (3σ) were estimated to be about 0.1 log units. The reproducibility of Quist, Marshall and Jolley's conductivity measurements on sulphuric acid was poor at

temperatures below 300 °C. They stated that corrosion of the fittings in their experimental equipment may have increased the overall error. Quist and Marshall considered their conductivity study on potassium bisulphate solutions, to be more reliable because of the better reproducibility obtained. The uncertainty in the pK_2^0 values derived by Ryzhenko from conductivity measurements on potassium bisulphate solutions are likely to be of the same order as those in the above conductivity studies. Ryzhenko's values listed in Table 6.6 are in molar units; however, the pK_2^0 values recalculated to molal units by Quist and Marshall are only 0.02 lower and 0.01 higher at 100 and 200 °C respectively.

The pK_2^0 values agree well with the spectrophotometric study of Pavlyuk, Smolyakov and Kryukov. Their experiments and numerical derivations were inherently simpler than the solubility and conductivity studies of Lietzke, Marshall, Quist and co-workers from the Oak Ridge National Laboratory. However Pavlyuk's method depends on knowing accurate ionization constants for the indicator 2,6-dinitrophenol. They estimated the errors to be between 0.01 and 0.02 log units.

Schöön and Wannholt published a graph (of small scale) consisting of smoothed lines representing the variation of the dissociation quotients with ionic strength between 0.25 and 3 mol dm⁻³ (NaCl) at temperatures from 75 to 150 °C. The maximum deviation from the mean values was stated to be about 0.05 log units. Dissociation quotients were read off their graph at ionic strengths of 0.25, 0.5 and 1 mol dm⁻³ NaCl and corrected for Debye-Hückel interactions using equation 3.29. The pK_2^0 values given in Table 6.6 were derived by linear extrapolation of the pK_2' values to zero ionic strength. These dissociation constants are strictly on the molar scale; however, adjustment of the values to the molal scale would entail only a minor correction because of the low hydrogen and sulphate ion concentrations used in their experiments. Schöön and Wannholt's

results agree well with the values derived in this work. The maximum difference of 0.1 in pK_2^0 at 150 °C represents a difference of about 0.001 log units between the hydrogen ion activities (assuming an analytical sulphuric acid concentration of 0.01 mol kg⁻¹). The good agreement is surprising and may be fortuitous because Schöön and Wannholt assumed, in using the Nernst equation, that the activity coefficient for the hydrogen ion is independent of the hydrogen ion concentration. They also assumed that any liquid junction potential and thermal effects between the salt bridge and the solution contained in the autoclave, were negligible and could be ignored.

It would be an advantage to adjust the published high temperature data to a common activity coefficient in an attempt to remove the discrepancies. This may still not result in more consistent values because of reasons previously discussed in relation to the low temperature data. However the major obstacle to recalculating the data is that values are often reported only at zero ionic strength, for example as in Pavlyuk's and Lietzke's study. This problem, coupled with complex mathematical procedures used in deriving the dissociation constants, as in the latter study, precludes an easy reanalysis of the data.

6.5.2 Trends of the Dissociation Constants with Temperature.

Extrapolation of the data to 225 °C from a fit of the data up to 150 °C using the CG3 equation, gives the same trends as found in all the other studies, i.e. progressively decreasing dissociation constants with no observed maximum or minimum. Plots of the experimental data in Figures C.1 to C.3 definitely show curvature above 150 °C. A consequence of the deviation from linearity is that the smoothed pK_2^0 values reach a maximum at about 217 °C, as shown in Figure 6.2. The calculated

TABLE 6.7

Sensitivity of pK'_2 to the Measured Hydrogen Ion Concentration in 0.10M KCl Solution.

	m_{H^+}	$m_{HSO_4^-}$	$m_{SO_4^{2-}}$	pK'_2	pQ_2
1) CG3 Equation, Extrapolated Values					
2) CG4 Equation					
$t = 200\ ^\circ C$					
1)	0.0100967	9.903×10^{-3}	9.699×10^{-5}	4.753	4.006
2)	0.0102693	9.731×10^{-3}	2.693×10^{-4}	4.294	3.546
$t = 225\ ^\circ C$					
1)	0.0100433	9.957×10^{-3}	4.325×10^{-5}	5.172	4.360
2)	0.0103032	9.697×10^{-3}	3.032×10^{-4}	4.305	3.492

dissociation constants are very sensitive to the measured hydrogen ion concentration. Table 6.7 shows the hydrogen ion concentration at $I=0.11$ needed to give the extrapolated dissociation constant predicted using the CG3 equation and that actually found using the CG4 equation (see also Table C.1). Thus at $225\ ^\circ C$ a very small shift of less than $0.0003\ \text{mol kg}^{-1}$ in the measured stoichiometric hydrogen ion concentration, changes the sulphate concentration by an order of magnitude and the calculated dissociation constant by 0.9 log units. The curvature above $150\ ^\circ C$ may be due to some unidentified systematic error, although this is unlikely in view of the good results obtained for the water and borax systems. Experimental failure may be eliminated as the probable cause since the curvature was observed at all ionic strengths and over a number of experimental runs. The difference of

about 0.01 log units between these calculated hydrogen ion concentrations is of the same order as the experimental error. Thus the magnification of the uncertainty, due to analytical errors in the sulphuric acid concentration and small errors in EMF discussed earlier, rather than any small unidentified systematic error, are likely to be of more significance in accounting for the non-linearity.

6.5.3 Ion Pair Formation.

One mechanism that may account for the observed curvature is the formation of KSO_4^- ion pairs. An upper limit for the molal dissociation constant of the KSO_4^- ion may be calculated from the results given in Table 6.7, if it is assumed that the extrapolated sulphate concentration calculated, using the CG3 equation, represents the lowest value of $m_{\text{SO}_4^{2-}}$ if no ion pair formation takes place. Thus the concentration of the ion pair is given by the difference in the hydrogen ion concentration found using the CG3 and CG4 equations. Table 6.8 shows the resulting concentrations of the various species at 200 °C. The calculated dissociation quotient is -1.25 log units and assuming the same activity coefficient term as for the bisulphate equilibrium, i.e. effectively a cancellation of the KSO_4^- and K^+ activity coefficients, a dissociation constant of -2.00 log units is obtained. The pK_2' values calculated before and after adjustment for ion pair formation are 4.29 and 4.74 log units respectively. Similarly a value for $\text{pK}_{\text{KSO}_4}'$ at 225 °C was calculated to be 2.6 log units.

The only high temperature KSO_4^- ion pair data available are the dissociation constants of this ion at 100 200 and 300°C* determined by Quist, Frank, Jolley and Marshall¹¹⁹ from the conductance of potassium

* The value at 300 °C was considered suspect by the authors.

TABLE 6.8

Calculation of the KSO_4^- Molal Ion Pair Dissociation Constant in
0.10 mol kg^{-1} KCl Solution and at 200°C.

m_{H^+}	0.0102693
m_{K^+}	0.099827
$m_{\text{KSO}_4^-}$	1.726×10^{-4}
$m_{\text{SO}_4^{2-}}$	9.669×10^{-5}
$m_{\text{HSO}_4^-}$	9.731×10^{-3}
pQ_2	4.00
pK_2'	4.74
$pQ_{\text{KSO}_4^-}$	1.25
pK_{KSO_4}'	2.00

sulphate solutions. The thermodynamic dissociation constants at 200 and 225 °C were estimated⁺ to be about -2 and -2.5 log units respectively. The agreement between these and the values calculated here, assuming that the dissociation constants are relatively independent of ionic strength, is quite remarkable but may be just fortuitous. The problem of not being able to estimate adequately the extent of sulphate hydrolysis limited the accuracy of the dissociation constants calculated from the conductivity data.

In the absence of suitable data, ion pair formation has been neglected in the analysis of this work as has been the case in all high temperature studies to date. A small amount of KSO_4^- ion pair formation may be disregarded as any ion association will be taken up by the term

⁺ Standard state molal dissociation constants were calculated by Helgeson¹²¹ from the results of Quist, Frank, Jolley and Marshall.¹¹⁹ The 225 °C value was extrapolated from data at temperatures up to 200 °C.

linear in ionic strength in the activity coefficient quotient expression^{114,120} (Eq. 3.29). The formation of ion pairs will affect the slope of the plots of pK_2' against I but not the extrapolated pK_2^0 values. The pK_2' values in Figure 6.1 (noting that these are smoothed points with large associated errors) show some curvature with ionic strength, suggesting more significant ion pair formation than in the room temperature results. To linearize these plots higher order terms would be necessary in the activity coefficient quotient expression.

If the formation of KSO_4^- ion pairs explains the observed curvature in pK_2' against temperature as the crude calculation in 0.11 mol kg^{-1} KCl suggests, then the question arises as to why the curvature was not observed in studies of other workers. It is expected* that the degree of ion association increases rapidly with increasing ion charge and decreasing dielectric constant. Thus ion pairs would be expected to form, for example, in the complex mixtures used by Marshall and Jones in their solubility studies of $CaSO_4$ in NaCl and in H_2SO_4 solutions up to 350 °C. Helgeson¹²¹ suggests that the almost uniform shift of Marshall and Jones's data from Lietzke's values was due to the formation of $CaSO_4$ ion pairs. It is likely that Lietzke's pK_2^0 values, which are also linear up to 225 °C, would be affected by the formation of $AgSO_4^-$ ion pairs, as silver sulphate is appreciably soluble¹²³⁺ in sulphuric acid solutions at elevated temperatures.

The pK_2^0 values at 200 °C derived by Quist and Marshall and Ryzhenko from the conductivity of potassium bisulphate solutions agree well with the extrapolated value derived using the CG3 equation. Both these

* Predicted by Bjerrum's electrostatic theory of ion association.¹²²

⁺ At 200 °C about 0.1 and 0.5 mol kg^{-1} Ag_2SO_4 in 0.1 and 1.0 mol kg^{-1} H_2SO_4 solution respectively.

studies took no account of the possible formation of KSO_4^- ion pairs. At first sight this result conflicts directly with the suggestion that the curvature observed in this work may have been caused by the formation of these ion pairs. However the solutions used by Quist and Marshall and Ryzhenko were very dilute, ranging in concentration from 0.00007 to 0.005 mol kg^{-1} and 0.0006 to 0.01 mol dm^{-3} respectively. The formation of KSO_4^- would be minimal at these low concentrations and accurate values for pK_2^0 may be derived by extrapolation to zero ionic strength. Quist, Marshall and Jolley in a similar conductivity study on sulphuric acid solutions, derived a value of 4.03 at 200 °C. A value some 0.6 log units lower than that given by Quist and Marshall. The agreement is poor and this result indicates the level of uncertainty associated with such measurements.

6.5.4 Reduction of Sulphate by Hydrogen.

Another marginally possible explanation for the apparent inconsistencies at elevated temperatures is provided by recent unpublished work¹²⁴ where the reduction of sulphate to hydrogen sulphide by hydrogen at elevated temperatures, was found to occur readily in low pH environments, in contrast to near neutral or alkaline solutions. Ohmoto and Lasaga¹²⁵ postulated that the reduction of sulphate to sulphide occurs via sulphur compounds with intermediate valency state, such as thiosulphate species. The speciation of these compounds depends on pH and thus the rate of reduction is pH dependent. The formation of H_2S may explain the slow attainment of equilibrium and also the increasing scatter of the experimental results at temperatures above 150 °C.

Malinin and Khitarov¹²⁶ studied the reduction of sulphate by hydrogen in aqueous solutions of zinc sulphate under hydrothermal conditions. They found that no noticeable reduction took place at

temperatures below 200 °C. At temperatures above 200 °C the reduction of zinc sulphate proceeded rapidly. Their investigations and thermodynamic calculations showed that a 50% reduction of a 0.1 mol dm⁻³ zinc sulphate solution at temperatures of 200-300 °C requires a partial pressure of hydrogen of only 0.1 kPa.

The deviation from linearity of the experimental curves (Figures C.1-C.3), may not have been observed in the "low" temperature experimental range, because these solutions were in contact with the hydrogen atmosphere for about half the time (less than 10 hours) than in the experiments at temperatures above 150 °C. Hydrogen Sulphide was not detected at any stage during the course of these experiments.

6.6 THERMODYNAMIC PARAMETERS.

6.6.1 Trends with Temperature.

The best available thermodynamic parameters as selected by Larson²³ et al. at 25 °C are listed in Table 6.9. The 25 °C extrapolated values derived using the CG3 equation are consistent with the literature results.

TABLE 6.9

Thermodynamic Values for the Dissociation of the Bisulphate Ion at 25°C.

	pK_2^0	ΔG^0 (kJ mol ⁻¹)	ΔH^0 (kJ mol ⁻¹)	ΔS^0 (J K ⁻¹ mol ⁻¹)
Larson ²³ <u>et al.</u>	1.979	11.3	-22.6	-113.7
CG3 Equation* to 150°C	1.9 ± 0.3	11 ± 2	-26 ± 14	-122 ± 42

* extrapolated

6.6.1.1 CG3 Equation.

The standard enthalpy change for the dissociation reaction derived using the CG3 equation rapidly becomes large and more negative with increasing temperature. The $-T\Delta S^\circ$ term dominates giving rise to progressively more positive standard Gibbs energy changes. Thus the bisulphate ion is becoming a weaker acid with increasing temperature. The trends in thermodynamic parameters for all the other literature studies listed in Table 6.6 are the same as that found using the CG3 equation. The agreement with Pavlyuk, Smolyakov and Kryukov's results which are listed at 75 and 150 °C in Table 6.10 is quite reasonable. Larson developed equations which apparently yield very accurate ionization constants up to 100 °C and moderately accurate values at temperatures to 200 °C. Their predictions of the thermodynamic parameters for the dissociation of the bisulphate ion agree with the results derived using the CG3 equation and also with previously published work.

6.6.1.2 CG4 Equation.

The thermodynamic parameters, obtained from a fit of the data using the CG4 equation over the whole temperature range, become more negative but as a consequence of the increasing curvature of the pK_2° curve with temperature, the thermodynamic parameters reach a minimum and then become progressively less negative. The $-T\Delta S^\circ$ term is still more positive than the enthalpy term and consequently the standard Gibbs energy change is still positive although tending towards a maximum. Curves of $\log K$ against temperature for dissociation reactions often pass through a minimum or maximum. However the slope observed in this work at temperatures above 150 °C is opposite to that reported in all other studies in aqueous media (see Section 6.7).

TABLE 6.10

Thermodynamic Values for the Dissociation of the Bisulphate Ion at 75° and 150°C.

t/°C	pK ₂ ^o	ΔG ^o (kJ mol ⁻¹)	ΔH ^o (kJ mol ⁻¹)	ΔS ^o (J K ⁻¹ mol ⁻¹)
Pavlyuk ¹¹⁰ <u>et al.</u>				
75	2.661	17.7	-32.6	-144.7
150	3.772	30.6	-52.9	-197.1
CG3 Equation				
75	2.653 ± 0.035	17.69 ± 0.23	-38 ± 6	-160 ± 17
150	3.893 ± 0.041	31.54 ± 0.33	-56 ± 7	-208 ± 18
CG4 Equation				
75	2.649 ± 0.048	17.65 ± 0.32	-38 ± 8	-159 ± 23
150	3.846 ± 0.030	31.15 ± 0.24	-43 ± 3	-175 ± 8

6.7 PREDICTED THERMODYNAMIC TRENDS.

The acid strength, as measured by the dissociation constant, is determined not only by the bond strength of the acid ion or molecule but also to a great extent, by the Gibbs energy (and hence the component enthalpy and entropy terms) of solvation of the complex and of the dissociated species.¹²⁷ The most convenient approach is to divide the thermodynamic properties into an internal part, intrinsic to the molecules and ion of the acid and an external or environmental part, arising from the interaction of these particles with the solvent.⁷⁵ The internal and external parts are regarded as the sum of the short range electrostatic and long range electrostatic interactions respectively.

It is usually assumed that the internal part of the Gibbs energy change for ionization is independent of temperature. It is therefore possible to predict the thermodynamic parameters, if the hydration process is entirely electrostatic, by calculating the loss of electrostatic energy due to solvation of the ions. Thus the change in the thermodynamic parameters with increasing temperature may be attributed to the changing electrostatic interaction between the ions and the solvent. Many models* have been proposed and the electrostatic approach has been successful in describing the solvent dependence of many dissociation constants.^{75,121,127-129} The theoretically expected Gibbs energies of solvation calculated by Born's equation become less negative, as the dielectric constant of water decreases, so that the stability of ions in water suffers a relative decrease. However the component enthalpy term (in ΔG°) which measures the strength of ion-solvent interactions becomes increasingly exothermic.¹²⁹ Thus the $-T\Delta S^\circ$ term must become increasingly large and more positive i.e. the ΔS° term becomes increasingly large and negative. The available experimental evidence^{121,130} shows that both the enthalpy and entropy of dissociation reactions in aqueous solution become increasingly negative with increasing temperature; for example : the ionization of water, aqueous ammonia¹³¹, first dissociation of boric⁹⁹ and phosphoric acids.¹³²⁺ This behaviour is in accord with the above predictions and is interpreted as a result of the increasing

* Born's model of an ion as a conducting sphere of radius r immersed in a homogeneous, isotropic, linear medium of dielectric constant ϵ is the simplest. However this model is crude and can only give a rough approximation to the electrostatic effect.

+ The values published in these latter two studies must be combined with the corresponding thermodynamic values for the ionization of water.

domination of the electrostatic terms as the dielectric constant of water decreases with increasing temperature.¹²¹ These same trends are observed for the dissociation of charged ions even though more electrical work is required to form the multiply charged species; for example, the second dissociation constants of phosphoric¹³², carbonic^{23,133} and sulphuric acids. Born's model predicts a linear relationship between ΔG and $1/\epsilon$ with a change in temperature. Pavlyuk found that this assumption agreed well with their results over the temperature interval 0 to 200 °C. Thus they concluded that the variation of pK_2^0 with temperature is primarily determined by electrostatic factors. The thermodynamic parameters for the bisulphate dissociation reaction at temperatures above 150 °C derived in this study, are inconsistent with the predicted behaviour and also with other dissociation reactions. This is not surprising in view of the large effect that small changes in the sulphate concentration have on the calculated dissociation constants (see Table 6.7 and Section 6.5.3). Thermodynamic parameters derived over the whole temperature range, using the CG3 equation from a fit of the data up to 150 °C, are in good accord with previous work and the above predictions.

6.8 RECOMMENDED VALUES FOR THE SECOND DISSOCIATION CONSTANT OF SULPHURIC ACID.

The difficulty of measuring the second dissociation constants at elevated temperatures is reflected in discrepancies between the results of previously published work. The data derived in this study are considered reliable within the calculated (random) errors of about 0.05 log units and the estimated uncertainties of 0.04 to 0.08 log units between temperatures of 75 and 225 °C. Recalculating these results in terms of the formation of $KS\bar{O}_4$ ion pairs, allowed the derivation of

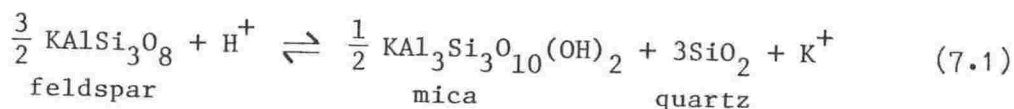
values for $pK'_{\text{KSO}_4^-}$ which were in good accord with previously published data. Thus the full interpretation of the dissociation constants derived in this work is limited by the lack of accurate molal dissociation constants of the KSO_4^- ion pair over the full range of ionic strength and temperature. The only other published studies, where dissociation constants have been derived over an extended range of temperature, are those of Lietzke⁶¹ and Marshall and Jones⁶². Helgeson suggests that the large difference between these two sets of results may be due to the formation of ion pairs. If ion pairing is of importance in such solutions, then the reason for the linear dependence of pK_2^0 with temperature found in their studies, in contrast to the behaviour observed in this work, is not clear. Lietzke's⁶¹ values, rather than Marshall and Jones's⁶² results, appear to be in better agreement with the dissociation constants extrapolated from the low temperature data derived in this study and also with the data calculated using Larson's equations. In view of the lack of any other reliable high temperature studies Lietzke's results, although limited by the neglect of ion pairing effects, may be used to estimate values for pK_2^0 above 150 °C.

Chapter 7

ACID HYDROLYSIS OF K-FELDSPAR TO K-MICA AND QUARTZ.

7.1 INTRODUCTION.

The suitability of the pH cell in physico-chemical studies has been well demonstrated in the previous three experimental systems. There are however, many important silicate mineral equilibria that occur in natural hydrothermal systems and which proceed via hydrogen ion exchange. For example, K-feldspar occurs commonly in silicic igneous rocks and hydrochloric acid is one of the more abundant acids in hydrothermal solutions. Thus, the acid hydrolysis of K-feldspar to K-mica and quartz, represented by the reaction



apparently buffers many hydrothermal fluids and is of fundamental importance in determining the chemistry of such systems. This equilibrium has been well studied^{13,134} and appears to be one of the least complicated. Feldspar-mica assemblages act as buffers for potassium-hydrogen ratios at a given pressure and temperature and they have been used to control acidity in geochemical solubility studies. The geological significance of such reactions and the importance of obtaining reliable dissociation constants has been well demonstrated by Gunter and Eugster.¹³⁵ Such information is used to estimate the abundances of solute species and is essential in understanding mineral dissolution, precipitation and mass transport in aqueous fluids.

7.1.1 Previous Work.

Nearly all previous investigations¹³⁶ have been undertaken at temperatures and pressures above 350 °C and 100 MPa respectively, and the results are not directly relevant to this work. Usdowski and Barnes²⁵ determined at SVP the equilibrium constant at 30, 60 and 300 °C and their results are more useful for comparison with those found in this study. A discussion of all the previously published work will be given in a following section.

7.1.2 Limitations of This Work.

The usual experimental technique for studying such reactions is periodic sampling and analysis of the quenched fluids. The assumption is then made that the analysed concentrations are representative of the solution under the high temperature and pressure conditions. This assumption is difficult to justify and therefore, the use of the present cell to make direct measurements of pH in situ at elevated temperatures would in principle be an advance over such a technique. In practice the study was severely limited by the very slow rate* of equilibration among the three minerals at temperatures less than 300 °C. The usual method of temperature scanning at different potassium ion concentrations could not be used and an alternative procedure was adopted where the stability field of the minerals was located by suitable adjustment of the initial hydrogen and potassium ion ratio's. The equilibrium constant at 225 °C was found by bracketing with different concentrations of the ions until a pH independent of time was achieved. Thus a considerable number of trial experimental runs were required to establish just one experimental point. The temperature of 225°C was chosen so that the teflon seals

* For example under hydrothermal conditions quartz dissolves reaching equilibrium in 4-6 days¹³⁷ at temperatures between 130 and 300 °C.

would last the required time (25 hours) and also to ensure adequate performance of the porous teflon plug.

7.2 RESULTS.

The successful experimental runs, representing about a third of all those attempted* are shown in Figure 7.1, where $\log Q$ is plotted against time. Q is the concentration ratio (m_{K^+}/m_{H^+}) calculated from the stoichiometric amounts of potassium and hydrogen ions. As the reaction proceeds towards equilibrium, the ratio becomes a better approximation to the equilibrium constant, assuming that the activity coefficient quotient ($\gamma_{K^+}/\gamma_{H^+}$) is near unity. The initial pH's at 225 °C⁺ and potassium ion concentrations are given in Table 7.1. Runs A and D contained no hydrochloric acid and the pH listed was that obtained from the ionization constant of water for 0.1 and 1 mol kg⁻¹ KCl at 225 °C. All the experimental results are listed in Appendix D.

* See Section 2.3.4, page 20 for possible reasons for the failure of these other experimental runs.

⁺ The pH's at zero time were calculated from the initial hydrogen ion concentrations and the Debye-Hückel equation (Eq. 3.14) at a temperature of 225 °C.

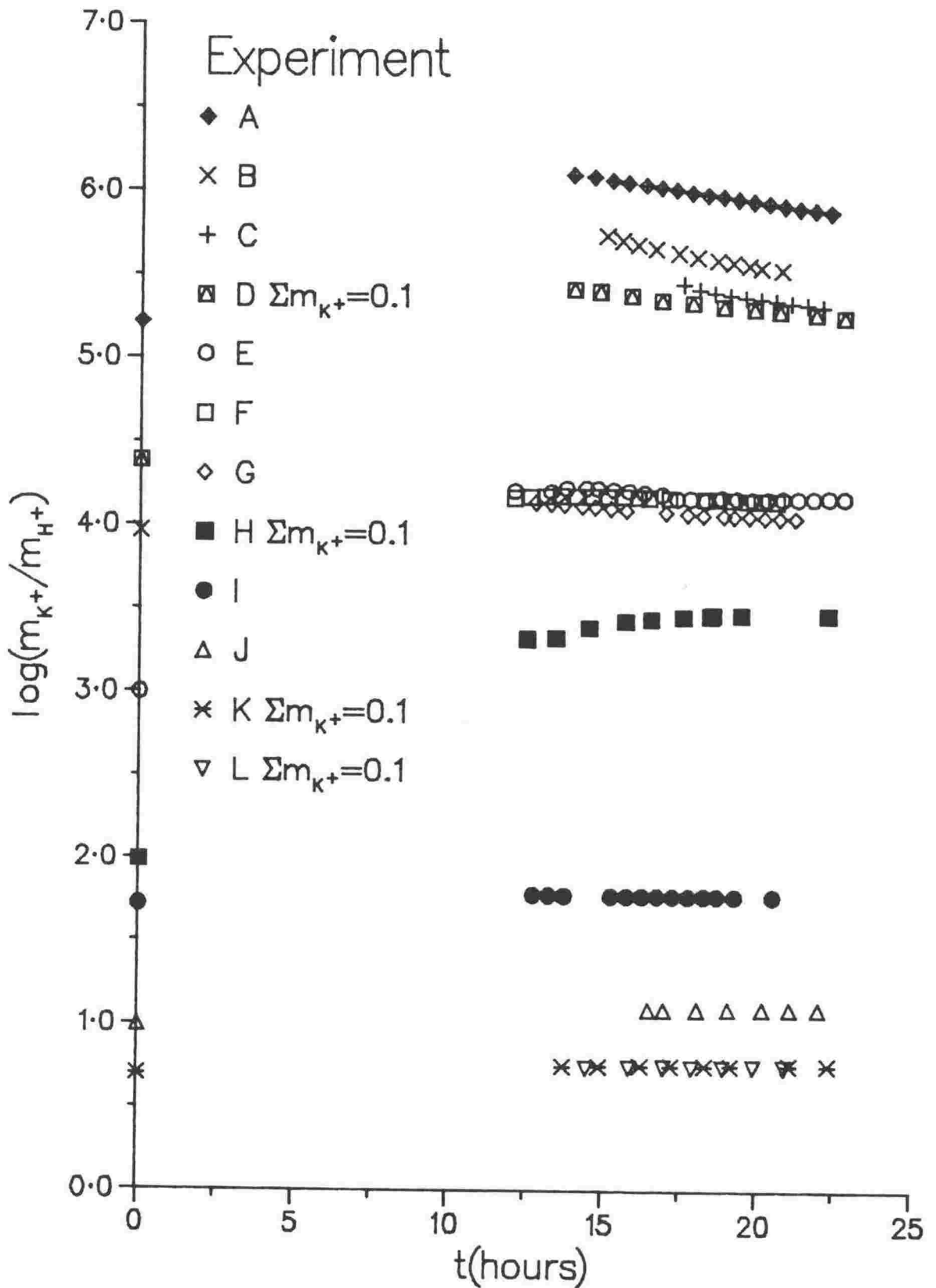


Figure 7.1: The Variation of $\log(m_{K^+}/m_{H^+})$ with Time of the Feldspar Hydrolysis Reaction at 225°C.

TABLE 7.1

Initial Solution Concentrations of the Feldspar Hydrolysis Experiments.

Experiment	Initial pH	m_K^+	logQ
A	5.475	1.0246	5.213
B,C	4.322 (4.396)*	1.0446	3.962 (4.036)
D	5.591	0.0977	4.384
E,F,G	3.356 (3.436)	1.0464	2.996 (3.077)
H	3.167 (3.209)	0.1040	1.987 (2.029)
I	2.074 (2.086)	1.0596	1.717 (1.730)
J	2.185	0.1027	0.992
K,L	1.903	0.1004	0.696

* Calculated at 225 °C.

+ The figures shown in brackets have been corrected for the effects of dissolved Fe^{2+} .

7.3 IRON CORRECTION.

A correction was necessary due to the presence of iron (about 3.6% FeO as determined by electron microprobe analysis) in the K-mica. This iron is soluble in media of low pH and the initial pH's and the corresponding concentration ratios shown in brackets in Table 7.1 have been corrected on the basis of the amount of iron found solution at the end of the experiment. The concentration of iron was determined by atomic absorption analysis. The initial acid strength determined the amount of iron present. For example, in experiment I the total iron accounted for a 3% change in the initial acid concentration of 0.02 mol kg^{-1} , while there was no detectable iron in the "neutral" solutions of experiments

A and D. The corrections to the initial pH's were small and less than 0.1 units, thus the observed changes in logQ of about 1-2 log units (Figure 7.1) are not fully accounted for by only the simple dissolution of iron oxide by acid.

7.4 ERROR.

The total error from all the combined uncertainties was about 0.01 pH units (calculated using the same techniques as those described in Chapter 5). The liquid junction potential represented only a minor correction to the measured potential which was always an order of magnitude greater.

7.5 DISCUSSION.

7.5.1 Experiments at Low pH.

Experiments I-L at low pH were well away from the expected equilibrium ratio as suggested by the literature results.¹³ The change in acid concentration was very small compared to the high initial concentration and there was almost no change from the initial pH. Thus the resulting logQ values were almost constant from the commencement of readings at 225 °C, because of the slow dissolution rate of the silicate minerals. The data from the experiments I,J,K summarized from Appendix D are listed in Table 7.2. There is considerable evidence that shows that the initial step in the acid hydrolysis of alkali feldspars¹³⁸ and micas¹³⁹ consists of the replacement of alkali ions by hydronium ions on the surface of the mineral structure. This is consistent with the behaviour observed in experiments I to J where the same proportion of hydrogen ion, independent of the K^+ concentration, has reacted by the end of the experiment and nearly all this change has occurred in the initial heating period. Runs I, J and K show a change in pH of 0.01 log

TABLE 7.2

Summarized Results for the Feldspar Hydrolysis Experiments I, J and K at Low pH.

Time (hours)	pH at 225°C	logQ	E (mV)	% m_{H^+} Reacted
Experiment I, m_{H^+} 0.020319, m_{K^+} 1.059582				
0	2.07 (2.09)	1.72 (1.73)		
12.75	2.13	1.78	5.77	13
15.25	2.13	1.77	5.23	
20.50	2.13	1.77	5.03	11
Experiment J, m_{H^+} 0.010453, m_{K^+} 0.102700				
0	2.19	0.99		
16.50	2.28	1.09	8.60	19
22	2.28	1.10	9.17	20
Experiment K, m_{H^+} 0.020234, m_{K^+} 0.100367				
0	1.90	0.70		
13.75	1.95	0.75	4.11	10
22.33	1.96	0.76	4.90	11

units after the initial heating up period to 225°C. The changes in pH of 0.01 log units at 225 °C over the day are very small and are of the same order as the experimental error and are therefore not at all significant.

The constant pH with time observed at 225 °C may be explained by the formation of a protective layer consisting of secondary minerals (e.g. Al-silicates, oxides and hydroxides). Thus the dissolution rate would be

controlled by diffusion of the feldspar components through a thickening layer of such products. It has been recently shown^{140,141} that no continuous layer of secondary products forms on the surface of the feldspar. Rather they occur as discrete particles occupying a very small fraction of the total surface. Thus dissolution is controlled by the rate of reaction at the feldspar-solution interface and not by the formation of diffusion barriers. The major factor determining the rate of equilibration is likely to be the transformation of a three dimensional feldspar lattice to a mica network sheet structure, a process that is both energetically and kinetically unfavourable.¹⁴¹ Formation of intermediate minerals by incongruent dissolution of the feldspar and mica is expected to occur¹³ and this will further impede and influence the buffered pH.

7.5.2 Experiments at High pH.

In experiments A-H the concentration ratios of the potassium to hydrogen ions were closer to the equilibrium ratios suggested by Usdowski and Barnes's results. The reaction rate is still slow, as in the low pH experiments, but now the small change in acid concentration is comparable in size to the initial starting pH and thus changes in logQ of 1-2 units are observed. In experiments A-D the initial increase in logQ is followed by a small progressive decrease. This is consistent with the experimental evidence¹³ that suggests that the equilibrium pH's are higher at lower temperatures. Thus in these cases the pH increases during heating to 180°C, and then as the temperature is finally set at about 225°C the pH slowly decreases. For experiment B there is a total decrease of pH (initially set at a pH of 4.32 in 1 mol kg⁻¹ KCl solution) from 6.10 to 5.90 and in logQ from 5.74 to 5.54. This small change represents a potential change of 20 mV, from 175 to 155 mV. Thus

the pH was precisely determined and would not be greatly affected by any small errors in potential. Experiment C which had the same initial solution concentrations as for B was heated overnight to about to 215 °C rather than the usual 180 °C. Consistent with the above explanation the measured pH's and logQ's are lower than the results for B.

Decreasing the initial pH by one log unit from that used in experiments B and C to 3.356 in experiments E,F and G results in the same initial increase in logQ but this then remains relatively constant with time, which would be expected if the system was at equilibrium. These experiments were performed in the sequence E-G-F. Experiment G deviates downwards by about 0.1 units, equivalent to about 10 mV, from E and F which are virtually overlapping. New cell seals were used with experiment G which may explain this slight deviation.

In order to approach the equilibrium from the reverse direction the forward reaction, i.e. the increase in pH, must be observed. Further reduction in pH in 1 mol kg⁻¹ KCl solution did not produce any significant changes (c.f. experiment I). In experiment H the same starting pH was used as in E, F and G but the potassium ion concentration was reduced to 0.1 mol kg⁻¹. Consistent with what would be expected, the reaction is driven towards the K-mica/quartz assemblage and a very slow increase in the measured pH and logQ results. Thus the equilibrium ratio is bracketed between logQ values of 3.7 and 5.5. The results of experiment E,F and G, where a constant pH with time was observed, give an equilibrium ratio close to 4.2 log units at 225°C.

The major part of the pH change in experiments A to H occurred during the overnight temperature equilibration at about 180 °C. This behaviour may be qualitatively explained by assuming high initial dissolution rates for the powdered minerals. It has been experimentally demonstrated¹³⁸ that initial dissolution rates depend upon the state of

TABLE 7.3

Summarized Results for the Feldspar Hydrolysis Experiments A, B, C and D at High pH.

Time (hours)	pH at 225°C	logQ	E (mV)
Experiment A, $m_H + 6.281 \times 10^{-6}$, $m_K + 1.0246$			
0	5.48	5.21	
13.92	6.47	6.10	218.3
17.75	6.37	6.00	209.2
22.25	6.25	5.88	197.7
Experiment B, $m_H + 1.141 \times 10^{-4}$, $m_K + 1.0446$			
0	4.32 (4.40)	3.96 (4.04)	
15.00	6.10	5.74	177.6
17.92	5.97	5.61	162.9
20.67	5.90	5.54	155.2
Experiment C			
17.50	5.81	5.45	147.0
19.00	5.75	5.38	140.7
22.00	5.67	5.31	133.5
Experiment D, $m_H + 4.036 \times 10^{-6}$, $m_K + 0.0977$			
0	5.59	4.38	
13.97	6.62	5.42	339.9
17.80	6.55	5.34	332.0
22.72	6.46	5.25	323.6

the starting materials. Grinding may produce enough surface strain or super soluble fine particles so that enhanced reactivity is observed. As the damaged surface and fine particles are consumed the dissolution rates decrease.

7.5.3 Previously Published Work.

Previously published data together with this work is shown in Figure 7.2, where $\log Q$ is plotted against temperature. Apart from Usdowski and Barnes's²⁵ work all the experimental studies were undertaken at 100 MPa pressure. The equilibrium quotients derived in these high temperature studies have been recalculated to 0.1 MPa using a value for ΔV^0 (assumed to be independent of pressure) of $-16.6 \text{ cm}^3 \text{ mol}^{-1}$ given by Usdowski and Barnes.* Pressure changes of several hundred bars usually have a small effect on equilibrium reactions in aqueous media. At 300 and 600 °C the calculated values for $\log Q$ at 0.1 MPa are lower than at 100 MPa, by only 0.15 and 0.10 log units respectively.

Significant disagreement between the literature results suggests that large uncertainties are associated with the reported equilibrium constants. The value at 225 °C derived in this study is in very good agreement with Hemley's¹⁴³ work but is about half a log unit lower and one log unit higher than the values interpolated from the results of Usdowski and Barnes and Ivanov¹⁴⁴ et al. respectively. Ivanov considered their results to be more reliable than those of Hemley because of an improved experimental procedure which involved determining the direction of reaction by comparing X-ray diffractions of the run product with standard mixtures. However the lack of experimental data points makes it difficult to fully evaluate their results.¹³⁶ Usdowski and Barnes's results were obtained by following the change in pH of dilute KOH/KCl solutions over a period of 12 days for experiments at 30

* Shade¹⁴² derived a ΔV^0 value of $-16.05 \text{ cm}^3 \text{ mol}^{-1}$.

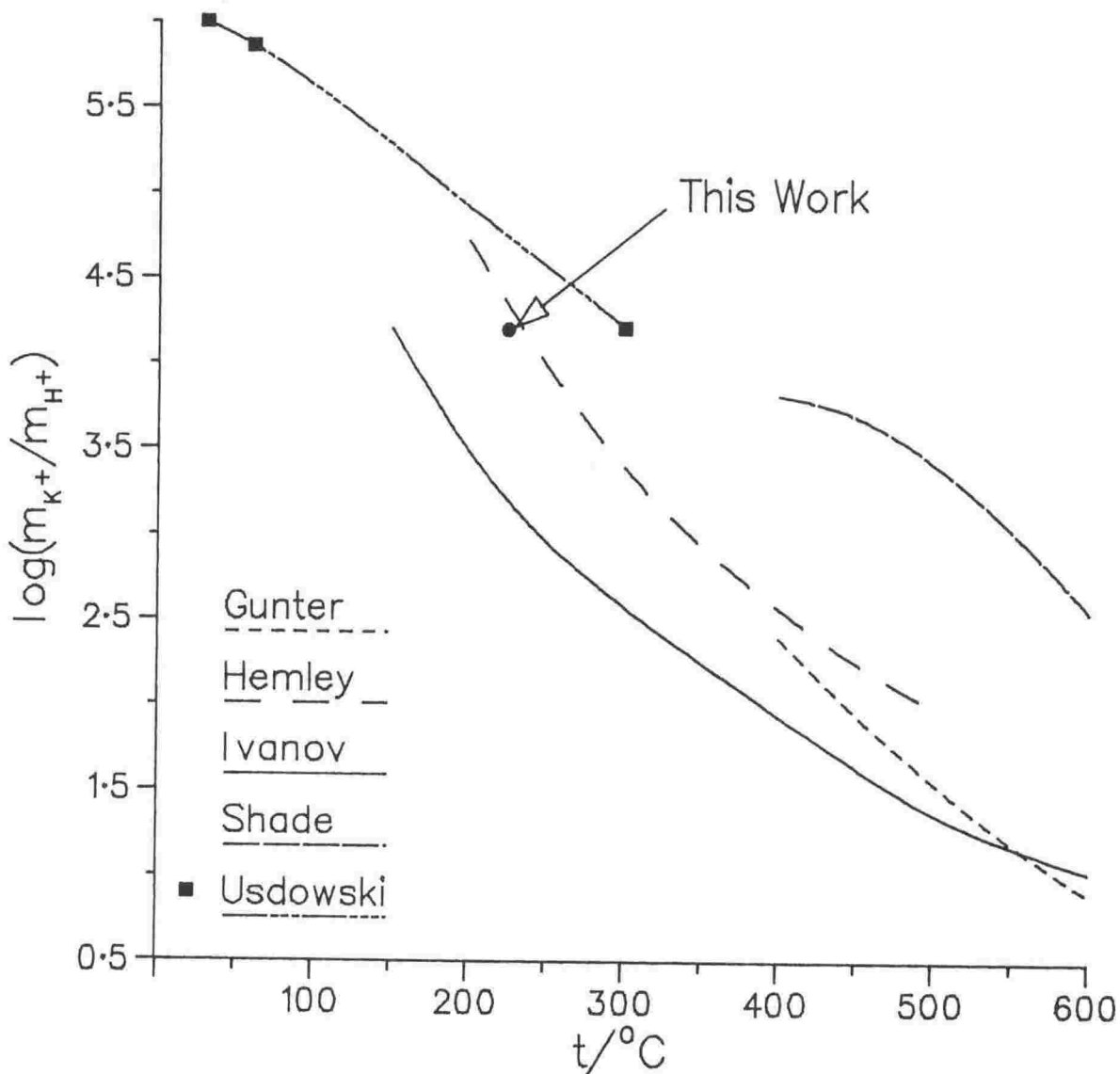


Figure 7.2: The Variation of $\log(m_{K^+}/m_{H^+})$ with Temperature Derived by Different Workers.

and 60°C , and over about 70 hours at 300°C . The total change in pH was small, usually less than 0.5 units (e.g. 8.7 to 8.2 at 30°C) and equilibrium was approached only from one side. This may explain why higher $\log Q$ values were obtained in their study. The changes in pH, observed by them and in this study, were such that the potassium ion concentration remained virtually constant over the time taken for the experimental run. In many cases Gunter and Eugster¹³⁵ could not detect any hydrolysis reaction (by potassium ion analysis) at temperatures

about 500 °C, even after several weeks. Thus a steady state condition does not necessarily imply that equilibrium has been established. This fact was given as one reason for the necessity of reversing the equilibrium in order to determine the stability field of the minerals.

Unfortunately because of the very slow rate of equilibration and the distance away from equilibrium it was not possible to determine the equilibrium quotient in this study with any degree of certainty. However, the derived logQ value of 4.2 was bounded by reactions where a reversal in pH with time was observed. The result is consistent with previously published data and the method is likely to give a more precise estimate of the equilibrium constant at 225 °C than the usual quenching techniques.

Appendix A
WATER RESULTS

TABLE A.1

Terms Contributing to the Final Smoothed Ionization Constants of Water
as a Function of Ionic Strength and Temperature.

t (°C)	E (V)	E _J (mV)	pQ' _W	pK' _W
$m_{\text{KOH}} = 0.01, m_{\text{KCl}} = 0.1 : m_{\text{HCl}} = 0.01, m_{\text{KCl}} = 0.1$				
75	-0.58129	4.811	12.485	12.721
100	-0.58739	4.556	11.995	12.247
125	-0.59717	4.308	11.614	11.887
150	-0.61045	4.077	11.319	11.616
175	-0.62690	3.845	11.093	11.416
200	-0.64603	3.608	10.920	11.275
225	-0.66750	3.370	10.787	11.182
$m_{\text{KOH}} = 0.01, m_{\text{KCl}} = 0.3 : m_{\text{HCl}} = 0.01, m_{\text{KCl}} = 0.3$				
75	-0.58015	1.800	12.425	12.717
100	-0.58561	1.694	11.932	12.246
125	-0.59398	1.593	11.539	11.880
150	-0.60520	1.501	11.226	11.597
175	-0.61889	1.409	10.976	11.382
200	-0.63456	1.318	10.773	11.221
225	-0.65179	1.227	10.607	11.106
$m_{\text{KOH}} = 0.01, m_{\text{KCl}} = 0.5 : m_{\text{HCl}} = 0.01, m_{\text{KCl}} = 0.5$				
75	-0.57922	1.107	12.401	12.703
100	-0.58358	1.040	11.896	12.222
125	-0.59091	0.977	11.492	11.848
150	-0.60115	0.920	11.171	11.560
175	-0.61388	0.863	10.913	11.342
200	-0.62857	0.806	10.704	11.179

225	-0.64479	0.750	10.531	11.063
$m_{\text{KOH}} = 0.01, m_{\text{KCl}} = 1.0 : m_{\text{HCl}} = 0.01, m_{\text{KCl}} = 1.0$				
75	-0.57781	0.564	12.373	12.648
100	-0.58351	0.530	11.888	12.192
125	-0.59082	0.497	11.485	11.825
150	-0.59979	0.467	11.150	11.529
175	-0.61006	0.438	10.866	11.291
200	-0.62110	0.409	10.620	11.100
225	-0.63252	0.380	10.403	10.949

TABLE A.2

Equation Coefficients for the Ionization Constant of Water.

$$\text{Valentiner Equation } pK'_W = a_1/T + a_2 + a_3 \log T$$

I	a_1	a_2	a_3	n	s_f
0*	7085.590	-82.946	29.634	127	0.015
0	7229.701	-85.007	30.285	163	0.017
0.1	7012.893	-81.365	29.091	51	0.012
0.3	6367.296	-69.202	25.034	39	0.016
0.5	6548.836	-71.840	25.861	37	0.017
1.0	5079.673	-45.959	17.317	36	0.021

* A fit of the data from I=0.5.

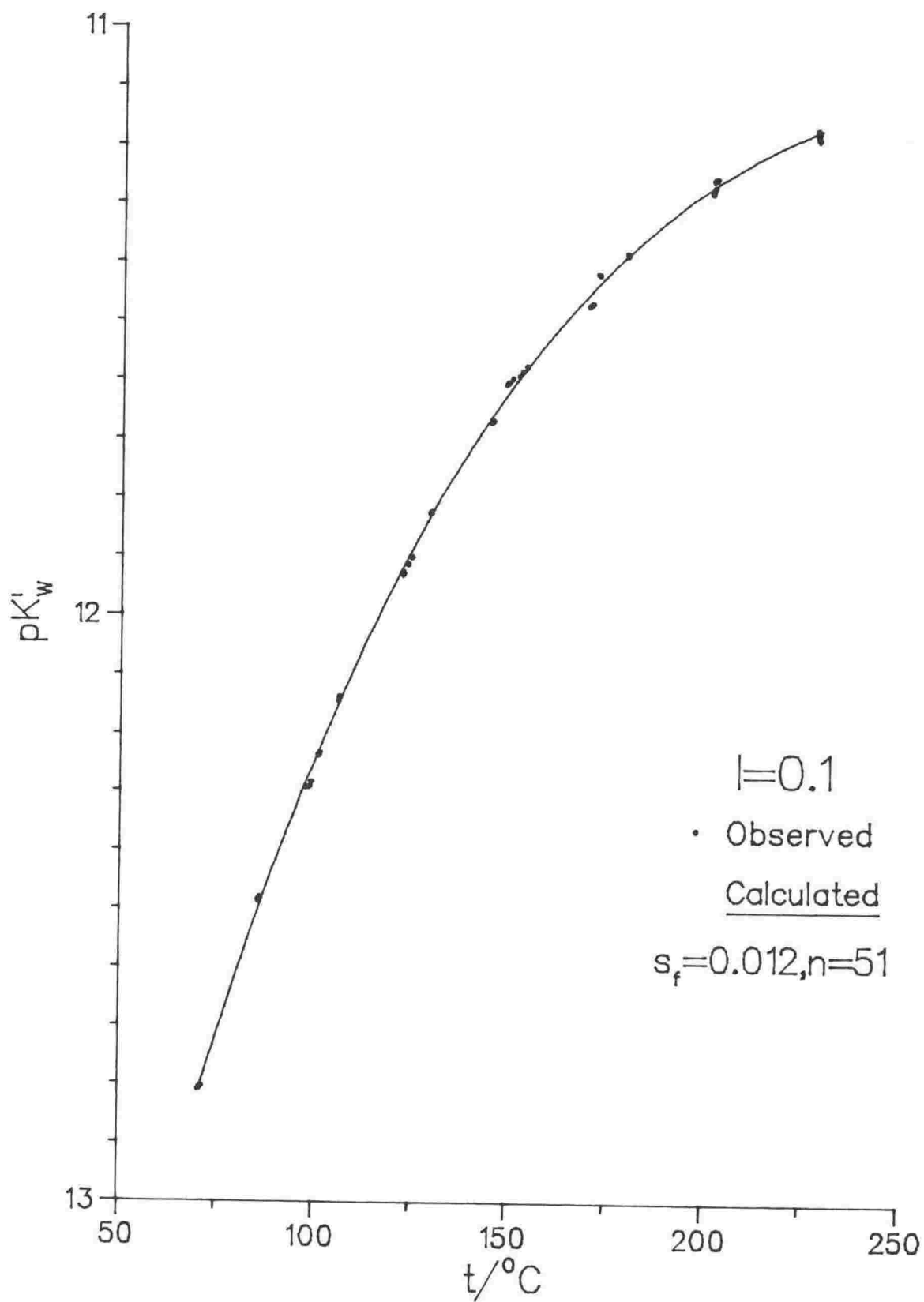


Figure A.1: The Temperature Dependence of pK'_w in 0.1 mol kg^{-1} KCl Solution.

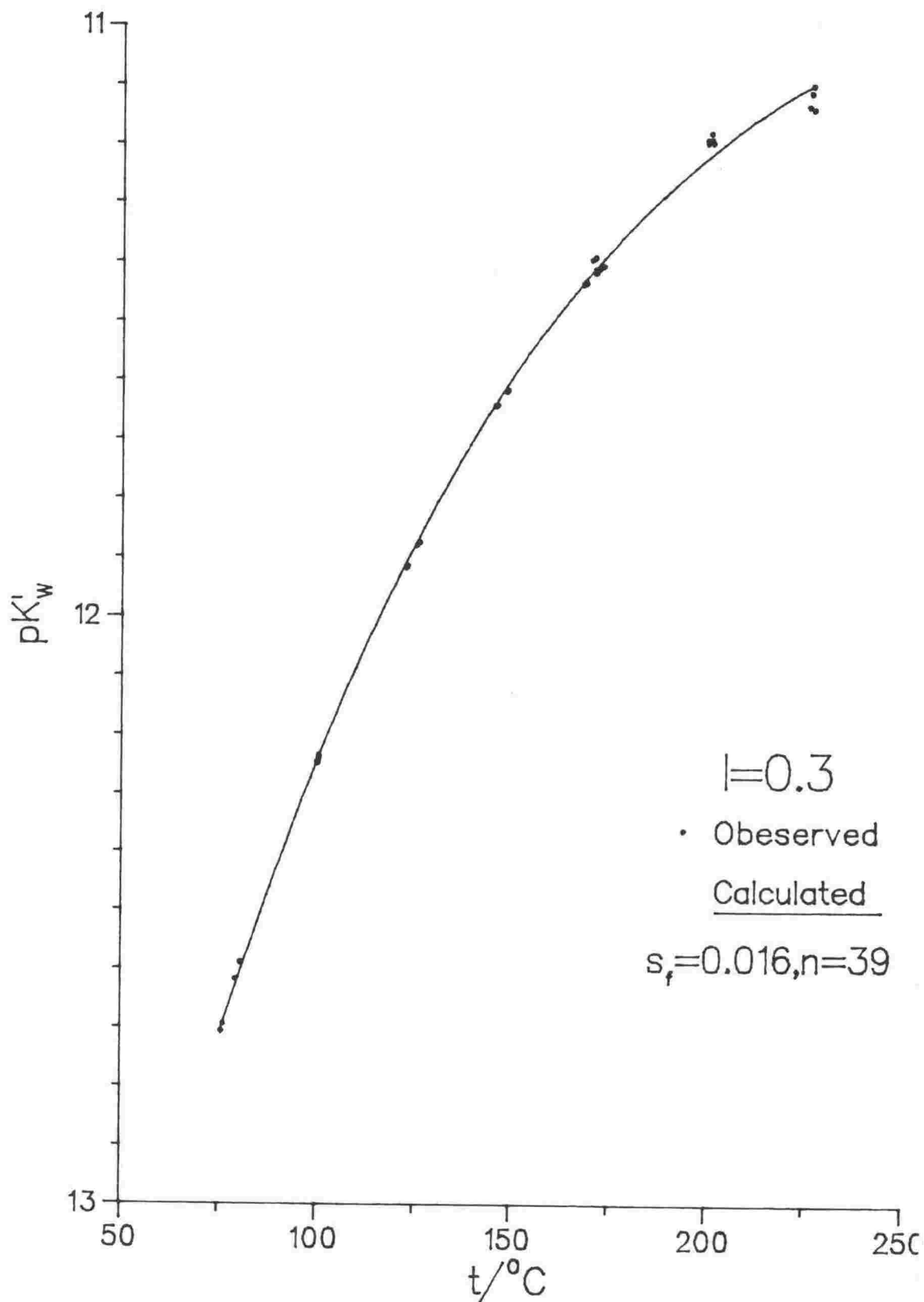


Figure A.2: The Temperature Dependence of pK'_w in 0.3 mol kg^{-1} KCl Solution.

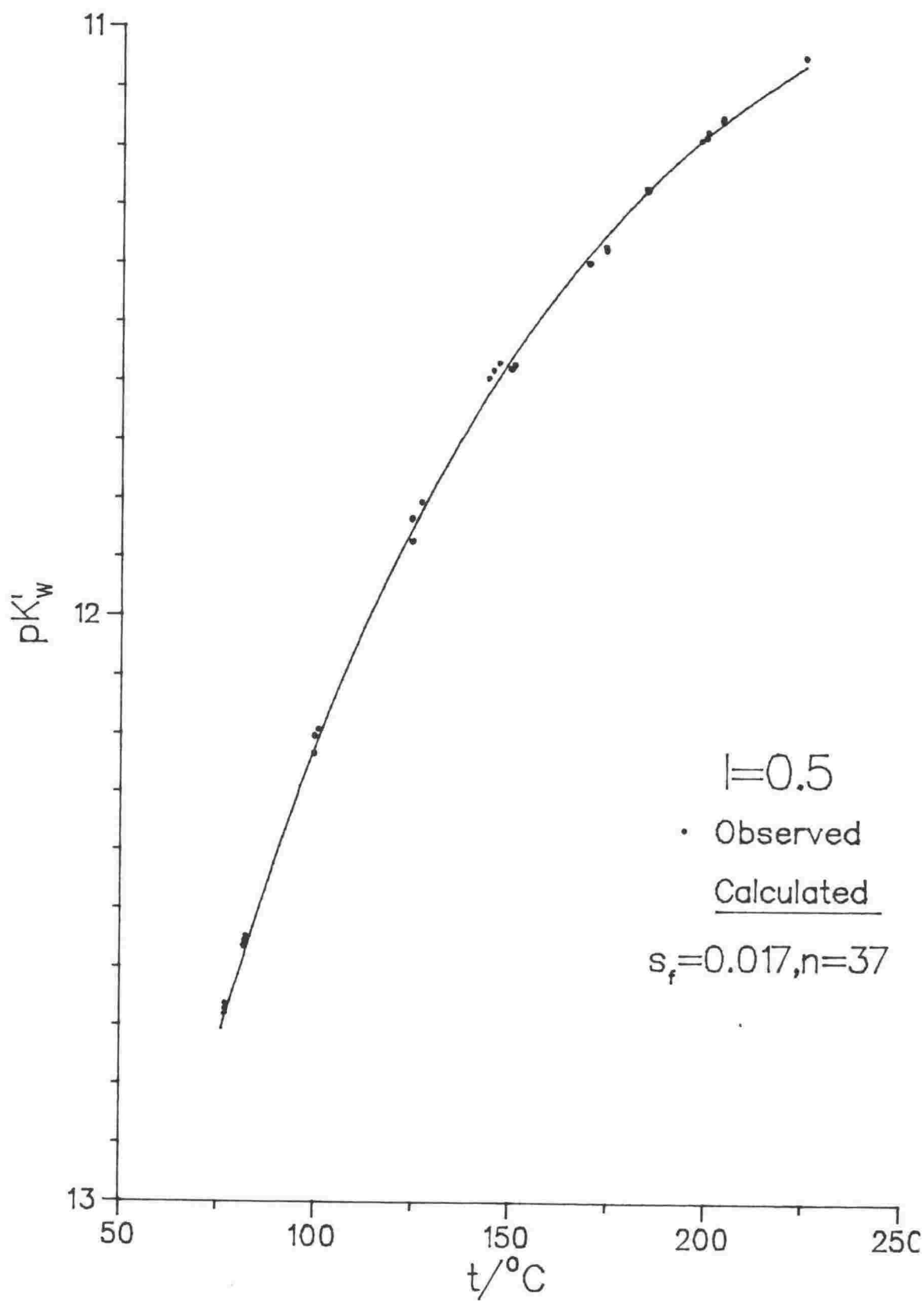


Figure A.3: The Temperature Dependence of pK'_w in 0.5 mol kg^{-1} KCl Solution.

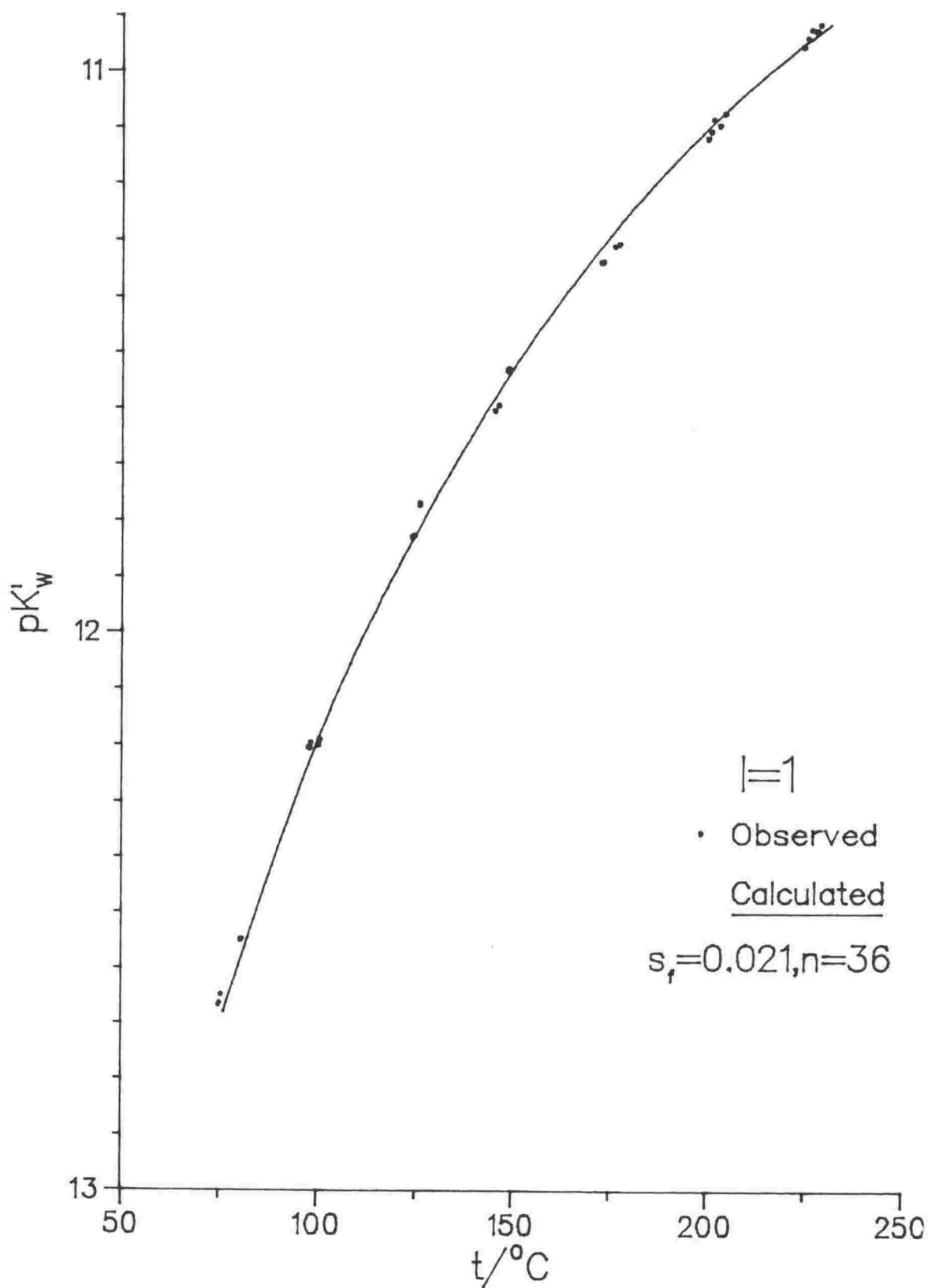


Figure A.4: The Temperature Dependence of pK'_w in 1.0 mol kg^{-1} KCl Solution.

TABLE A.3

Solution Concentrations used in Determining the Ionization Constant of Water.

Experiment	m_{KOH}	m_{KCl}	:	m_{HCl}	m_{KCl}
1	8.054×10^{-3}	0.078042		8.049×10^{-3}	0.078707
2	9.953×10^{-3}	0.100982		0.010205	0.102256
3	0.010117	0.110356		0.010214	0.099008
4	0.010091	0.099181		0.010250	0.099748
5	0.010340	0.313107		0.010453	0.309221
6	0.010157	0.311251		0.010195	0.301589
7	0.010167	0.302757		0.010274	0.303883
8	0.010167	0.302757		0.010274	0.303883
9	0.010145	0.490395		0.010049	0.493432
10	0.010221	0.505774		9.717×10^{-3}	0.494442
11	0.010340	0.526248		0.010460	0.513929
12	0.010168	0.510255		0.010316	0.501365
13	0.010294	0.516350		0.010199	0.502211
14	9.167×10^{-3}	0.906923		9.354×10^{-3}	0.908033
15	0.010481	1.062303		0.010511	1.046644
16	0.010304	1.040392		0.010375	1.036742
17	0.010485	1.027168		0.010556	1.022757
18	0.010438	1.036455		0.010389	1.018501

TABLE A.4

Experimental Data of the Ionization Constant of Water in 0.1 mol kg⁻¹ KCl Solution.

Experiment	t (°C)	E (V)	pQ' _W	pK' _W	pK' _W (fitted)
2	70.64	-0.58066	12.576	12.811	12.817
2	71.03	-0.58105	12.572	12.807	12.808
2	71.42	-0.58156	12.570	12.806	12.800
3	85.66	-0.58305	12.243	12.486	12.504
3	85.88	-0.58323	12.240	12.483	12.499
3	86.18	-0.58353	12.238	12.481	12.494
1	98.01	-0.57493	12.059	12.293	12.281
1	98.73	-0.57599	12.058	12.292	12.269
1	99.16	-0.57598	12.048	12.283	12.261
2	100.91	-0.58835	11.981	12.235	12.233
2	100.97	-0.58849	11.982	12.236	12.232
2	101.30	-0.58870	11.978	12.232	12.226
3	106.14	-0.58995	11.886	12.143	12.149
3	106.35	-0.58975	11.879	12.136	12.146
3	106.46	-0.58997	11.879	12.137	12.145
2	122.48	-0.59734	11.658	11.930	11.919
2	122.50	-0.59703	11.653	11.925	11.918
2	122.51	-0.59720	11.655	11.927	11.918
1	123.87	-0.58405	11.658	11.912	11.901
1	124.63	-0.58416	11.646	11.900	11.891
1	124.75	-0.58438	11.646	11.901	11.890
3	129.45	-0.59980	11.549	11.826	11.833
3	129.58	-0.59992	11.548	11.825	11.831
3	129.65	-0.59988	11.546	11.823	11.830
1	144.97	-0.59412	11.400	11.672	11.664
1	144.99	-0.59405	11.399	11.671	11.664
1	145.33	-0.59438	11.397	11.669	11.660
3	148.80	-0.60922	11.313	11.607	11.627
3	149.30	-0.60962	11.309	11.604	11.622
3	150.30	-0.61043	11.301	11.597	11.613
2	152.00	-0.61178	11.293	11.593	11.597
2	152.82	-0.61228	11.285	11.585	11.590
2	153.91	-0.61308	11.276	11.577	11.580
4	169.75	-0.62620	11.156	11.473	11.453
4	170.56	-0.62689	11.151	11.469	11.447
2	172.10	-0.62380	11.098	11.418	11.436
2	172.44	-0.62435	11.098	11.420	11.434
1	179.46	-0.61471	11.076	11.382	11.387
1	179.49	-0.61512	11.080	11.387	11.387
1	179.54	-0.61496	11.078	11.384	11.387
4	201.14	-0.64924	10.923	11.280	11.270
4	201.36	-0.64916	10.919	11.276	11.269
1	201.42	-0.63061	10.924	11.257	11.269
4	201.67	-0.64896	10.913	11.270	11.268
1	201.77	-0.63086	10.922	11.255	11.267
1	202.19	-0.63127	10.920	11.254	11.265
1	227.93	-0.65368	10.797	11.170	11.174

1	228.03	-0.65508	10.810	11.183	11.173
1	228.03	-0.65407	10.800	11.173	11.173
4	228.23	-0.67318	10.786	11.186	11.173
4	228.32	-0.67204	10.774	11.174	11.173

TABLE A.5

Experimental Data of the Ionization Constant of Water in 0.3 mol kg⁻¹ KCl Solution.

Experiment	t (°C)	E (V)	pQ' _W	pK' _W	pK' _W (fitted)
6	75.74	-0.58162	12.413	12.707	12.702
6	76.18	-0.58144	12.400	12.694	12.692
5	79.41	-0.58258	12.320	12.617	12.625
5	80.65	-0.58262	12.291	12.589	12.600
5	80.66	-0.58265	12.291	12.589	12.600
5	99.97	-0.58802	11.932	12.247	12.247
5	100.26	-0.58720	11.933	12.248	12.242
6	100.44	-0.58806	11.922	12.237	12.239
5	100.55	-0.58803	11.920	12.235	12.237
5	100.56	-0.58712	11.926	12.241	12.237
6	122.74	-0.59621	11.577	11.916	11.909
5	122.83	-0.59623	11.575	11.915	11.908
5	123.06	-0.59643	11.574	11.913	11.905
5	125.54	-0.59578	11.537	11.878	11.873
6	126.12	-0.59623	11.531	11.873	11.865
6	145.76	-0.60465	11.278	11.643	11.640
6	146.03	-0.60486	11.276	11.642	11.637
6	146.15	-0.60503	11.276	11.642	11.636
5	148.66	-0.60801	11.249	11.619	11.610
5	148.95	-0.60817	11.246	11.616	11.607
5	168.34	-0.61812	11.039	11.436	11.433
5	168.79	-0.61845	11.035	11.433	11.430
5	168.99	-0.61877	11.036	11.434	11.428
7	170.34	-0.61582	10.996	11.395	11.417
7	171.25	-0.61659	10.990	11.391	11.410
6	171.27	-0.61811	11.011	11.411	11.410
7	171.34	-0.61872	11.017	11.417	11.409
6	171.63	-0.61870	11.012	11.413	11.407
8	172.13	-0.61944	11.009	11.410	11.403
8	173.26	-0.62040	11.002	11.405	11.395
7	199.68	-0.63313	10.744	11.192	11.223
8	199.76	-0.63373	10.749	11.197	11.222
7	200.59	-0.63317	10.731	11.181	11.218
8	200.75	-0.63444	10.743	11.192	11.217
8	201.01	-0.63515	10.746	11.197	11.216
8	225.70	-0.65718	10.633	11.134	11.103
8	226.36	-0.65574	10.610	11.113	11.100
8	226.81	-0.65491	10.595	11.099	11.099
7	226.88	-0.65894	10.635	11.139	11.098

TABLE A.6

Experimental Data of the Ionization Constant of Water in 0.5 mol kg⁻¹
KCl Solution.

Experiment	t (°C)	E (V)	pQ' _W	pK' _W	pK' _W (fitted)
9	76.90	-0.58123	12.376	12.680	12.662
9	77.02	-0.58080	12.367	12.671	12.659
9	77.06	-0.58030	12.359	12.663	12.659
11	81.72	-0.58261	12.256	12.564	12.562
11	82.03	-0.58247	12.247	12.555	12.555
11	82.33	-0.58238	12.239	12.547	12.549
11	99.73	-0.58640	11.906	12.231	12.226
9	99.80	-0.58256	11.878	12.204	12.225
11	99.81	-0.58662	11.907	12.233	12.225
9	99.82	-0.58244	11.876	12.202	12.225
9	100.73	-0.58299	11.865	12.191	12.209
9	124.46	-0.58976	11.480	11.835	11.855
11	124.56	-0.59482	11.516	11.872	11.854
9	124.67	-0.58983	11.477	11.832	11.852
11	124.67	-0.59497	11.516	11.872	11.852
11	124.77	-0.59511	11.516	11.872	11.851
9	126.95	-0.59093	11.448	11.806	11.823
9	144.02	-0.59685	11.214	11.594	11.622
9	145.24	-0.59736	11.199	11.581	11.609
9	146.73	-0.59830	11.184	11.569	11.594
11	149.75	-0.60517	11.189	11.578	11.563
11	150.02	-0.60540	11.187	11.577	11.560
11	150.70	-0.60583	11.181	11.572	11.553
11	169.47	-0.61490	10.978	11.397	11.385
11	169.53	-0.61500	10.978	11.398	11.384
11	169.84	-0.61536	10.977	11.397	11.382
12	173.85	-0.61675	10.943	11.369	11.350
12	174.00	-0.61751	10.949	11.376	11.349
10	184.10	-0.61818	10.826	11.270	11.276
10	184.36	-0.61882	10.830	11.274	11.275
10	184.76	-0.61917	10.827	11.273	11.272
12	198.11	-0.62918	10.717	11.188	11.190
13	199.40	-0.63019	10.709	11.183	11.182
13	199.74	-0.62978	10.700	11.175	11.181
10	203.47	-0.63001	10.674	11.156	11.160
10	203.66	-0.62971	10.668	11.150	11.159
13	224.84	-0.64527	10.517	11.049	11.063

TABLE A.7

Experimental Data of the Ionization Constant of Water in 1.0 mol kg⁻¹
KCl Solution.

Experiment	t (°C)	E (V)	pQ' _W	pK' _W	pK' _W (fitted)
14	74.76	-0.57361	12.384	12.667	12.652
14	75.05	-0.57379	12.380	12.663	12.646
14	75.52	-0.57354	12.365	12.649	12.637
16	80.44	-0.58185	12.273	12.550	12.540
16	80.65	-0.58205	12.270	12.548	12.536
16	97.67	-0.58326	11.906	12.203	12.230
16	97.93	-0.58371	11.906	12.204	12.226
16	98.23	-0.58346	11.896	12.194	12.221
14	100.07	-0.57867	11.888	12.198	12.190
14	100.32	-0.57864	11.883	12.193	12.186
14	100.49	-0.57852	11.877	12.188	12.184
14	123.98	-0.58408	11.486	11.829	11.838
14	124.24	-0.58433	11.484	11.828	11.834
14	124.52	-0.58458	11.482	11.826	11.831
16	125.88	-0.59037	11.434	11.772	11.813
16	125.96	-0.59020	11.430	11.769	11.812
15	145.25	-0.60370	11.236	11.604	11.580
15	146.22	-0.60416	11.224	11.594	11.569
14	148.44	-0.59207	11.150	11.531	11.545
14	148.70	-0.59232	11.149	11.531	11.543
14	148.75	-0.59214	11.146	11.528	11.542
17	172.62	-0.61540	10.919	11.338	11.311
17	173.19	-0.61589	10.916	11.336	11.306
15	176.09	-0.61692	10.884	11.309	11.281
15	177.30	-0.61798	10.877	11.305	11.271
18	199.90	-0.62598	10.639	11.118	11.101
18	200.73	-0.62576	10.625	11.106	11.095
17	201.34	-0.62526	10.602	11.084	11.091
15	203.01	-0.62796	10.609	11.095	11.080
15	204.32	-0.62734	10.584	11.073	11.071
18	224.53	-0.63613	10.411	10.955	10.951
18	225.66	-0.63583	10.393	10.940	10.945
18	226.66	-0.63520	10.374	10.924	10.940
15	227.86	-0.63729	10.373	10.926	10.933
15	228.89	-0.63713	10.358	10.915	10.928
15	230.21	-0.63586	10.328	10.889	10.921

Appendix B

SODIUM TETRABORATE BUFFER RESULTS

TABLE B.1

Activity Coefficients at Ionic Strengths of 0.02 and 0.1, as a Function of Temperature.

Ionic Strength = 0.02

t/°C	Bates-Guggenheim Convention	Liu and Lindsay's γ_{NaCl} Data
75	0.066	0.066
100	0.070	0.070
125	0.075	0.075
150	0.081	0.081
175	0.087	0.088
200	0.095	0.096
225	0.103	0.106
250	0.114	0.118

Ionic Strength = 0.1

75	0.121	0.121
100	0.129	0.127
125	0.138	0.137
150	0.148	0.149
175	0.160	0.163
200	0.174	0.179
225	0.190	0.199
250	0.210	0.222

TABLE B.2

Clark-Glew Temperature Variable Terms.

$t/^{\circ}\text{C}$	t_1	t_2	t_3
$\theta = 373.15 \text{ K}$			
25	-0.25155131E+00	0.27167481E-01	-0.37752583E-02
50	-0.15472695E+00	0.10863041E-01	-0.99353635E-03
75	-0.71808149E-01	0.24610678E-02	-0.11119051E-03
100	0.00000000E+00	0.00000000E+00	0.00000000E+00
125	0.62790421E-01	0.20579305E-02	0.90921561E-04
150	0.11816144E+00	0.75848377E-02	0.66329613E-03
175	0.16735472E+00	0.15792841E-01	0.20512117E-02
200	0.21134951E+00	0.26082525E-01	0.44742552E-02
225	0.25092848E+00	0.37992334E-01	0.80728655E-02
250	0.28672470E+00	0.51163119E-01	0.12932282E-01
$\theta = 423.15 \text{ K}$			
25	-0.41925219E+00	0.69122084E-01	-0.14395566E-01
50	-0.30945391E+00	0.39843722E-01	-0.65564074E-02
75	-0.21542445E+00	0.20331092E-01	-0.24798912E-02
100	-0.13399441E+00	0.82481338E-02	-0.66329613E-03
125	-0.62790421E-01	0.18924991E-02	-0.75295096E-04
150	0.00000000E+00	0.00000000E+00	0.00000000E+00
175	0.55784906E-01	0.16163790E-02	0.63054361E-04
200	0.10567475E+00	0.60110062E-02	0.46466828E-03
225	0.15055709E+00	0.12617454E-01	0.14501540E-02
250	0.19114980E+00	0.20991746E-01	0.31895774E-02

TABLE B.3

Terms Contributing to the Final Smoothed pOH's as a Function of Ionic Strength and Temperature.

$$m_{\text{Na}_2\text{B}_4\text{O}_7} = 0.01, \quad m_{\text{NaCl}} = 0.09 : \quad m_{\text{NaOH}} = 0.01, \quad m_{\text{NaCl}} = 0.1$$

$t/^{\circ}\text{C}$	$E \text{ (V)}$	$E_J \text{ (mV)}$	$-\log m_{\text{OH}^-}$	pOH	$\log Q_b^*$
75	-0.115922	4.275	3.740	3.865	3.732
100	-0.096047	4.067	3.352	3.485	3.333
125	-0.078388	3.770	3.040	3.182	3.000
150	-0.063059	3.369	2.791	2.944	2.721
175	-0.049906	2.896	2.594	2.759	2.483
200	-0.039001	2.361	2.441	2.620	2.282
225	-0.030081	1.829	2.323	2.519	2.113
250	-0.022978	1.351	2.234	2.451	1.973

$$m_{\text{Na}_2\text{B}_4\text{O}_7} = 0.01, \quad m_{\text{NaCl}} = 0.3 : \quad m_{\text{NaOH}} = 0.01, \quad m_{\text{NaCl}} = 0.3$$

75	-0.120352	1.141	3.757	3.930	3.749
100	-0.100891	1.067	3.376	3.559	3.358
125	-0.083358	0.969	3.066	3.262	3.029
150	-0.067989	0.832	2.818	3.029	2.752
175	-0.054605	0.680	2.620	2.848	2.515
200	-0.043366	0.496	2.465	2.713	2.315
225	-0.034015	0.311	2.345	2.616	2.145
250	-0.026555	0.150	2.255	2.554	2.007

$$m_{\text{Na}_2\text{B}_4\text{O}_7} = 0.01, \quad m_{\text{NaCl}} = 0.5 : \quad m_{\text{NaOH}} = 0.01, \quad m_{\text{NaCl}} = 0.5$$

75	-0.123459	0.703	3.797	3.992	3.790
100	-0.103533	0.658	3.406	3.614	3.389
125	-0.085739	0.600	3.092	3.314	3.057

$$* Q_b = (0.02 - m_{\text{OH}^-}) / ((0.02 + m_{\text{OH}^-}) m_{\text{OH}^-})$$

150	-0.070105	0.518	2.840	3.079	2.777
175	-0.056470	0.426	2.639	2.897	2.539
200	-0.044813	0.313	2.479	2.760	2.334
225	-0.034952	0.198	2.354	2.661	2.159
250	-0.026663	0.093	2.256	2.595	2.009

$$m_{\text{Na}_2\text{B}_4\text{O}_7} = 0.05, \quad m_{\text{NaCl}} = 0 \quad : \quad m_{\text{NaOH}} = 0.01, \quad m_{\text{NaCl}} = 0.1$$

$t/^{\circ}\text{C}$	$E \text{ (V)}$	$E_J \text{ (mV)}$	$-\log m_{\text{OH}^-}$	pOH	$\log Q_b^*$
75	-0.105303	5.568	3.609	3.730	3.607
100	-0.085759	5.323	3.234	3.363	3.229
125	-0.066884	4.923	2.913	3.051	2.902
150	-0.049144	4.357	2.642	2.790	2.622
175	-0.032859	3.582	2.415	2.575	2.382
200	-0.018325	2.665	2.229	2.403	2.178
225	-0.005705	1.693	2.081	2.271	2.009
250	0.005189	0.765	1.964	2.174	1.869

$$m_{\text{Na}_2\text{B}_4\text{O}_7} = 0.05, \quad m_{\text{NaCl}} = 0.21 \quad : \quad m_{\text{NaOH}} = 0.01, \quad m_{\text{NaCl}} = 0.3$$

75	-0.114837	1.545	3.685	3.856	3.683
100	-0.095753	1.465	3.313	3.495	3.309
125	-0.077292	1.348	2.995	3.190	2.986
150	-0.059834	1.180	2.727	2.936	2.711
175	-0.043653	0.961	2.502	2.728	2.475
200	-0.029088	0.693	2.317	2.563	2.275
225	-0.016230	0.404	2.168	2.437	2.109

$$^* Q_b = (0.1 - m_{\text{OH}^-}) / ((0.1 + m_{\text{OH}^-}) m_{\text{OH}^-})$$

250 -0.004888 0.123 2.048 2.345 1.970

$m_{\text{Na}_2\text{B}_4\text{O}_7} = 0.05$, $m_{\text{NaCl}} = 0.41$: $m_{\text{NaOH}} = 0.01$, $m_{\text{NaCl}} = 0.5$

$t/^{\circ}\text{C}$	$E \text{ (V)}$	$E_J \text{ (mV)}$	$-\log m_{\text{OH}^-}$	pOH	$\log Q_b$
75	-0.118036	0.945	3.722	3.917	3.720
100	-0.098852	0.898	3.347	3.554	3.343
125	-0.080531	0.830	3.030	3.251	3.022
150	-0.063256	0.733	2.762	3.000	2.747
175	-0.047395	0.609	2.540	2.797	2.515
200	-0.032934	0.456	2.356	2.635	2.318
225	-0.019838	0.287	2.204	2.509	2.150
250	-0.008263	0.121	2.081	2.418	2.009

TABLE B.4

Equation Coefficients For the 0.01 mol kg⁻¹ and 0.05 mol kg⁻¹ Sodium Tetraborate Buffers.

$$\text{Clark-Glew Equation } \text{pOH} = a_0 + a_1 t_1 + a_2 t_2 + a_3 t_3$$

I	a ₀	a ₁	a ₂	a ₃	n	s _f
Bates-Guggenheim activity coefficients, 0.01 mol kg ⁻¹ Sodium Tetraborate.						
0	2.91188	-3.55981	8.25061	6.25317	216	0.010
0.11	2.94395	-3.55047	8.19944	4.17842	73	0.003
0.32	3.02877	-3.47975	8.16629	5.84045	72	0.006
0.52	3.07896	-3.50728	8.25006	4.10322	71	0.006

Bates-Guggenheim activity coefficients, 0.05 mol kg ⁻¹ Sodium Tetraborate.						
0	2.74998	-4.05604	5.21532	14.18170	207	0.019
0.10	2.79007	-4.01737	5.26425	13.05119	71	0.003
0.31	2.93597	-3.89335	5.47358	12.16570	69	0.003
0.51	3.00041	-3.82480	5.68302	9.28676	68	0.003

I	a ₀	a ₁	a ₂	a ₃
NaCl activity coefficients, 0.01 mol kg ⁻¹ Sodium Tetraborate.				
0	2.91428	-3.53569	8.31877	5.01562
0.11	2.94339	-3.52131	8.47770	4.23432
0.32	3.02318	-3.41986	8.68022	6.23263
0.52	3.06985	-3.41284	8.99525	3.91005

I	a_0	a_1	a_2	a_3
NaCl activity coefficients, 0.05 mol kg ⁻¹ Sodium Tetraborate.				
0	2.75293	-4.03873	5.35807	14.16244
0.10	2.79032	-3.98361	5.57344	12.90579
0.31	2.93021	-3.83018	5.94834	11.89968
0.51	2.99186	-3.72799	6.39562	9.03763

Fit at the buffer ionic strength, 0.01 mol kg⁻¹ Sodium Tetraborate.

- 1) pOH, Bates-Guggenheim convention.
- 2) pOH, NaCl activity coefficients
- 3) pH, NaCl activity coefficients, pK_W^0 from I=0.5
- 4) pH, NaCl activity coefficients, pK_W^0 from I=1.0
- 5) pH, NaCl activity coefficients, IAPS equation

1)	0.02	2.91865	-3.55799	8.24180	6.36600
2)	0.02	2.92042	-3.52852	8.35158	4.96479
3)	0.02	8.70838	-0.39934	5.01979	3.76938
4)	0.02	8.69832	-0.48303	5.56916	7.71667
5)	0.02	8.71474	-0.53740	4.10494	16.74368

Fit at the buffer ionic strength, 0.05 mol kg⁻¹ Sodium Tetraborate.

1)	0.10	2.80124	-4.00942	5.34710	13.51753
2)	0.10	2.80318	-3.96607	5.52200	12.46913
3)	0.10	8.82562	0.03820	7.84937	-3.73496
4)	0.10	8.81556	-0.04549	8.39874	0.21232
5)	0.10	8.83198	-0.09986	6.93452	9.23934

TABLE B.5

Solution Concentrations Used in Determining the pOH's of 0.01 mol kg⁻¹
Sodium Tetraborate.

Experiment	$m_{\text{Na}_2\text{B}_4\text{O}_7}$	m_{NaCl} :	m_{NaOH}	m_{NaCl}
1,2,3	0.010033	0.100766	9.999×10^{-3}	0.099832
7,8,9	0.010009	0.298667	9.826×10^{-3}	0.295761
13,14,15,16	0.010259	0.514834	9.031×10^{-3}	0.515462
10,11,12	0.010265	0.303404	9.385×10^{-3}	0.305758
4,5,6	0.010180	0.101416	9.225×10^{-3}	0.102603
17,18	0.010279	0.509764	9.880×10^{-3}	0.511051

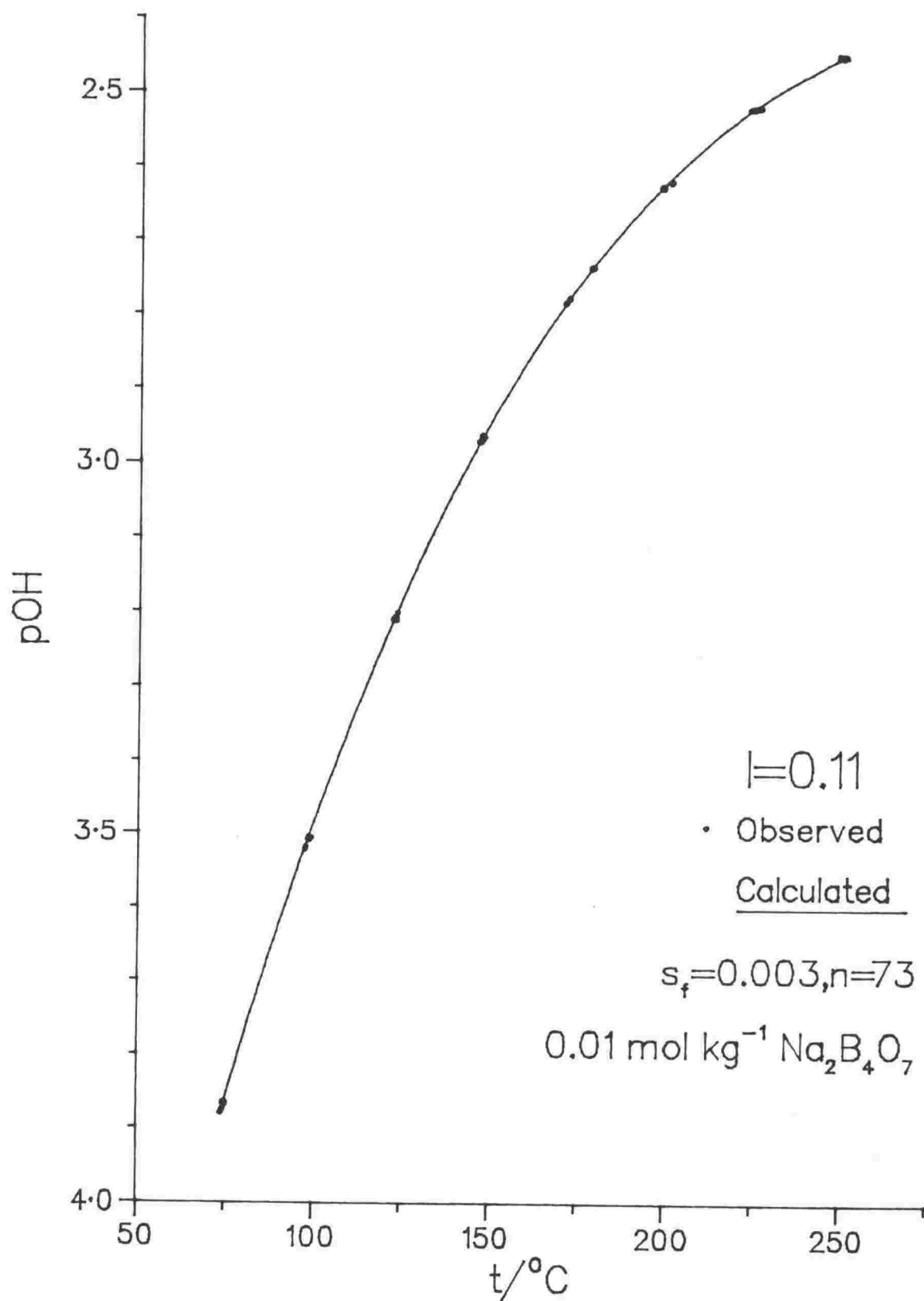


Figure B.1: The Temperature Dependence of pOH of 0.01 mol kg^{-1} Sodium Tetraborate in 0.1 mol kg^{-1} NaCl Solution.

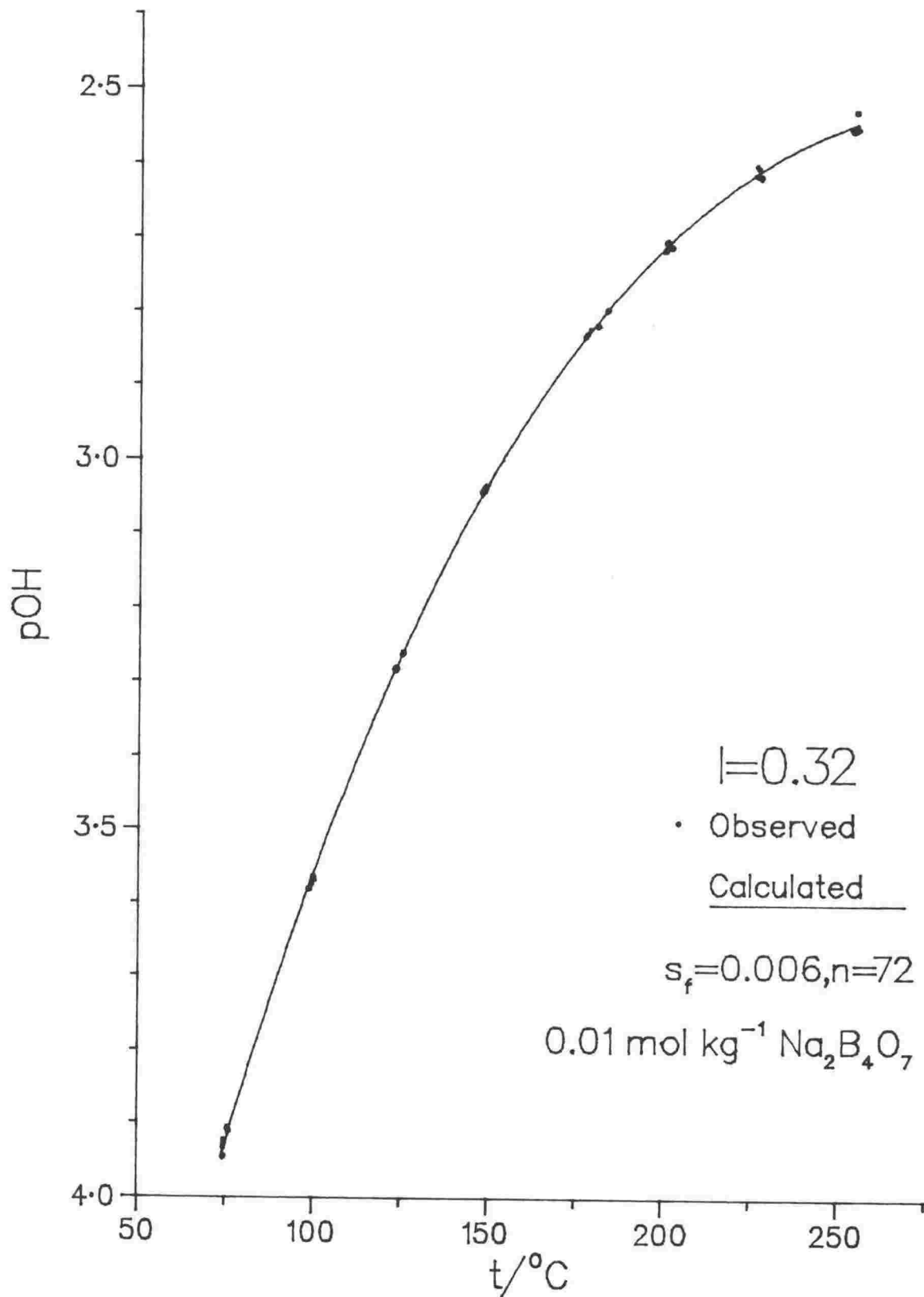


Figure B.2: The Temperature Dependence of pOH of 0.01 mol kg^{-1} Sodium Tetraborate in 0.3 mol kg^{-1} NaCl Solution.

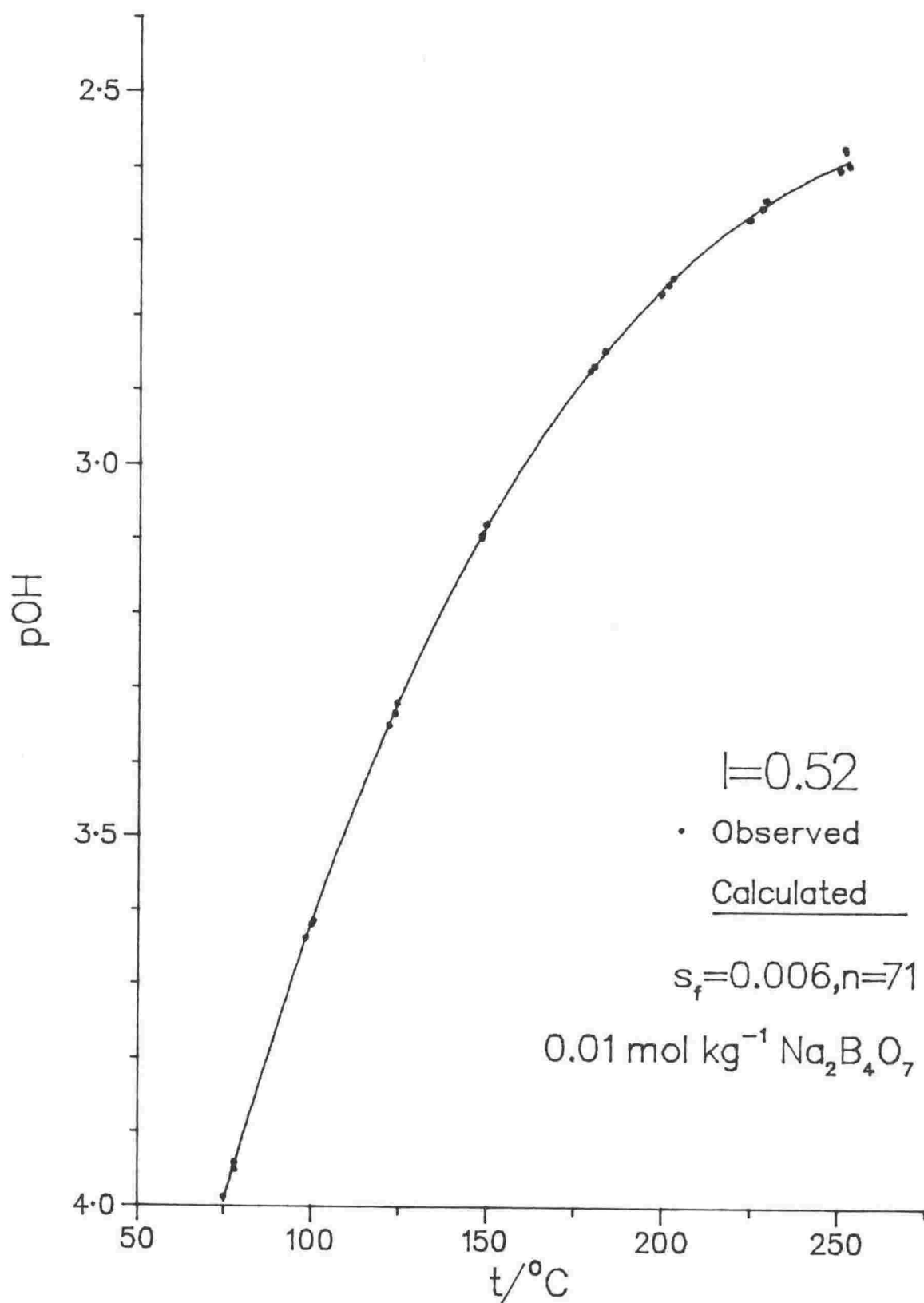


Figure B.3: The Temperature Dependence of pOH of 0.01 mol kg⁻¹ Sodium Tetraborate in 0.5 mol kg⁻¹ NaCl Solution.

TABLE B.6

Experimental pOH data of 0.01 mol kg⁻¹ Sodium Tetraborate in
0.1 mol kg⁻¹ NaCl Solution.

Experiment	t/°C	E (V)	-logm _{OH⁻}	pOH	pOH (fitted)
3	73.99	-0.117972	3.752	3.880	3.882
3	74.33	-0.117782	3.747	3.876	3.877
3	74.40	-0.117755	3.746	3.875	3.875
1	74.49	-0.117137	3.737	3.866	3.874
1	74.69	-0.117207	3.737	3.866	3.870
1	74.75	-0.117229	3.738	3.866	3.869
2	75.06	-0.117509	3.740	3.869	3.864
2	75.12	-0.117352	3.737	3.866	3.863
2	75.12	-0.117294	3.736	3.865	3.863
1	97.46	-0.099472	3.386	3.522	3.519
1	97.70	-0.099254	3.382	3.518	3.516
2	98.28	-0.098595	3.371	3.508	3.508
2	98.53	-0.098405	3.368	3.504	3.505
2	98.54	-0.098425	3.368	3.505	3.504
3	98.65	-0.098808	3.372	3.509	3.503
3	98.70	-0.098730	3.371	3.508	3.502
3	98.90	-0.098591	3.369	3.505	3.500
2	122.09	-0.081375	3.065	3.210	3.214
2	122.23	-0.081239	3.063	3.209	3.212
2	122.25	-0.081229	3.063	3.208	3.212
3	122.84	-0.081400	3.063	3.209	3.206
3	122.87	-0.081370	3.063	3.209	3.205
3	122.90	-0.081349	3.063	3.208	3.205
1	122.91	-0.081092	3.059	3.205	3.205
1	123.33	-0.080817	3.055	3.200	3.200
1	123.37	-0.080781	3.054	3.200	3.200
2	146.21	-0.066113	2.816	2.971	2.976
3	147.03	-0.066197	2.815	2.971	2.969
1	147.07	-0.065845	2.811	2.967	2.969
1	147.08	-0.065797	2.810	2.966	2.969
2	147.16	-0.065613	2.808	2.964	2.968
3	147.30	-0.066033	2.812	2.969	2.967
1	147.31	-0.065648	2.808	2.964	2.967
2	147.37	-0.065489	2.806	2.962	2.966
3	147.83	-0.065707	2.807	2.964	2.962
1	170.74	-0.053066	2.617	2.785	2.787
1	170.95	-0.052961	2.615	2.784	2.786
1	171.19	-0.052925	2.614	2.783	2.784
2	171.82	-0.052635	2.610	2.779	2.780
2	171.84	-0.052669	2.611	2.779	2.780
2	172.07	-0.052507	2.608	2.777	2.779
6	178.15	-0.046519	2.565	2.738	2.740
6	178.16	-0.046422	2.564	2.737	2.739
6	178.19	-0.046527	2.565	2.738	2.739
5	178.37	-0.046589	2.566	2.738	2.738
5	178.57	-0.046525	2.565	2.737	2.737
5	178.75	-0.046459	2.564	2.737	2.736

6	198.17	-0.037688	2.444	2.628	2.629
6	198.30	-0.037624	2.443	2.627	2.628
6	198.37	-0.037590	2.442	2.627	2.628
5	198.53	-0.037758	2.444	2.629	2.627
5	198.67	-0.037727	2.443	2.628	2.626
5	198.76	-0.037676	2.443	2.628	2.626
4	200.78	-0.037086	2.435	2.621	2.616
4	200.98	-0.037026	2.434	2.620	2.615
4	201.18	-0.037036	2.434	2.620	2.614
6	223.32	-0.028167	2.321	2.522	2.525
6	224.06	-0.028084	2.319	2.521	2.522
5	224.22	-0.028017	2.318	2.521	2.522
6	224.35	-0.028014	2.318	2.521	2.521
5	224.53	-0.028070	2.319	2.521	2.520
5	224.71	-0.028010	2.318	2.521	2.520
4	226.06	-0.027846	2.315	2.519	2.515
4	226.27	-0.027940	2.316	2.520	2.515
4	226.30	-0.027881	2.316	2.519	2.515
4	248.68	-0.020706	2.229	2.452	2.454
4	248.79	-0.020356	2.226	2.449	2.453
5	249.24	-0.020467	2.227	2.450	2.452
5	249.49	-0.020586	2.228	2.451	2.452
5	249.67	-0.020461	2.227	2.450	2.451
6	249.77	-0.020569	2.228	2.451	2.451
6	250.00	-0.020504	2.227	2.451	2.451
6	250.27	-0.020383	2.226	2.450	2.450

TABLE B.7

Experimental pOH data of 0.01 mol kg⁻¹ Sodium Tetraborate in
0.3 mol kg⁻¹ NaCl Solution.

Experiment	t/°C	E (V)	-log _m OH ⁻	pOH	pOH (fitted)
7	74.37	-0.120919	3.774	3.946	3.940
7	74.48	-0.120835	3.772	3.945	3.939
8	74.61	-0.120020	3.760	3.932	3.936
7	74.62	-0.120818	3.771	3.944	3.936
8	74.68	-0.119784	3.756	3.928	3.935
8	74.78	-0.119468	3.751	3.923	3.934
9	75.81	-0.118686	3.734	3.907	3.917
9	75.92	-0.118911	3.737	3.910	3.915
9	75.99	-0.119073	3.739	3.912	3.914
7	98.67	-0.101841	3.399	3.581	3.576
7	98.80	-0.101779	3.397	3.580	3.575
7	98.84	-0.101754	3.397	3.580	3.574
8	99.33	-0.101454	3.391	3.574	3.567
9	99.58	-0.101132	3.386	3.569	3.564
8	99.79	-0.101087	3.384	3.567	3.561
9	99.82	-0.100870	3.381	3.564	3.561
9	99.87	-0.100767	3.380	3.563	3.560
8	99.94	-0.100968	3.382	3.565	3.559
7	122.93	-0.084239	3.088	3.283	3.284
7	122.93	-0.084271	3.088	3.283	3.284
8	122.93	-0.084329	3.089	3.284	3.284
7	122.98	-0.084218	3.088	3.282	3.284
8	123.08	-0.084182	3.087	3.282	3.283
8	123.22	-0.084067	3.085	3.280	3.281
9	124.92	-0.082969	3.066	3.262	3.263
9	125.21	-0.082761	3.063	3.259	3.260
9	125.23	-0.082728	3.062	3.259	3.260
8	147.72	-0.068455	2.834	3.043	3.048
8	147.77	-0.068442	2.833	3.043	3.047
8	147.79	-0.068486	2.834	3.043	3.047
7	148.26	-0.068130	2.829	3.038	3.043
9	148.27	-0.068276	2.830	3.040	3.043
9	148.28	-0.068268	2.830	3.040	3.043
9	148.28	-0.068321	2.831	3.041	3.043
7	148.36	-0.068125	2.828	3.038	3.042
7	148.53	-0.068001	2.826	3.036	3.041
10	177.03	-0.050909	2.603	2.833	2.836
10	177.64	-0.050578	2.598	2.829	2.832
10	178.54	-0.050105	2.592	2.823	2.826
11	180.68	-0.049792	2.585	2.819	2.814
11	180.79	-0.049776	2.585	2.818	2.813
11	180.81	-0.049729	2.584	2.818	2.813
12	183.27	-0.048048	2.563	2.798	2.799
12	183.51	-0.047992	2.562	2.797	2.797
12	183.62	-0.047923	2.561	2.796	2.797
12	199.81	-0.041074	2.468	2.717	2.714
12	200.09	-0.041042	2.468	2.716	2.712

10	200.27	-0.040026	2.457	2.706	2.712
12	200.33	-0.040973	2.467	2.716	2.711
10	200.55	-0.039915	2.455	2.704	2.710
10	200.62	-0.039860	2.454	2.704	2.710
11	201.88	-0.040602	2.461	2.712	2.704
11	201.90	-0.040691	2.462	2.713	2.704
11	201.92	-0.040624	2.461	2.712	2.704
12	225.89	-0.030950	2.341	2.614	2.614
10	226.11	-0.029817	2.329	2.602	2.613
12	226.29	-0.030916	2.340	2.614	2.612
10	226.51	-0.030097	2.332	2.605	2.612
12	226.55	-0.031092	2.342	2.615	2.612
10	226.76	-0.030050	2.331	2.605	2.611
11	227.33	-0.031134	2.342	2.616	2.609
11	227.46	-0.031323	2.344	2.618	2.609
11	227.46	-0.031074	2.341	2.616	2.609
12	253.26	-0.023112	2.248	2.552	2.548
11	253.49	-0.023386	2.250	2.555	2.547
11	253.55	-0.023151	2.248	2.553	2.547
12	253.88	-0.023211	2.248	2.554	2.547
11	254.02	-0.023348	2.250	2.555	2.546
10	254.45	-0.020654	2.223	2.529	2.546
10	254.58	-0.020653	2.223	2.529	2.545
10	254.76	-0.020583	2.222	2.529	2.545
12	255.10	-0.022901	2.245	2.552	2.545

TABLE B.8

Experimental pOH data of 0.01 mol kg⁻¹ Sodium Tetraborate in
0.5 mol kg⁻¹ NaCl Solution.

Experiment	t/°C	E (V)	-log _m OH ⁻	pOH	pOH (fitted)
17	74.84	-0.122631	3.790	3.987	3.995
17	74.88	-0.122674	3.791	3.987	3.994
17	74.88	-0.122696	3.791	3.988	3.994
18	77.78	-0.121107	3.754	3.951	3.946
13	77.89	-0.117883	3.744	3.942	3.944
13	77.89	-0.117903	3.744	3.942	3.944
13	77.91	-0.117983	3.745	3.944	3.944
18	77.92	-0.121076	3.753	3.950	3.943
18	78.00	-0.121115	3.753	3.950	3.942
17	98.12	-0.104371	3.430	3.638	3.640
17	98.14	-0.104386	3.430	3.638	3.639
17	98.15	-0.104317	3.429	3.637	3.639
18	99.79	-0.103461	3.411	3.620	3.617
18	99.89	-0.103397	3.410	3.619	3.616
13	100.28	-0.100387	3.405	3.615	3.610
13	100.40	-0.100383	3.405	3.614	3.609
13	100.48	-0.100330	3.404	3.613	3.608
18	121.75	-0.087472	3.128	3.350	3.350
18	121.75	-0.087432	3.128	3.349	3.350
18	121.77	-0.087447	3.128	3.349	3.349
13	123.43	-0.083470	3.110	3.332	3.331
13	123.55	-0.083690	3.113	3.335	3.330
13	123.60	-0.083503	3.110	3.333	3.329
17	124.01	-0.085545	3.097	3.320	3.325
17	124.02	-0.085629	3.098	3.321	3.325
17	124.05	-0.085653	3.099	3.321	3.325
13	147.96	-0.067732	2.859	3.098	3.096
13	147.97	-0.067646	2.858	3.097	3.096
18	148.03	-0.070609	2.855	3.094	3.095
13	148.04	-0.067676	2.858	3.097	3.095
18	148.11	-0.070529	2.854	3.093	3.095
18	148.17	-0.070517	2.854	3.093	3.094
17	149.21	-0.069591	2.841	3.080	3.086
17	149.23	-0.069614	2.841	3.081	3.085
17	149.60	-0.069406	2.838	3.078	3.082
15	178.89	-0.050554	2.610	2.873	2.873
15	179.07	-0.050469	2.609	2.872	2.872
15	179.08	-0.050419	2.608	2.872	2.872
16	179.84	-0.049943	2.602	2.866	2.867
16	180.11	-0.049944	2.602	2.866	2.865
16	180.18	-0.049903	2.601	2.866	2.865
14	182.96	-0.048196	2.579	2.846	2.849
14	183.00	-0.048105	2.578	2.844	2.848
14	183.04	-0.048122	2.578	2.845	2.848
15	198.95	-0.041487	2.488	2.770	2.765
15	199.13	-0.041468	2.488	2.769	2.764
15	199.17	-0.041362	2.487	2.768	2.764

16	200.98	-0.040264	2.473	2.757	2.755
16	201.03	-0.040271	2.473	2.757	2.755
16	201.04	-0.040259	2.473	2.757	2.755
14	202.27	-0.039469	2.463	2.748	2.749
14	202.47	-0.039387	2.462	2.747	2.748
14	202.52	-0.039396	2.462	2.747	2.748
15	223.67	-0.031399	2.362	2.670	2.665
15	224.28	-0.031310	2.361	2.669	2.663
15	224.40	-0.031294	2.361	2.669	2.663
16	227.53	-0.029755	2.343	2.655	2.653
16	227.64	-0.029712	2.343	2.655	2.653
16	227.78	-0.029680	2.342	2.654	2.652
14	228.30	-0.028548	2.331	2.643	2.650
14	228.71	-0.028502	2.330	2.643	2.649
14	228.93	-0.028458	2.329	2.643	2.649
15	249.72	-0.022840	2.263	2.604	2.595
15	249.79	-0.022734	2.262	2.603	2.595
15	249.88	-0.022848	2.263	2.604	2.595
14	251.10	-0.019550	2.230	2.573	2.593
14	251.27	-0.019718	2.232	2.575	2.592
14	251.46	-0.020031	2.235	2.578	2.592
16	252.44	-0.021847	2.252	2.597	2.590
16	252.46	-0.021840	2.252	2.597	2.590
16	252.48	-0.021856	2.252	2.597	2.590

TABLE B.9

Solution Concentrations used in Determining the pOH's of 0.05 mol kg⁻¹
Sodium Tetraborate.

Experiment	$m_{\text{Na}_2\text{B}_4\text{O}_7}$	m_{NaCl}	:	m_{NaOH}	m_{NaCl}
13,14,15	0.050531	0.399917		0.011769	0.509416
7,8,9	0.051370	0.208432		0.014320	0.306979
1,2,3	0.050153	0.0		0.013418	0.101893
16,17,18	0.050436	0.404028		0.013199	0.510464
10,11,12	0.051536	0.204285		0.012362	0.312917
4,5,6	0.050373	0.0		0.012632	0.101826

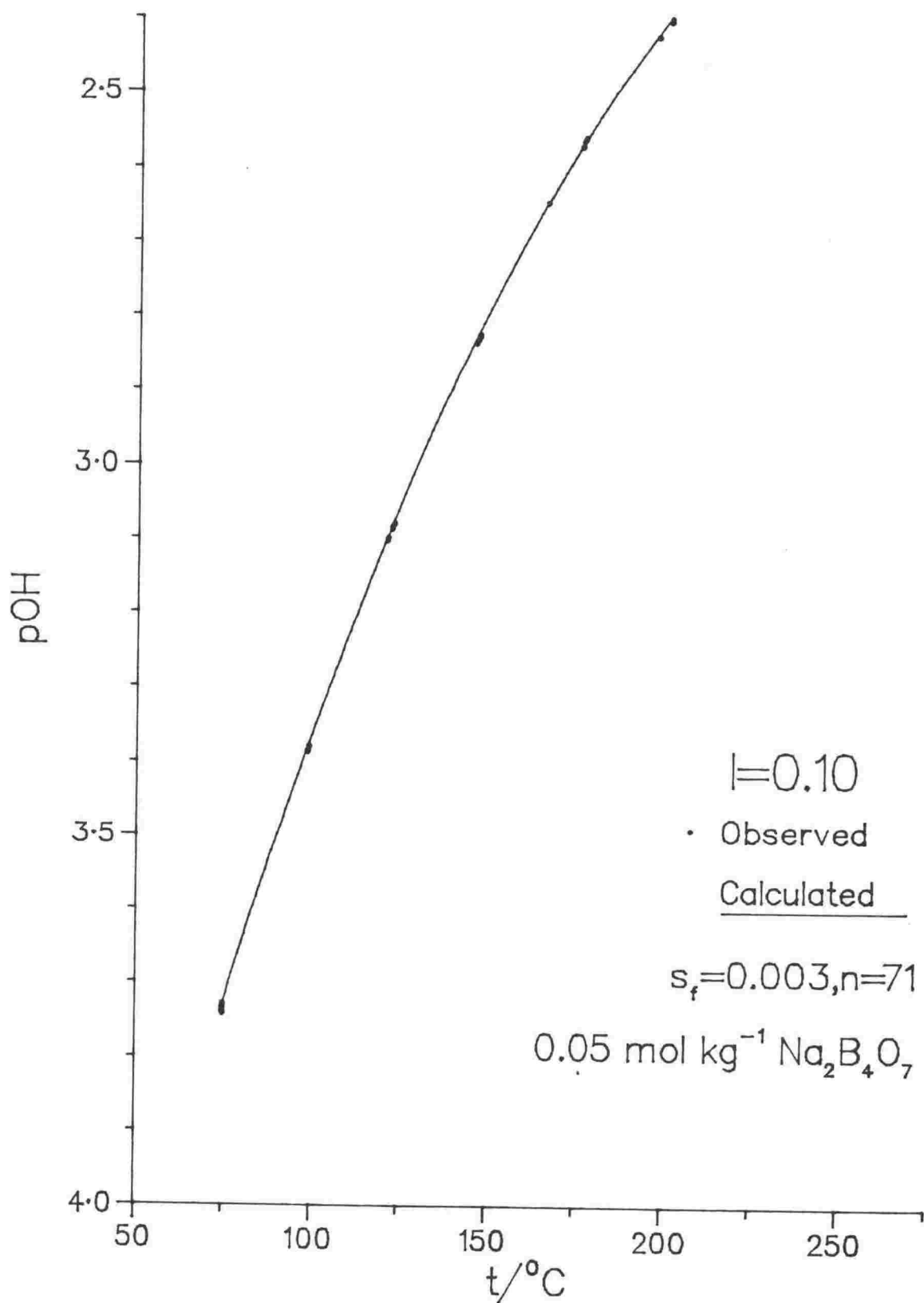


Figure B.4: The Temperature Dependence of pOH of 0.05 mol kg^{-1} Sodium Tetraborate Solution, No Added NaCl.

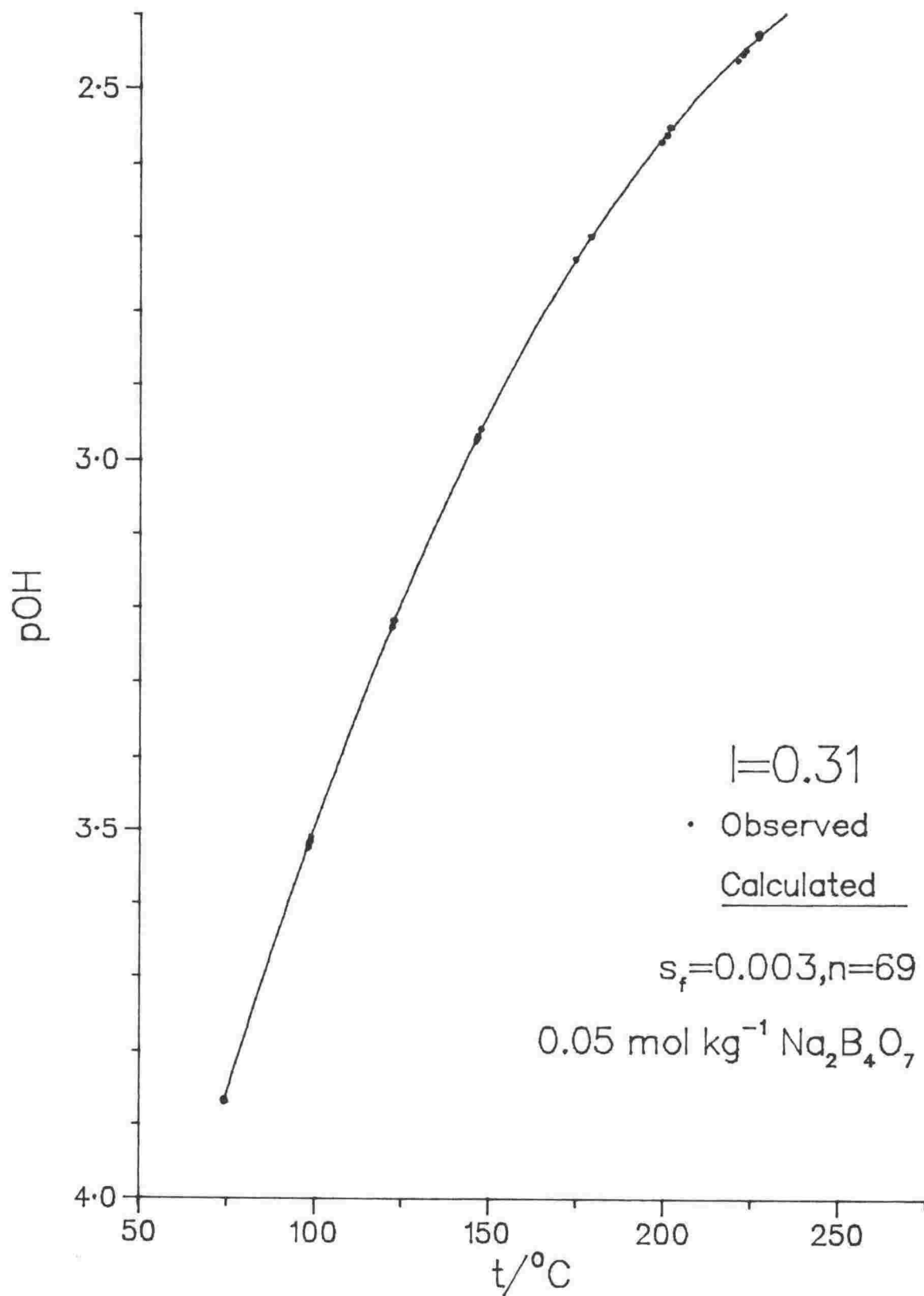


Figure B.5: The Temperature Dependence of pOH of 0.05 mol kg^{-1} Sodium Tetraborate in 0.2 mol kg^{-1} NaCl Solution.

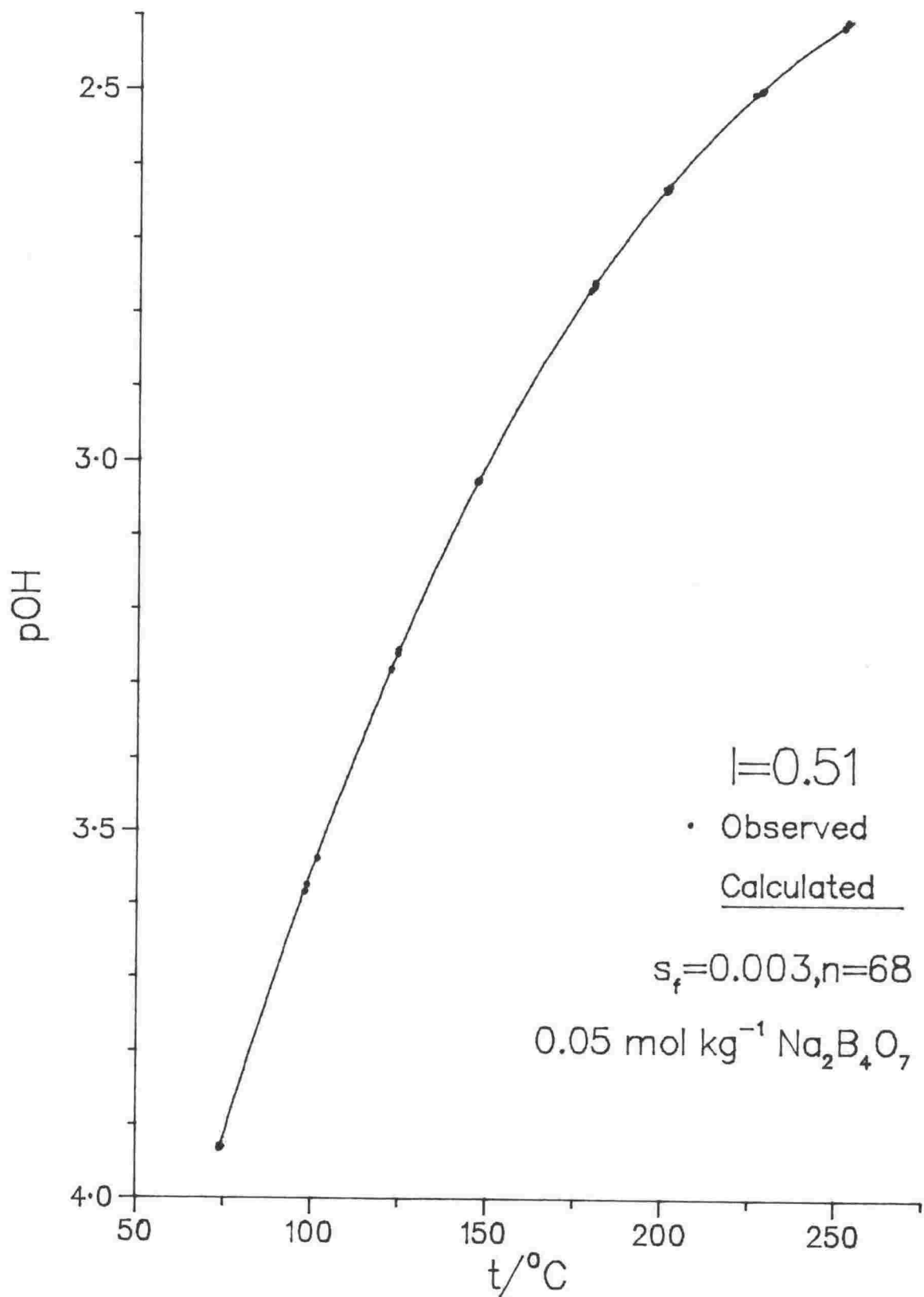


Figure B.6: The Temperature Dependence of pOH of 0.05 mol kg^{-1} Sodium Tetraborate in 0.4 mol kg^{-1} NaCl Solution.

TABLE B.10

Experimental pOH data of 0.05 mol kg⁻¹ Sodium Tetraborate Solution, No Added NaCl.

Experiment	t/°C	E (V)	-logm _{OH⁻}	pOH	pOH (fitted)
3	74.60	-0.112805	3.621	3.742	3.737
2	74.61	-0.112398	3.615	3.736	3.736
2	74.62	-0.112341	3.614	3.735	3.736
2	74.62	-0.112376	3.615	3.736	3.736
3	74.62	-0.112750	3.620	3.741	3.736
3	74.65	-0.112854	3.622	3.743	3.736
1	74.67	-0.111971	3.609	3.730	3.735
1	74.73	-0.112033	3.609	3.730	3.734
1	74.78	-0.112139	3.611	3.732	3.734
1	98.18	-0.094406	3.257	3.385	3.388
1	98.31	-0.094385	3.256	3.384	3.386
3	98.38	-0.094518	3.258	3.386	3.385
3	98.40	-0.094481	3.257	3.385	3.385
3	98.43	-0.094480	3.257	3.385	3.385
1	98.61	-0.094203	3.253	3.381	3.382
2	98.61	-0.094044	3.251	3.379	3.382
2	98.74	-0.094021	3.250	3.378	3.380
2	98.78	-0.094067	3.250	3.379	3.380
1	120.60	-0.078157	2.967	3.103	3.102
1	120.66	-0.078063	2.965	3.101	3.102
1	120.82	-0.077906	2.962	3.098	3.100
3	121.98	-0.077105	2.949	3.086	3.086
3	122.09	-0.076989	2.947	3.083	3.085
3	122.19	-0.076922	2.946	3.082	3.084
2	122.70	-0.076683	2.942	3.079	3.078
2	122.71	-0.076697	2.942	3.079	3.078
2	122.74	-0.076646	2.941	3.078	3.077
2	145.64	-0.061077	2.690	2.836	2.832
2	146.01	-0.060849	2.686	2.832	2.829
2	146.26	-0.060667	2.683	2.830	2.826
3	146.47	-0.060564	2.682	2.828	2.824
3	146.55	-0.060449	2.680	2.827	2.823
3	146.57	-0.060404	2.679	2.826	2.823
1	146.60	-0.060348	2.679	2.825	2.823
1	146.75	-0.060299	2.678	2.824	2.821
1	146.75	-0.060306	2.678	2.825	2.821
6	165.72	-0.045727	2.491	2.646	2.650
6	165.74	-0.045673	2.490	2.646	2.650
6	165.76	-0.045693	2.490	2.646	2.650
5	175.46	-0.039980	2.410	2.570	2.572
5	175.54	-0.040015	2.410	2.570	2.571
5	175.64	-0.039995	2.410	2.570	2.570
4	175.89	-0.039393	2.402	2.563	2.568
4	176.28	-0.039169	2.399	2.560	2.565
4	176.48	-0.039018	2.397	2.558	2.564
6	196.81	-0.028081	2.251	2.423	2.423
6	196.96	-0.028052	2.251	2.423	2.422

6	197.12	-0.028017	2.250	2.423	2.421
5	200.43	-0.026353	2.229	2.403	2.401
5	200.58	-0.026329	2.228	2.403	2.400
5	200.66	-0.026265	2.228	2.402	2.399
4	200.76	-0.025933	2.224	2.398	2.399
4	200.93	-0.025824	2.223	2.397	2.398
4	201.13	-0.025684	2.221	2.396	2.396
6	222.08	-0.015523	2.096	2.284	2.284
6	222.21	-0.015424	2.095	2.283	2.284
6	222.26	-0.015369	2.094	2.283	2.283
5	222.74	-0.015337	2.094	2.282	2.281
5	223.37	-0.014924	2.089	2.278	2.278
5	223.65	-0.014752	2.087	2.276	2.277
4	224.49	-0.014442	2.083	2.273	2.273
4	224.97	-0.014317	2.082	2.272	2.271
4	225.33	-0.014166	2.080	2.271	2.269
5	248.32	-0.003853	1.964	2.173	2.180
5	249.17	-0.003776	1.963	2.173	2.177
6	249.86	-0.004085	1.967	2.177	2.175
6	249.92	-0.003839	1.964	2.174	2.175
6	249.92	-0.004026	1.966	2.176	2.175
4	252.34	-0.003023	1.955	2.168	2.167
4	252.81	-0.002949	1.954	2.167	2.166
4	253.03	-0.002967	1.955	2.168	2.165

TABLE B.11

Experimental pOH data of 0.05 mol kg⁻¹ Sodium Tetraborate in
0.2 mol kg⁻¹ NaCl Solution.

Experiment	t/°C	E (V)	-logm _{OH⁻}	pOH	pOH (fitted)
9	73.92	-0.124893	3.697	3.868	3.873
9	73.96	-0.124959	3.697	3.868	3.872
9	74.03	-0.125024	3.698	3.869	3.871
7	74.16	-0.124796	3.694	3.865	3.869
7	74.17	-0.124948	3.696	3.867	3.869
7	74.21	-0.125121	3.699	3.870	3.868
8	74.42	-0.124933	3.694	3.865	3.865
8	74.46	-0.125027	3.696	3.867	3.864
8	74.55	-0.125139	3.697	3.868	3.863
7	98.12	-0.107844	3.343	3.524	3.520
7	98.13	-0.107728	3.342	3.523	3.520
7	98.14	-0.107783	3.342	3.524	3.520
8	98.26	-0.107426	3.337	3.518	3.518
8	98.40	-0.107374	3.336	3.517	3.516
9	98.54	-0.107365	3.335	3.517	3.514
8	98.60	-0.107324	3.334	3.516	3.513
9	98.73	-0.107146	3.331	3.513	3.512
9	98.89	-0.106920	3.328	3.509	3.510
7	121.90	-0.090681	3.033	3.226	3.225
7	121.99	-0.090621	3.032	3.225	3.224
7	122.04	-0.090603	3.031	3.224	3.223
8	122.30	-0.090071	3.024	3.217	3.220
8	122.31	-0.090101	3.024	3.217	3.220
9	122.38	-0.090136	3.024	3.217	3.219
8	122.45	-0.090048	3.023	3.216	3.219
9	122.48	-0.090148	3.024	3.217	3.218
9	122.57	-0.090105	3.023	3.217	3.217
7	146.01	-0.074460	2.767	2.974	2.973
7	146.21	-0.074314	2.765	2.972	2.971
7	146.29	-0.074239	2.764	2.971	2.971
9	146.54	-0.073920	2.760	2.967	2.968
9	146.56	-0.073960	2.760	2.967	2.968
9	146.60	-0.073920	2.760	2.967	2.968
8	147.48	-0.073331	2.750	2.958	2.959
8	147.53	-0.073280	2.750	2.958	2.959
8	147.62	-0.073240	2.749	2.957	2.958
12	174.65	-0.050651	2.503	2.729	2.731
12	174.69	-0.050706	2.504	2.729	2.731
12	174.71	-0.050653	2.503	2.729	2.731
11	178.90	-0.048141	2.469	2.698	2.700
11	179.07	-0.048220	2.470	2.699	2.699
11	179.12	-0.048172	2.469	2.698	2.698
12	199.22	-0.037146	2.326	2.570	2.568
12	199.31	-0.037118	2.325	2.570	2.567
12	199.31	-0.037082	2.325	2.570	2.567
11	200.71	-0.036340	2.316	2.561	2.559
11	200.84	-0.036265	2.315	2.561	2.558

11	200.88	-0.036237	2.314	2.560	2.558
10	201.44	-0.035359	2.305	2.551	2.555
10	201.78	-0.035325	2.304	2.550	2.553
10	201.88	-0.035279	2.303	2.550	2.552
12	221.07	-0.026525	2.197	2.461	2.454
12	222.54	-0.025729	2.188	2.453	2.447
12	223.46	-0.025113	2.181	2.447	2.443
10	226.55	-0.022780	2.155	2.425	2.430
11	227.01	-0.023169	2.159	2.429	2.428
11	227.01	-0.023186	2.159	2.429	2.428
10	227.05	-0.022729	2.154	2.424	2.428
11	227.05	-0.023215	2.159	2.429	2.428
10	227.10	-0.022701	2.154	2.424	2.428
12	250.07	-0.013549	2.053	2.349	2.345
12	250.26	-0.013012	2.048	2.344	2.345
12	250.40	-0.013285	2.050	2.347	2.344
11	251.33	-0.012923	2.047	2.344	2.342
10	251.40	-0.011853	2.036	2.334	2.341
11	251.45	-0.012878	2.046	2.344	2.341
11	251.51	-0.012734	2.045	2.343	2.341
10	251.93	-0.011845	2.038	2.334	2.340
10	252.20	-0.011850	2.036	2.335	2.339

TABLE B.12

Experimental pOH data of 0.05 mol kg⁻¹ Sodium Tetraborate in
0.4 mol kg⁻¹ NaCl Solution.

Experiment	t/°C	E (V)	-log _m OH ⁻	pOH	pOH (fitted)
15	73.70	-0.122890	3.740	3.933	3.938
15	73.89	-0.122860	3.739	3.932	3.935
13	73.93	-0.122626	3.735	3.928	3.934
15	74.02	-0.122856	3.738	3.931	3.932
13	74.09	-0.122618	3.734	3.927	3.931
13	74.22	-0.122696	3.735	3.928	3.929
14	74.31	-0.122853	3.736	3.930	3.928
14	74.35	-0.122911	3.737	3.930	3.927
14	74.40	-0.122965	3.737	3.931	3.926
13	97.83	-0.105092	3.380	3.585	3.583
13	97.98	-0.105053	3.379	3.584	3.581
13	98.06	-0.105042	3.378	3.583	3.580
14	98.57	-0.104527	3.369	3.575	3.573
14	98.57	-0.104597	3.370	3.575	3.573
14	98.63	-0.104474	3.368	3.574	3.572
15	101.48	-0.102511	3.331	3.538	3.534
15	101.54	-0.102539	3.331	3.538	3.533
15	101.59	-0.102508	3.331	3.537	3.533
13	122.21	-0.087287	3.063	3.281	3.282
13	122.23	-0.087323	3.063	3.282	3.281
13	122.38	-0.087238	3.062	3.280	3.280
14	123.97	-0.085901	3.040	3.260	3.262
15	124.09	-0.086021	3.041	3.261	3.261
14	124.14	-0.085758	3.038	3.257	3.260
15	124.19	-0.085973	3.040	3.260	3.260
15	124.19	-0.085970	3.040	3.260	3.260
14	124.45	-0.085498	3.034	3.254	3.257
14	146.49	-0.070461	2.794	3.029	3.033
13	146.59	-0.070505	2.795	3.029	3.032
14	146.67	-0.070370	2.793	3.027	3.031
13	146.69	-0.070423	2.793	3.028	3.031
13	146.70	-0.070451	2.794	3.028	3.031
14	146.75	-0.070312	2.792	3.026	3.030
15	146.86	-0.070410	2.793	3.028	3.029
15	147.06	-0.070212	2.790	3.025	3.027
15	147.08	-0.070235	2.790	3.025	3.027
16	178.79	-0.055112	2.511	2.770	2.770
16	178.95	-0.055055	2.510	2.770	2.769
16	179.16	-0.054957	2.508	2.768	2.767
17	179.97	-0.054238	2.499	2.760	2.761
18	180.00	-0.054565	2.503	2.763	2.761
17	180.04	-0.054184	2.498	2.759	2.761
17	180.13	-0.054082	2.497	2.758	2.760
18	180.17	-0.054589	2.503	2.764	2.760
18	180.18	-0.054472	2.502	2.762	2.760
17	200.13	-0.043146	2.353	2.632	2.634
17	200.27	-0.043132	2.353	2.632	2.633

17	200.29	-0.043156	2.353	2.632	2.633
18	200.41	-0.043483	2.357	2.636	2.632
18	200.64	-0.043367	2.355	2.635	2.631
18	200.85	-0.043217	2.354	2.633	2.630
16	201.15	-0.042957	2.350	2.630	2.628
16	201.35	-0.042809	2.349	2.629	2.627
16	201.40	-0.042782	2.348	2.628	2.627
17	225.52	-0.030419	2.199	2.504	2.507
17	225.86	-0.030387	2.199	2.504	2.506
17	225.97	-0.030355	2.198	2.504	2.506
16	227.42	-0.029963	2.193	2.501	2.499
16	227.52	-0.029891	2.192	2.500	2.499
16	227.56	-0.029846	2.192	2.500	2.499
18	227.64	-0.029965	2.193	2.501	2.499
18	227.94	-0.029870	2.192	2.500	2.497
18	228.12	-0.029783	2.191	2.499	2.497
18	251.32	-0.019322	2.075	2.414	2.414
18	251.37	-0.019600	2.078	2.416	2.414
17	252.21	-0.018580	2.068	2.407	2.412
17	252.29	-0.018862	2.071	2.410	2.411
17	252.35	-0.018763	2.070	2.409	2.411

Appendix C

SULPHURIC ACID RESULTS

TABLE C.1

Terms Contributing to the Final Smoothed pK'_2 as a Function of Ionic Strength and Temperature.

Clark-Glew Equation, Three Terms, Values above 150 °C are extrapolated.

t/°C	E (mV)	E_J (mV)	pQ_2	pK'_2
$m_{H_2SO_4} = 0.01, m_{KCl} = 0.10, : m_{HCl} = 0.01, m_{KCl} = 0.1$				
75	-7.140	1.687	2.136	2.680
100	-4.711	1.152	2.507	3.078
125	-2.533	0.808	2.888	3.492
150	-1.083	0.620	3.267	3.911
175	-0.281	0.535	3.640	4.332
200	0.121	0.503	4.006	4.753
225	0.308	0.488	4.360	5.172
$m_{H_2SO_4} = 0.01, m_{KCl} = 0.30, : m_{HCl} = 0.01, m_{KCl} = 0.3$				
75	-10.340	0.794	1.916	2.670
100	-7.581	0.547	2.276	3.070
125	-5.017	0.384	2.612	3.454
150	-3.078	0.285	2.925	3.823
175	-1.802	0.232	3.215	4.178
200	-1.028	0.206	3.481	4.519
225	-0.578	0.191	3.722	4.848
$m_{H_2SO_4} = 0.01, m_{KCl} = 0.51, : m_{HCl} = 0.01, m_{KCl} = 0.5$				
75	-11.004	0.483	1.877	2.746
100	-8.512	0.337	2.201	3.116
125	-5.828	0.229	2.530	3.500
150	-3.552	0.158	2.857	3.892

175	-1.954	0.118	3.179	4.288
200	-0.982	0.095	3.489	4.684
225	-0.434	0.083	3.784	5.078

Clark-Glew Equation, Four Terms.

$t/^{\circ}\text{C}$	$E \text{ (mV)}$	$E_J \text{ (mV)}$	pQ_2	pK'_2
----------------------	------------------	--------------------	--------	---------

$m_{\text{H}_2\text{SO}_4} = 0.01, m_{\text{KCl}} = 0.10, :$ $m_{\text{HCl}} = 0.01, m_{\text{KCl}} = 0.1$

75	-7.157	1.690	2.134	2.678
100	-4.673	1.146	2.512	3.083
125	-2.484	0.802	2.897	3.501
150	-1.222	0.634	3.225	3.869
175	-0.660	0.567	3.451	4.143
200	-0.504	0.549	3.546	4.294
225	-0.690	0.554	3.491	4.305

$m_{\text{H}_2\text{SO}_4} = 0.01, m_{\text{KCl}} = 0.30, :$ $m_{\text{HCl}} = 0.01, m_{\text{KCl}} = 0.3$

75	-10.312	0.792	1.919	2.673
100	-7.648	0.551	2.269	3.063
125	-4.992	0.383	2.616	3.457
150	-3.163	0.289	2.911	3.809
175	-2.186	0.244	3.126	4.089
200	-1.827	0.227	3.236	4.275
225	-1.982	0.224	3.226	4.353

$m_{\text{H}_2\text{SO}_4} = 0.01, m_{\text{KCl}} = 0.51, :$ $m_{\text{HCl}} = 0.01, m_{\text{KCl}} = 0.5$

75	-10.937	0.480	1.884	2.753
100	-8.634	0.341	2.189	3.104
125	-5.765	0.227	2.537	3.507

150	-3.612	0.159	2.848	3.883
175	-2.476	0.128	3.069	4.178
200	-2.147	0.114	3.161	4.356
225	-2.590	0.113	3.097	4.393

TABLE C.2

pK'_2 Values as a Function of Ionic Strength and Temperature, CG3 Equation.

Ionic Strength

t/°C	0.11	0.31	0.52
75	2.680 ± 0.028	2.670 ± 0.017	2.746 ± 0.017
100	3.079 ± 0.021	3.070 ± 0.014	3.116 ± 0.013
125	3.492 ± 0.020	3.454 ± 0.013	3.500 ± 0.012
150	3.911 ± 0.033	3.823 ± 0.019	3.892 ± 0.017
n	45	36	24
s_f	0.035	0.019	0.015

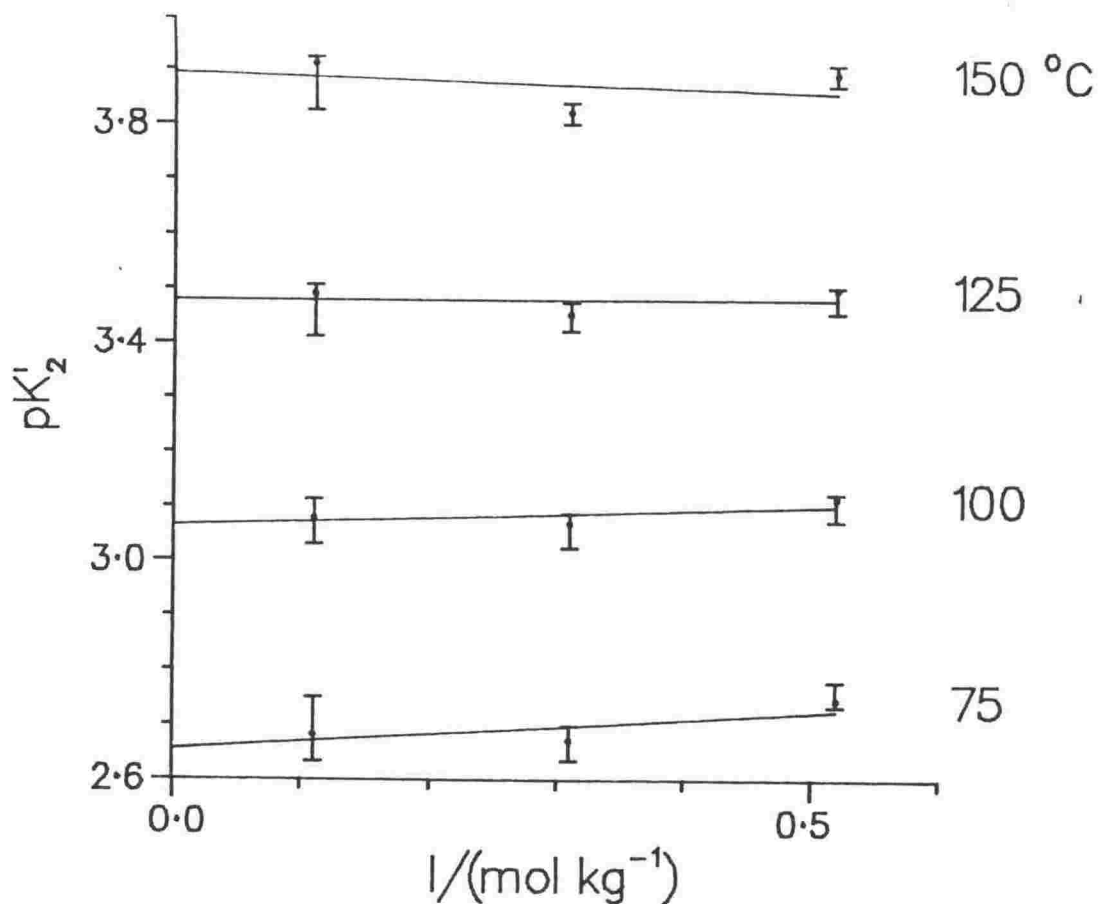


Figure C.1: The Variation of pK'_2 as a Function of Ionic Strength at Various Temperatures, CG3 Equation to 150°C.

TABLE C.3

Thermodynamic Values for the Dissociation of the Bisulphate Ion, CG3
Equation To 150°C.

t/°C	pK ₂ ^o	ΔG ^o	ΔH ^o	ΔS ^o
		(kJ mol ⁻¹)	(kJ mol ⁻¹)	(J K ⁻¹ mol ⁻¹)
25*	1.9 ± 0.3	11 ± 2	-26 ± 14	-122 ± 42
75	2.65 ± 0.04	17.7 ± 0.2	-38 ± 6	-160 ± 17
100	3.07 ± 0.03	21.9 ± 0.2	-44 ± 2	-177 ± 6
125	3.48 ± 0.03	26.5 ± 0.2	-50 ± 3	-193 ± 9
150	3.89 ± 0.04	31.5 ± 0.3	-56 ± 7	-208 ± 18
175*	4.3 ± 0.1	37 ± 1	-62 ± 12	-222 ± 28
200*	4.7 ± 0.2	43 ± 2	-69 ± 16	-235 ± 37
225*	5.1 ± 0.3	49 ± 3	-75 ± 20	-248 ± 46

$$\Delta C_p^o = -244 \pm 171 \text{ J K}^{-1} \text{ mol}^{-1}$$

$$n = 105, s_f = 0.036$$

* extrapolated values at these temperatures

TABLE C.4

Equation Coefficients For Dissociation Constant of the Bisulphate Ion.

Clark-Glew Equation, Three Terms, Data smoothed between 75 and 150 °C.

$$\theta = 373.15 \text{ K} \quad pK'_2 = a_0 + a_1 t_1 + a_2 t_2$$

I	a_0	a_1	a_2	n	s_f
0	3.06596	6.18148	12.73008	105	0.036
0.11	3.07934	6.07910	14.92303	45	0.035
0.31	3.06996	5.85319	8.13211	36	0.019
0.52	3.11597	5.65025	14.32977	24	0.015

Clark-Glew Equation, Four Terms , Data smoothed between 75 and 225 °C.

$$\theta = 423.15 \text{ K} \quad pK'_2 = a_0 + a_1 t_1 + a_2 t_2 + a_3 t_3$$

I	a_0	a_1	a_2	a_3	n	s_f
0	3.84577	5.33528	-15.95180	-111.49278	199	0.049
0.11	3.86911	5.52787	-16.18507	-132.39960	74	0.050
0.31	3.80942	5.41856	-10.35450	-97.34010	63	0.033
0.52	3.88294	5.80322	-11.94680	-146.61691	62	0.046

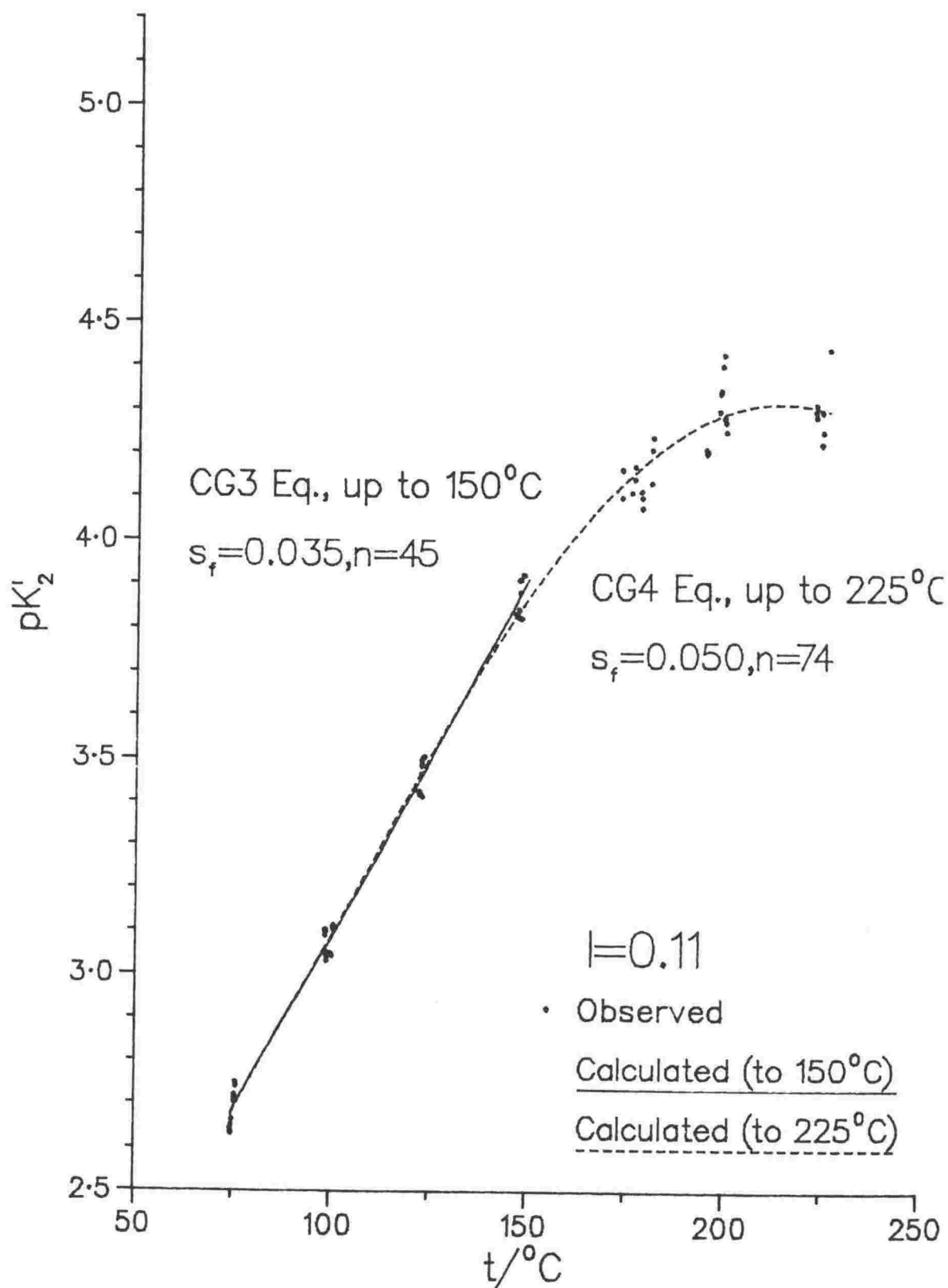


Figure C.2: The Temperature Dependence of pK'_2 in 0.1 mol kg⁻¹ KCl Solution.

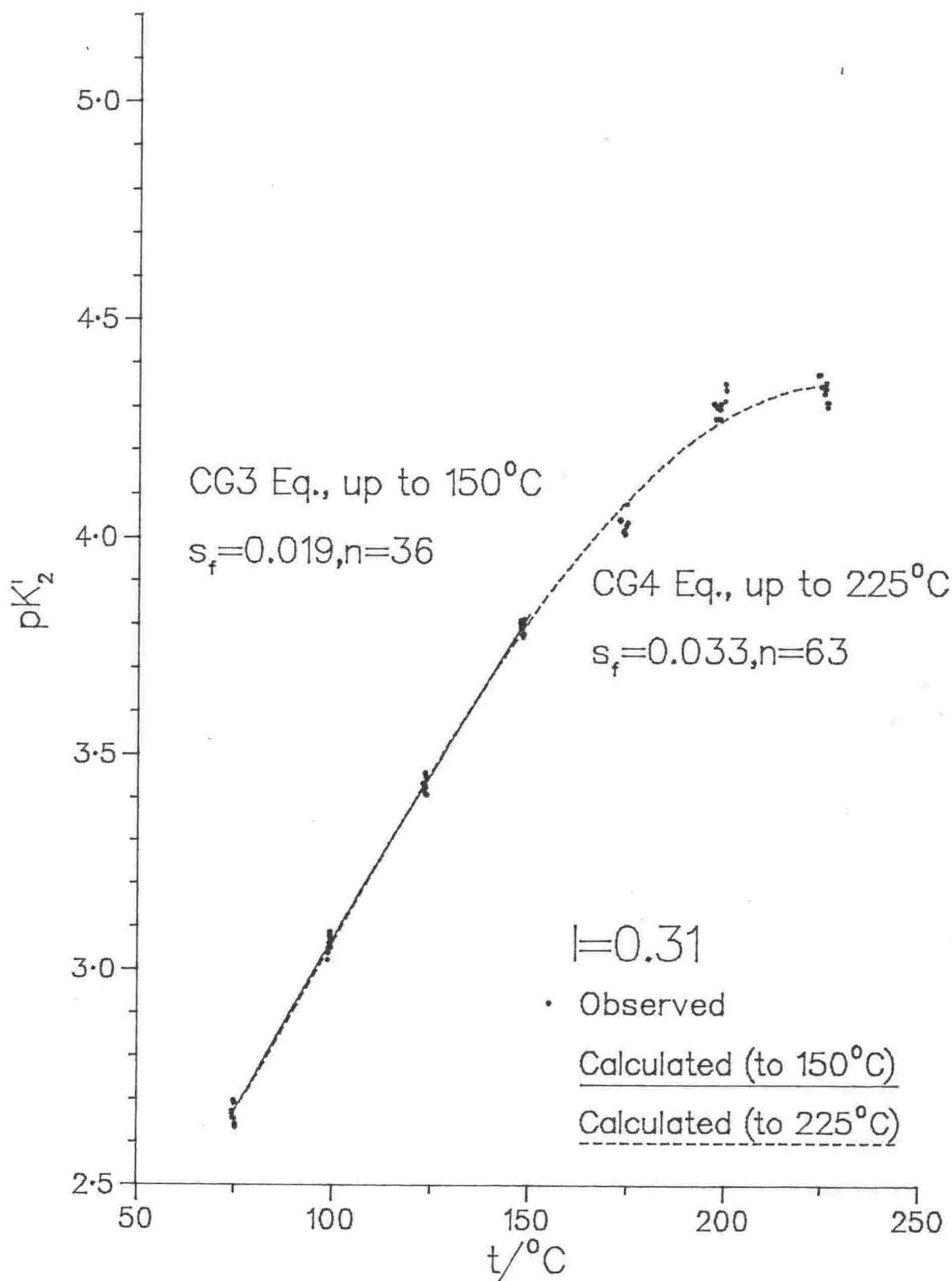


Figure C.3: ^{Temp.} The Dependence of pK'_2 in 0.3 mol kg⁻¹ KCl Solution

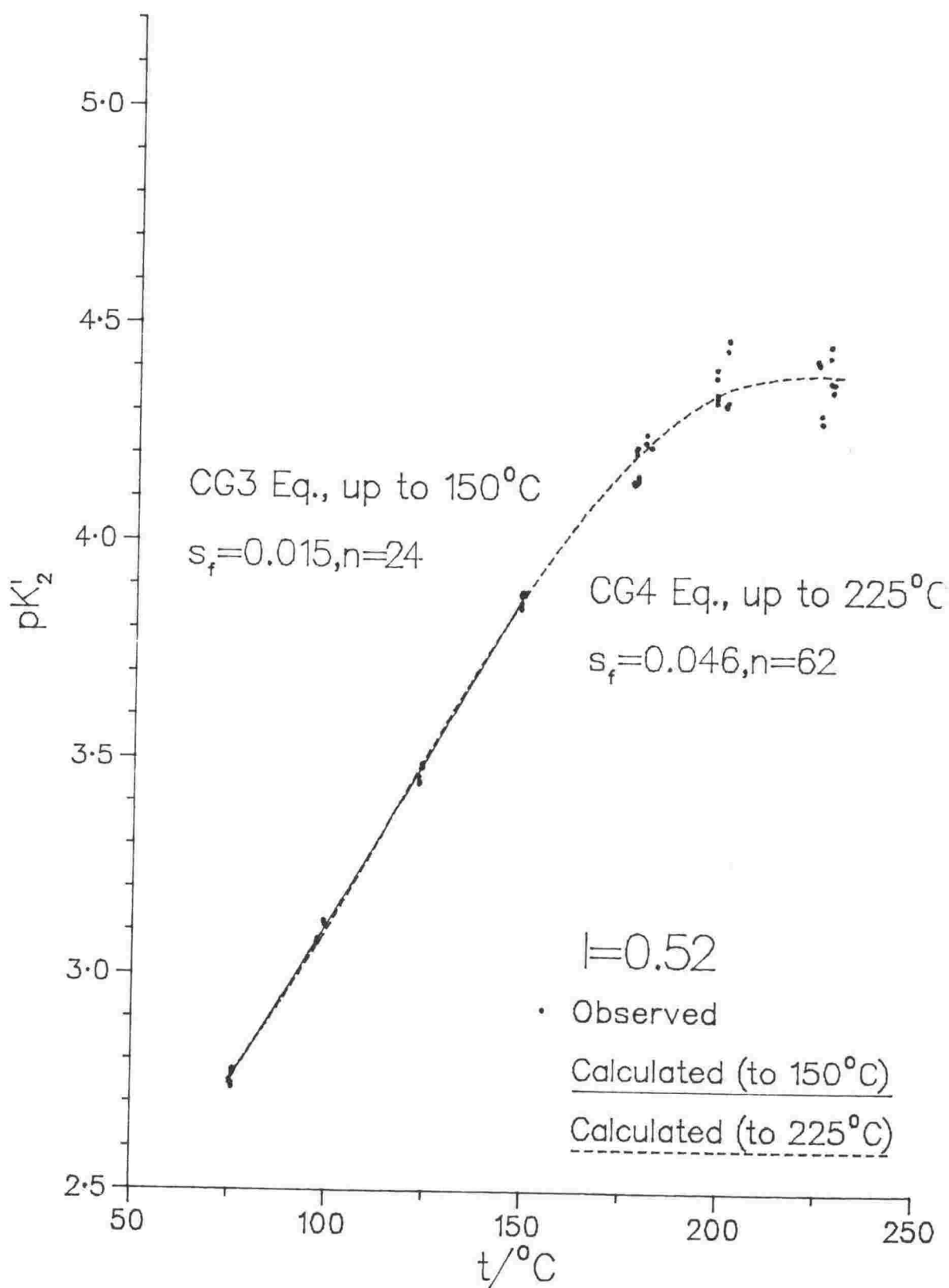


Figure C.4: The Temperature Dependence of pK'_2 in 0.5 mol kg⁻¹ KCl Solution.

TABLE C.5

Solution Concentrations Used in Determining The Dissociation Constant of the Bisulphate Ion.

Experiment	m_{KCl}	$m_{\text{H}_2\text{SO}_4}$:	m_{KCl}	m_{HCl}
1,2,3,4	0.095154	8.729×10^{-3}		0.095985	8.274×10^{-3}
9,10	0.283959	8.623×10^{-3}		0.285577	8.222×10^{-3}
15,16	0.486750	8.817×10^{-3}		0.488459	8.471×10^{-3}
11	0.287844	8.780×10^{-3}		0.286655	7.694×10^{-3}
5,6	0.101766	0.010229		0.101309	0.010645
7,8	0.101566	0.010546		0.101111	0.010841
12,13,14	0.309720	0.010362		0.307861	9.878×10^{-3}
17	0.514603	0.010517		0.504520	0.010969
18,19,20	0.516565	0.010628		0.514670	0.012076
21	0.493176	8.921×10^{-3}		0.487337	7.911×10^{-3}

TABLE C.6

Experimental Data of the Dissociation Constant of the Bisulphate Ion in
0.1 mol kg⁻¹ KCl Solution.

Experiment	t/°C	E (mV)	pQ ₂	pK' ₂	Fitted pK' ₂	
					(to 225°C)	(to 150°C)
2	74.72	-9.536	2.098	2.632	2.673	2.675
2	74.74	-9.467	2.106	2.640	2.674	2.675
2	74.76	-9.432	2.111	2.644	2.674	2.676
1	74.89	-9.535	2.098	2.632	2.676	2.678
1	74.95	-9.386	2.116	2.650	2.677	2.679
1	75.00	-9.282	2.129	2.662	2.678	2.680
3	75.67	-8.977	2.168	2.702	2.688	2.690
3	75.69	-8.900	2.178	2.711	2.688	2.690
3	75.69	-8.832	2.186	2.719	2.688	2.690
4	75.94	-8.592	2.216	2.749	2.692	2.694
4	76.01	-8.637	2.210	2.744	2.693	2.695
4	76.01	-8.672	2.206	2.740	2.693	2.695
3	98.61	-6.615	2.533	3.090	3.059	3.057
3	98.68	-6.505	2.547	3.104	3.060	3.058
3	98.69	-6.549	2.542	3.099	3.060	3.058
1	98.90	-6.952	2.491	3.050	3.064	3.061
1	98.91	-7.032	2.482	3.040	3.064	3.062
1	98.95	-7.117	2.471	3.030	3.065	3.062
2	99.81	-6.992	2.489	3.048	3.080	3.076
2	100.10	-7.029	2.485	3.045	3.084	3.081
2	100.39	-7.069	2.481	3.041	3.089	3.086
4	100.57	-6.545	2.548	3.108	3.092	3.089
4	100.67	-6.508	2.553	3.113	3.094	3.090
4	100.69	-6.575	2.544	3.104	3.094	3.091
4	122.40	-4.917	2.838	3.426	3.459	3.448
4	122.51	-4.971	2.830	3.418	3.461	3.450
4	122.53	-4.928	2.836	3.425	3.461	3.451
1	122.53	-4.939	2.835	3.423	3.461	3.451
1	122.76	-4.979	2.829	3.418	3.465	3.454
2	122.99	-4.686	2.878	3.466	3.469	3.458
3	123.00	-4.508	2.908	3.497	3.469	3.458
2	123.03	-4.572	2.897	3.486	3.470	3.459
2	123.12	-4.510	2.908	3.497	3.471	3.460
1	123.20	-5.020	2.824	3.413	3.472	3.462
3	123.37	-4.467	2.915	3.504	3.475	3.465
3	123.83	-4.475	2.916	3.506	3.482	3.472
4	146.85	-3.399	3.198	3.834	3.827	3.858
1	147.53	-3.333	3.217	3.844	3.836	3.869
3	147.56	-3.090	3.284	3.910	3.837	3.870
4	147.59	-3.408	3.198	3.825	3.837	3.870
1	147.75	-3.190	3.255	3.883	3.839	3.873
3	147.96	-3.092	3.284	3.912	3.842	3.877
4	148.21	-3.424	3.195	3.824	3.845	3.881
3	148.45	-3.061	3.294	3.922	3.849	3.885
2	148.88	-3.073	3.293	3.922	3.854	3.892

5	173.54	0.707	3.408	4.101	4.130	-
5	173.57	0.863	3.473	4.166	4.130	-
6	176.05	0.723	3.413	4.113	4.152	-
6	176.76	0.798	3.443	4.144	4.158	-
6	176.89	0.868	3.473	4.174	4.159	-
7	178.48	0.328	3.411	4.116	4.172	-
7	178.65	0.285	3.396	4.101	4.173	-
7	178.74	0.220	3.372	4.076	4.174	-
8	180.99	0.360	3.426	4.135	4.191	-
8	181.20	0.532	3.502	4.212	4.193	-
8	181.49	0.588	3.529	4.240	4.195	-
5	195.00	0.891	3.474	4.214	4.275	-
5	195.13	0.866	3.463	4.204	4.276	-
5	195.32	0.874	3.468	4.210	4.276	-
8	198.38	0.645	3.553	4.301	4.289	-
8	198.56	0.717	3.593	4.342	4.289	-
8	198.76	0.731	3.598	4.348	4.290	-
6	199.17	1.252	3.654	4.404	4.292	-
6	199.52	1.297	3.679	4.429	4.293	-
7	199.66	0.605	3.533	4.285	4.293	-
7	200.02	0.583	3.523	4.275	4.295	-
7	200.11	0.535	3.500	4.253	4.295	-
5	223.14	0.957	3.487	4.300	4.309	-
5	223.21	0.995	3.503	4.316	4.309	-
5	223.29	0.926	3.475	4.288	4.309	-
7	224.72	0.301	3.407	4.225	4.306	-
7	224.82	0.313	3.411	4.299	4.306	-
7	225.05	0.380	3.434	4.253	4.305	-
8	226.57	0.791	3.619	4.442	4.301	-

TABLE C.7

Experimental Data of the Dissociation Constant of the Bisulphate Ion in
0.3 mol kg⁻¹ KCl Solution.

Experiment	t/°C	E (mV)	pQ ₂	pK' ₂	Fitted pK' ₂	
					(to 225°C)	(to 150°C)
11	74.44	-14.739	1.913	2.656	2.665	2.661
11	74.45	-14.662	1.922	2.665	2.665	2.661
11	74.47	-14.601	1.928	2.671	2.665	2.661
10	74.88	-12.026	1.956	2.697	2.671	2.668
10	74.96	-12.045	1.954	2.695	2.672	2.669
9	75.07	-12.436	1.913	2.654	2.674	2.671
10	75.07	-12.095	1.949	2.690	2.674	2.671
9	75.22	-12.561	1.900	2.641	2.676	2.673
9	75.29	-12.634	1.892	2.634	2.677	2.674
9	98.79	-10.035	2.244	3.023	3.043	3.051
9	98.93	-9.875	2.261	3.040	3.045	3.053
9	98.98	-9.767	2.272	3.051	3.046	3.054
10	99.22	-9.654	2.284	3.063	3.050	3.058
11	99.32	-12.076	2.294	3.076	3.052	3.059
11	99.33	-12.025	2.299	3.081	3.052	3.059
11	99.34	-11.960	2.206	3.088	3.052	3.060
10	99.39	-9.717	2.278	3.058	3.053	3.060
10	99.54	-9.779	2.273	3.052	3.055	3.063
9	122.95	-7.171	2.611	3.434	3.426	3.423
10	123.36	-7.373	2.589	3.413	3.432	3.429
11	123.45	-9.709	2.631	3.459	3.433	3.431
9	123.48	-7.230	2.605	3.430	3.434	3.431
10	123.53	-7.419	2.584	3.409	3.435	3.432
9	123.61	-7.285	2.600	3.424	3.436	3.433
11	123.61	-9.792	2.622	3.450	3.436	3.433
10	123.85	-7.435	2.583	3.408	3.439	3.437
11	123.87	-9.843	2.617	3.445	3.440	3.437
9	147.74	-5.182	2.926	3.804	3.780	3.791
9	147.78	-5.256	2.915	3.793	3.781	3.791
9	147.78	-5.140	2.933	3.810	3.781	3.791
11	148.14	-8.146	2.917	3.799	3.785	3.796
11	148.18	-8.098	2.924	3.806	3.786	3.797
11	148.25	-8.329	2.890	3.772	3.787	3.798
10	148.40	-5.363	2.900	3.779	3.789	3.800
10	148.44	-5.249	2.917	3.797	3.789	3.801
10	148.50	-5.153	2.932	3.812	3.790	3.802
14	172.70	-4.089	3.077	4.043	4.067	-
14	172.85	-4.107	3.074	4.040	4.068	-
14	172.98	-4.095	3.076	4.043	4.069	-
12	173.67	-4.241	3.049	4.017	4.076	-
12	173.86	-4.267	3.044	4.013	4.078	-
12	174.12	-4.295	3.039	4.009	4.080	-
13	174.39	-4.197	3.059	4.029	4.083	-
13	174.56	-3.962	3.107	4.078	4.085	-
13	174.67	-4.170	3.064	4.036	4.086	-

4	196.78	-3.471	3.272	4.310	4.256	-
14	197.30	-3.614	3.236	4.275	4.259	-
14	197.43	-3.509	3.264	4.303	4.260	-
12	198.27	-3.636	3.232	4.275	4.265	-
12	198.33	-3.550	3.254	4.297	4.265	-
12	198.43	-3.509	3.266	4.309	4.266	-
13	199.56	-3.505	3.269	4.316	4.272	-
13	199.72	-3.366	3.308	4.355	4.273	-
13	199.89	-3.421	3.293	4.341	4.274	-
14	223.64	-3.797	3.244	4.376	4.352	-
14	224.09	-3.804	3.244	4.377	4.353	-
14	224.35	-3.930	3.214	4.349	4.353	-
13	225.24	-4.025	3.194	4.333	4.354	-
13	225.51	-3.986	3.204	4.343	4.354	-
13	225.59	-3.925	3.218	4.358	4.354	-
12	225.86	-4.129	3.173	4.313	4.354	-
12	226.07	-4.141	3.171	4.312	4.354	-

TABLE C.8

Experimental Data of the Dissociation Constant of the Bisulphate Ion in
0.5 mol kg⁻¹ KCl Solution.

Experiment	t/°C	E (mV)	pQ ₂	pK' ₂	Fitted pK' ₂	
					(to 225°C)	(to 150°C)
16	75.82	-12.739	1.888	2.747	2.763	2.757
16	75.85	-12.853	1.876	2.735	2.763	2.758
16	75.88	-12.789	1.883	2.742	2.764	2.758
15	76.04	-12.450	1.919	2.778	2.766	2.761
15	76.05	-12.506	1.913	2.773	2.766	2.761
15	76.06	-12.562	1.907	2.767	2.766	2.761
16	97.40	-10.609	2.177	3.075	3.064	3.077
16	97.65	-10.630	2.175	3.074	3.067	3.080
16	97.66	-10.535	2.185	3.084	3.068	3.081
15	99.15	-10.171	2.225	3.126	3.091	3.103
15	99.24	-10.234	2.219	3.121	3.092	3.104
15	99.39	-10.291	2.213	3.116	3.094	3.107
16	123.09	-7.954	2.508	3.462	3.476	3.471
16	123.17	-8.117	2.491	3.445	3.478	3.472
16	123.19	-8.058	2.497	3.451	3.478	3.472
15	123.83	-7.760	2.530	3.486	3.488	3.482
15	123.87	-7.700	2.534	3.492	3.489	3.483
15	124.00	-7.801	2.526	3.482	3.491	3.485
16	148.48	-5.645	2.832	3.850	3.862	3.868
16	148.54	-5.560	2.844	3.862	3.863	3.869
15	148.58	-5.393	2.867	3.885	3.863	3.870
16	148.59	-5.438	2.861	3.879	3.863	3.870
15	148.89	-5.383	2.869	3.888	3.868	3.875
15	149.24	-5.422	2.864	3.884	3.872	3.880
17	176.87	-0.966	3.024	4.142	4.196	-
17	176.97	-0.990	3.025	4.144	4.197	-
17	177.11	-1.030	3.018	4.137	4.198	-
18	177.46	2.581	3.102	4.218	4.201	-
18	177.55	2.530	3.086	4.208	4.202	-
18	177.74	2.609	3.097	4.224	4.204	-
20	177.97	2.194	3.020	4.143	4.206	-
20	178.03	2.238	3.028	4.151	4.207	-
20	178.04	2.274	3.035	4.158	4.207	-
19	179.82	2.639	3.106	4.235	4.222	-
19	179.91	2.639	3.106	4.235	4.223	-
19	180.04	2.722	3.124	4.253	4.224	-
21	181.34	-7.282	3.104	4.224	4.235	-
21	181.40	-7.263	3.107	4.224	4.236	-
20	197.57	3.145	3.195	4.385	4.345	-
20	197.67	3.144	3.194	4.385	4.345	-
20	197.73	3.227	3.214	4.405	4.346	-
19	197.78	2.890	3.137	4.328	4.346	-
19	197.81	2.938	3.147	4.338	4.346	-
19	197.82	2.978	3.156	4.347	4.346	-
17	200.12	-0.527	3.123	4.322	4.357	-

17	200.39	-0.548	3.119	4.319	4.358	-
18	200.40	3.382	3.248	4.449	4.358	-
18	200.67	3.474	3.272	4.474	4.359	-
17	200.74	-0.499	3.129	4.330	4.359	-
18	200.76	3.467	3.270	4.472	4.360	-
20	223.33	3.036	3.134	4.427	4.396	-
20	223.66	2.994	3.126	4.419	4.395	-
20	223.73	2.978	3.122	4.416	4.395	-
19	224.47	2.326	3.005	4.302	4.394	-
19	224.70	2.200	2.984	4.283	4.394	-
19	224.82	2.196	2.983	4.283	4.394	-
18	226.53	3.022	3.128	4.434	4.391	-
18	226.66	3.146	3.153	4.460	4.390	-
18	226.73	3.155	3.155	4.462	4.390	-
17	226.77	-0.842	3.069	4.376	4.390	-
17	227.35	-0.978	3.046	4.355	4.389	-
17	227.64	-0.877	3.063	4.373	4.388	-

Appendix D

FELDSPAR HYDROLYSIS RESULTS

TABLE D.1

Feldspar Hydrolysis Experimental Results.

Refer to Table 7.1 for Solution Concentrations

Exp.	time(hr.)	t/°C	E (mV)	E _J (mV)	m _K ⁺	pH	log(m _K ⁺ /m _H ⁺)
A	0.00	225.00	-	-	-	5.475	5.213
A	13.92	221.57	218.320	-0.403	1.024550	6.468	6.102
A	14.58	223.09	217.650	"	"	6.457	6.089
A	15.17	223.85	216.240	"	"	6.440	6.071
A	15.67	233.77	214.820	"	"	6.426	6.057
A	16.25	223.79	213.450	"	"	6.412	6.043
A	16.75	223.71	212.100	"	"	6.398	6.030
A	17.25	223.63	210.680	"	"	6.384	6.016
A	17.75	223.61	209.160	"	"	6.369	6.000
A	18.25	223.60	207.770	"	"	6.355	5.986
A	18.75	223.45	206.620	"	"	6.343	5.975
A	19.25	223.83	205.400	"	"	6.330	5.961
A	19.75	223.70	203.970	"	"	6.316	5.947
A	20.25	223.79	202.870	"	"	6.304	5.936
A	20.75	223.98	201.400	"	"	6.289	5.920
A	21.25	223.97	199.780	"	"	6.275	5.906
A	21.75	223.83	198.720	"	"	6.262	5.894
A	22.25	223.80	197.695	"	"	6.252	5.883
B	0.00	225.00	-	-	-	4.322	3.962
B	15.00	223.31	177.586	-0.002	1.042317	6.100	5.740
B	15.50	223.82	175.286	"	"	6.070	5.709
B	16.00	223.97	172.450	"	"	6.045	5.684
B	16.58	223.93	170.000	"	"	6.024	5.663
B	17.33	223.97	167.886	"	"	5.998	5.637
B	17.92	224.05	162.851	"	"	5.973	5.611
B	18.58	223.97	161.026	"	"	5.954	5.593
B	19.08	223.84	159.836	"	"	5.942	5.582
B	19.62	223.72	157.990	"	"	5.924	5.563
B	20.00	223.73	156.781	"	"	5.912	5.551
B	20.67	223.75	155.234	"	"	5.895	5.535
C	17.50	224.92	147.021	-0.002	1.042317	5.811	5.448
C	18.00	225.29	143.995	"	"	5.779	5.417
C	18.50	225.32	142.179	"	"	5.761	5.398
C	19.00	225.37	140.684	"	"	5.746	5.383
C	19.50	224.73	139.339	"	"	5.733	5.371
C	20.00	224.33	138.228	"	"	5.722	5.361
C	20.50	224.10	137.112	"	"	5.712	5.350
C	21.00	223.98	135.742	"	"	5.698	5.337
C	21.50	224.11	134.773	"	"	5.688	5.327
C	22.00	224.15	133.461	"	"	5.674	5.313
D	0.00	225.00	-	-	-	5.591	4.384
D	13.97	225.32	339.930	-1.710	0.097657	6.624	5.415
D	14.80	224.67	338.230	"	0.976566	6.611	5.403
D	15.80	225.08	336.250	"	"	6.588	5.380
D	16.80	225.62	333.910	"	"	6.562	5.353

Exp.	time(hr.)	t/°C	E (mV)	E _J (mV)	m _K ⁺	pH	log(m _K ⁺ /m _H ⁺)
D	17.80	224.99	332.040	"	"	6.546	5.338
D	18.80	225.47	330.260	"	"	6.525	5.317
D	19.80	224.99	328.400	"	"	6.509	5.301
D	20.63	224.99	327.210	"	"	6.497	5.289
D	21.80	224.91	325.170	"	"	6.477	5.269
D	22.72	224.79	323.630	"	"	6.462	5.254
E	0.00	225.00	-	-	-	3.356	2.996
E	12.08	194.60	112.053	-0.024	1.047420	4.530	4.203
E	13.25	222.06	118.214	"	"	4.556	4.199
E	13.75	223.31	120.659	"	"	4.580	4.221
E	14.38	224.79	121.235	-0.022	"	4.584	4.223
E	14.75	224.82	120.968	"	"	4.581	4.220
E	15.25	224.89	120.303	"	"	4.574	4.213
E	15.75	224.91	119.557	"	"	4.567	4.206
E	16.25	224.99	118.631	"	"	4.557	4.196
E	16.83	225.03	117.765	"	"	4.548	4.187
E	17.33	224.91	117.048	"	"	4.541	4.161
E	17.75	224.84	117.156	"	"	4.543	4.162
E	18.25	224.72	116.205	"	"	4.533	4.153
E	18.75	224.76	115.676	"	"	4.528	4.167
E	19.25	224.81	115.285	"	"	4.524	4.163
E	19.75	224.80	114.794	"	"	4.519	4.158
E	20.25	224.82	114.907	"	1.047410	4.520	4.159
E	20.75	224.68	115.226	"	"	4.523	4.162
E	21.25	224.61	115.212	"	"	4.523	4.162
E	21.75	224.75	115.309	-0.021	1.047410	4.524	4.163
E	22.25	224.54	115.592	"	"	4.527	4.166
E	22.75	224.50	115.490	"	"	4.526	4.165
F	11.00	195.26	108.650	-0.042	1.044720	4.492	4.165
F	12.08	222.40	114.632	-0.041	1.047129	4.520	4.162
F	12.58	224.94	116.048	"	"	4.531	4.170
F	13.08	225.60	116.505	"	"	4.535	4.173
F	13.58	225.81	116.685	"	"	4.537	4.175
F	14.08	225.90	116.638	"	"	4.536	4.174
F	14.58	225.96	116.554	"	"	4.535	4.173
F	15.08	225.92	116.659	"	"	4.536	4.174
F	15.58	225.84	116.442	"	"	4.534	4.172
F	16.08	225.81	116.172	"	"	4.532	4.169
F	16.42	225.81	115.823	"	"	4.528	4.166
F	17.08	225.95	115.743	"	"	4.527	4.165
F	18.25	226.06	115.415	"	"	4.524	4.161
F	18.58	226.20	115.171	"	"	4.521	4.158
F	19.08	226.21	114.971	"	"	4.519	4.156
F	19.58	226.06	114.540	"	"	4.515	4.152
F	19.83	226.19	114.400	"	"	4.513	4.151
F	20.08	226.11	114.200	"	"	4.511	4.149
F	20.58	225.97	114.131	"	"	4.511	4.148
G	10.67	182.54	102.006	-0.025	1.045635	4.439	4.124
G	12.75	224.28	112.383	-0.021	1.045611	4.495	4.135
G	13.25	224.42	111.966	"	"	4.490	4.130
G	13.67	224.25	111.382	"	"	4.485	4.124
G	14.25	224.38	110.692	"	"	4.478	4.117

Exp.	time(hr.)	t/°C	E (mV)	E _J (mV)	m _K ⁺	pH	log(m _K ⁺ /m _H ⁺)
G	14.67	224.48	110.191	"	"	4.472	4.112
G	15.17	224.67	109.340	"	1.045635	4.464	4.103
G	15.67	224.17	108.143	"	"	4.452	4.092
G	16.97	223.93	106.849	"	"	4.439	4.079
G	17.67	223.84	106.005	"	"	4.431	4.071
G	18.17	223.74	105.361	"	"	4.428	4.065
G	18.83	223.70	104.973	"	"	4.420	4.061
G	19.17	224.48	104.733	"	"	4.417	4.057
G	19.67	224.48	104.624	"	"	4.416	4.056
G	20.17	224.41	104.102	"	"	4.411	4.050
G	20.67	224.35	103.843	"	"	4.408	4.048
G	21.17	224.35	103.626	"	"	4.406	4.046
H	0.00	225.00	-	-	-	3.167	1.987
H	12.50	196.54	123.286	-0.243	0.104954	4.477	3.316
H	13.43	218.57	129.758	-0.226	0.104877	4.497	3.323
H	14.50	225.07	137.788	-0.223	0.104882	4.566	3.387
H	15.67	225.51	141.660	"	"	4.604	3.425
H	16.50	225.51	143.277	"	"	4.620	3.440
H	17.55	225.37	144.577	"	"	4.634	3.454
H	18.42	225.49	145.155	"	0.104884	4.639	3.460
H	18.50	225.45	145.685	"	"	4.645	3.465
H	19.42	225.27	145.817	-0.224	"	4.646	3.467
H	22.25	225.59	146.024	-0.223	"	4.648	3.468
I	0.00	225.00	-	-	-	2.074	1.717
I	12.75	224.32	5.774	-0.054	1.061402	2.133	1.777
I	13.25	224.32	5.682	-0.053	1.061353	2.132	1.776
I	13.75	224.26	5.429	-0.051	1.061256	2.130	1.773
I	15.25	224.47	5.231	-0.049	1.061158	2.128	1.771
I	15.75	224.58	5.207	"	1.061133	2.128	1.771
I	16.25	224.75	5.314	"	1.061207	2.129	1.772
I	16.75	224.71	5.295	"	1.061182	2.129	1.772
I	17.25	224.35	5.243	"	1.061158	2.128	1.771
I	17.75	224.38	5.143	"	1.061109	2.127	1.770
I	18.25	224.46	5.175	"	1.061133	2.127	1.771
I	18.67	224.33	5.188	"	1.061158	2.127	1.771
I	19.25	224.29	5.096	"	1.061085	2.126	1.770
I	20.50	224.01	5.030	"	1.061085	2.125	1.769
J	0.00	225.00	-	-	-	2.185	0.992
J	16.50	225.66	8.600	-0.378	0.104621	2.277	1.091
J	17.00	225.73	8.663	-0.381	0.104636	2.278	1.092
J	18.08	225.56	8.840	-0.388	0.104672	2.279	1.094
J	19.08	225.47	8.937	-0.392	0.104691	2.280	1.095
J	20.20	225.59	8.960	-0.393	0.104695	2.281	1.095
J	21.08	225.73	9.094	-0.398	0.104722	2.282	1.097
J	22.00	225.65	9.165	-0.401	0.104739	2.283	1.098
K	0.00	225.00	-	-	-	1.903	0.696
K	13.75	224.42	4.105	-0.348	0.102329	1.948	0.749

Exp. time(hr.)		$t/^{\circ}\text{C}$	E (mV)	E_J (mV)	m_{K^+}	pH	$\log(m_{K^+}/m_{H^+})$
K	14.92	224.65	4.349	-0.368	0.102442	1.951	0.752
K	16.25	224.89	4.463	-0.376	0.102492	1.952	0.754
K	17.25	224.85	4.518	-0.380	0.102518	1.953	0.754
K	18.33	224.45	4.491	-0.379	0.102506	1.953	0.754
K	19.17	224.76	4.472	-0.393	0.102588	1.954	0.756
K	21.08	224.93	4.832	-0.405	0.102660	1.956	0.758
K	22.33	224.80	4.896	-0.410	0.102687	1.957	0.759
L	14.50	224.86	3.572	-0.304	0.102082	1.942	0.742
L	15.87	224.90	3.794	-0.322	0.102187	1.945	0.745
L	17.00	224.73	4.027	-0.342	0.102294	1.947	0.748
L	17.92	224.68	3.871	-0.330	0.102224	1.946	0.746
L	18.92	224.89	3.944	-0.334	0.102256	1.947	0.747
L	19.92	224.66	4.028	-0.346	0.102318	1.948	0.749
L	20.92	224.78	4.022	-0.341	0.102290	1.947	0.748

REFERENCES

1. Macdonald D.D., Butler P., Owen D., Can. J. Chem. 51, 2590 (1973).
2. Bolton P.D., J. Chem. Educ. 47, 638 (1970).
3. Richard D.T., Wickman F.E., (Editors) Chemistry and Geochemistry of Solutions at High Temperatures and Pressures, Pergamon Press, 321 (1981).
4. Staehle R.W., Jones de D.G., Slater J.E., (Editors) High Temperature High Pressure Electrochemistry in Aqueous Solutions NACE-4 (1973).
5. Tödheide K., Ber Bunsenges. Phys. Chem. 86, 1005 (1982).
6. Cobble J.W., Science 152, 1479 (1966).
7. Helgeson H.C. in: Chemistry and Geochemistry of Solutions at High Temperatures and Pressures (ed. Richard D.T., Wickman F.E.), Pergamon Press, 133 (1981).
8. Reed M.H., Geochim. Cosmochim. Acta 46, 513 (1982).
9. Mann G.M.W. in: High Temperature High Pressure Electrochemistry in Aqueous Solutions (ed. Jones D. de G., Slater J., Staehle R.W.), NACE-4, 34 (1973).
10. Kwok O.J., Robins R.G., International Symposium on Hydrometallurgy, 1033 (1973).
11. Tomlinson M. in: High Temperature High Pressure Electrochemistry in Aqueous Solutions (ed. Jones D. de G., Slater J., Staehle R.W.), NACE-4, 221 (1973).
12. Barnes H.L. in: High Temperature High Pressure Electrochemistry in Aqueous Solutions (ed. Jones D. de G., Slater J., Staehle R.W.), NACE-4, 14 (1973).
13. Barnes H.L. in: Chemistry and Geochemistry of Solutions at High Temperatures and Pressures (ed. Richard D.T., Wickman F.E.), Pergamon Press, 321 (1981).
14. Dobson J.V., Adv. Corros. Sci. Technol. 7, 177 (1980).
15. Macdonald D.D. in: Modern Aspects of Electrochemistry (ed. Conway B.E., Bockris J.O'M.), Butterworths, 2, 141 (1975).
16. Macdonald D.D., Corrosion 34, 75 (1978).
17. Kryukov P.A., Starostina L.I., Izv. Sib. Otd. Akad. Nauk SSSR, Ser. Khim. Nauk No. 3, 27 (1970).

18. Seward T.M., *Geochim. Cosmochim. Acta* 40, 1329 (1976).
19. Mesmer R.E., Baes C.F., Sweeton F.H., *J. Phys. Chem.* 74, 1937 (1970).
20. Haar L., Gallagher J.S., Kell G.S., *A Thermodynamic Surface for Water : The Formulation and Computing Programs*, NBSIR 81 2253.
21. Pitzer K.S., Roy R.N., Silvester L.F., *J. Am. Chem. Soc.* 99, 4930 (1977).
22. Young T.F., Singleterry C.R., Klotz I.M., *J. Phys. Chem.* 82, 671 (1978).
23. Larson J.W., Zeeb K.G., Hepler L.G., *Can. J. Chem.* 60, 2141 (1982).
24. Hepler L.G., Hopkins H.P., *Rev. Inorg. Chem.* 1, 303 (1979).
25. Usdowski H.E., Barnes H.L., *Contr. Mineral. Petrol.* 36, 207 (1972).
26. Jones D. de G. in: *High Temperature High Pressure Electrochemistry in Aqueous Solutions* (ed. Jones D. de G., Slater J., Staehle R.W.), NACE-4, 265 (1973).
27. AEI Plastics (Aldridge) Ltd., *Fluorocarbons* (1971).
28. Danielson M.J., Koski O.H., Shannon D.W., *Development of Electrochemical Probes for Down Hole and In Line Chemical Analysis of High Temperature High Pressure Geothermal Fluids*. Interim Report No. 2459, Pacific Northwest Laboratories (1977).
29. Atlas Stainless Steels Co., *Technical Data*.
30. Benedict R.R., *Fundamentals of temperature, pressure and flow measurements*, 2nd Ed., John Wiley (1977).
31. Fellows S.K., *Conductance measurements on Aqueous Solutions over Extended Ranges of Concentration and Temperature*, PhD Thesis, Victoria University of Wellington (1971).
32. Pound B.G., *The Polarization Behaviour of Silver in Potassium Hydroxide Solution at Elevated Temperatures*, PhD Thesis, Victoria University of Wellington (1977).
33. Feltham A.M., Spiro M., *Chem. Rev.* 71, 177 (1971).
34. Ives D.J.G and Janz G.J., *Reference Electrodes*, Academic Press (1961).
35. Vogel A.I., *Textbook of Quantitative Inorganic Analysis*, 4th Ed., Longmans (1979).
36. Bangham A.D., Hill M.W., *Nature* 237, 408 (1972).
37. Nakamura S., Fudagawa N., Kawase A., *Bruneski Kayaku* 28, T39 (1979).
38. New Zealand Industrial Gases Ltd., *Personal Communications*.

39. Cox R.A., Haldna U.L., Idler K.L., Yates K., Can. J. Chem. 59, 2591 (1981).
40. MacInnes D.A., The Principles of Electrochemistry, Dover, (1961).
41. Manning G.D., Faraday Trans. 74, 2434 (1978).
42. McKubre M., Personal Communications.
43. Henderson P., Z. Phys. Chem. 59, 118 (1907).
44. Kortüm G., Bockris J.O'M., Textbook of Electrochemistry, Vol 1, Elsevier (1951).
45. Hewlett-Packard, HP-25 Application Programs (1975).
46. Helgeson H.C., Kirkham D.H., Am. J. Sci. 274, 1199 (1974).
47. Lewis G.N., Randall M., Revised by Pitzer K.S., Brewer L., 2nd. Ed., McGraw-Hill (1965), page 318 and references therein.
48. Lietzke M.H., Stoughton R.W., J. Chem. Educ. 39, 230 (1962).
49. Readnour J.M., Cobble J.W., Inorg. Chem. 8, 2174 (1969).
50. Pitzer K.S., J. Phys. Chem. 77, 268 (1973).
51. Pitzer K.S., Acc. Chem. Res. 10, 371 (1977).
52. Pitzer K.S. in: Chemistry and Geochemistry of Solutions at High Temperatures and Pressures (ed. Richard D.T., Wickman F.E.), Pergamon Press, 249 (1981).
53. Millero F.J., Schreiber D.R., Amer. J. Sci. 282, 1508 (1982).
54. Bates R.G., Determination of pH, 2nd Ed., John Wiley (1973).
55. Liu C., Lindsay W.T., J. Soln. Chem. 1, 45 (1972).
56. Covington A.K., Anal. Chim. Acta. 127, 1 (1981).
57. Robinson R.A., Stokes R.H., Electrolyte Solutions, 2nd Ed., Butterworths (1959).
58. Harned H.S., Cook M.A., J. Am. Chem. Soc. 59, 2304 (1937).
59. Akerlof G.C., Oshry H.I., J. Am. Chem. Soc. 72, 2846 (1950).
60. Sweeton F.H., Mesmer R.E., Baes C.F., J. Soln. Chem. 3, 191 (1974).
61. Lietzke M.H., Stoughton R.W., Young T.F., J. Phys. Chem. 65, 2247 (1961).
62. Marshall W.L., Jones E.V., J. Phys. Chem. 70, 4028 (1966).
63. Naumov G.B., Ryzhenko B.N., Khodakovskiy I.L., Handbook of Thermodynamic Data, USGS Transl., USGS-WRD-74-001, (1971).
64. IUPAC Commission 1.2, J. Chem. Thermodyn. 14, 805 (1982).

65. Blandamer M.J., Burgess J., Robertson R.E., Scott J.M.W., Chem. Rev. 82, 259 (1982).
66. Dobson J.V., Thirsk H.R., Electrochim. Acta 16, 315 (1971).
67. Valentiner S., Z. Phys. Chem. 42, 853 (1907).
68. Clark E.C.W., Glew D.N., Trans. Faraday Soc. 62, 539 (1966).
69. SAS Institute Inc., SAS Users Guide (ed. Helwig J.T., Council K.A.), (1975).
70. Bütikofer H.P., Covington A.K., Evans D.A., Electrochim. Acta 24, 1071 (1979).
71. Quist A.S., Marshall W.L., J. Phys. Chem. 69, 2984, (1965).
72. Bates R.G., CRC Crit. Rev. Anal. Chem. 10, 247 (1981).
73. Rock P.A., Electrochim. Acta 12, 1531 (1967).
74. IUPAC Commission 1.2, J. Chem. Thermodyn. 13, 603 (1981).
75. King E.J., Acid-Base Equilibria (The International Encyclopedia of Physical Chemistry and Chemical Physics, Vol. 4, ed. Guggenheim E.A., Mayer J.E., Tompkins F.C.), Pergamon Press (1965).
76. Timini B.A., Electrochim. Acta 19, 149 (1974).
77. Harned H.S., Owen B.B., Physical Chemistry of Electrolyte Solutions, 3rd Ed., Reinhold Press (1958).
78. Clever H.L.J., J. Chem. Educ. 45, 231 (1968).
79. Chatfield C., Statistics for Technology, Penguin (1970).
80. Perkovets V.D., Kryukov P.A., Izv. Sibirsk. Otd. Akad. Nauk SSSR, Ser Khim. Nauk No. 3, 9 (1969).
81. Greeley R.S., Smith W.T., Stoughton R.W., Lietzke M.H., J. Phys. Chem. 64, 652 (1960).
82. Bezboruah C.P., Filomena M., Camoes G.F.C., Covington A.K., Dobson J.V., Trans. Faraday Soc. 69, 949 (1973).
83. Bates R.G., Bower V.E., J. Res. Nat. Bur. Stand. 53, 283 (1954).
84. Bignold G.J., Brewer A.D., Hearn B., Trans. Faraday Soc. 67, 2419 (1971).
85. Fisher J.R., Barnes H.L., J. Phys. Chem. 76, 90 (1972).
86. Fisher J.R., Haas, Jr., J.L., Unpublished Results USGS (1973).
87. Busey R.H., Mesmer R.E., J. Soln. Chem. 5, 147 (1976).
88. Olofsson G., Hepler L.G., J. Soln. Chem. 4, 127 (1975).
89. Marshall W.L., Franck E.U., J. Phys. Chem. Ref. Data 10, 295 (1981).

90. Busey R.H., Mesmer R.E., J. Chem. Eng. Data 23, 175 (1978).
91. Olofsson G., Olofsson I., J. Chem. Thermodyn. 13, 437 (1981).
92. Ramette R.W., J. Chem. Educ. 54, 280 (1977).
93. Covington A.K., Bates R.G., Durst R.A., Pure & Appl. Chem. 55, 1467 (1983).
94. Le Peintre M., Soc. Franc. Elect. Bull. 8, 584 (1960).
95. Chaudon L., A Method for Measuring pH at High Temperature is Presented, PhD Thesis, Commissariat a l'Energie Atomique-France, CEA-R-4964, (1979).
96. Kryukov P.A., Perkovets V.D., Starostina L.I., Smolyakov B.S., Izv. Sib. Otd. Akad. Nauk SSSR, Ser. Khim. Nauk No. 2, 29 (1966).
97. Perkovets V.D., Kryukov P.A., Izv. Sibirsk. Otd. Akad. Nauk SSSR, Ser. Khim. Nauk No. 6, 22 (1968).
98. Mesmer R.E., Baes C.F., Sweeton F.H., Proc. International Water Conference 32nd, Pittsburgh, Pa., 55 (1971).
99. Mesmer R.E., Baes C.F., Sweeton F.H., Inorg Chem. 11, 537 (1972).
100. Seward T.M., Geochim. Cosmochim. Acta 38, 1651 (1974).
101. Greeley R.S., Smith W.T., Stoughton R.W., Lietzke M.H., J. Phys. Chem. 64, 1445 (1960).
102. Greeley R.S., Smith W.T., Stoughton R.W., Lietzke M.H., J. Phys. Chem. 64, 1861 (1960).
103. Stark J.G., Wallace H.G., Chemistry Data Book, John Murray Ltd (1970).
104. Hamer J.W., J. Am. Chem. Soc. 56, 860 (1934).
105. Davies C.W., Jones H.W., Monk C.B., Trans. Faraday Soc. 48, 921 (1952).
106. Covington A.K., Dobson J.V., Srinivasan K.V., Faraday Trans. I, 69, 94 (1973).
107. Ryzhenko B.N., Geochem. Intern. 1, 8 (1964).
108. Quist A.S., Marshall W.L., Jolley H.R., J. Phys. Chem. 69, 2726 (1965).
109. Quist A.S., Marshall W.L., J. Phys. Chem. 70, 3714 (1966).
110. Pavlyuk L.A., Smolyakov B.S., Kryukov P.A., Izv. Sib. Otd. Akad. Nauk SSSR, Ser. Khim. Nauk No. 3, 3 (1972).
111. Schöön N.H., Wannholt I., Svensk Papperstidn. 72, 431 (1969).
112. Cabani S., Gianni P., Anal. Chem. 44, 253 (1972).

113. King E.J., King G.W., J. Am. Chem. Soc. 74, 1212 (1952).
114. Covington A.K., Dobson J.V., Wynne-Jones W.F.K., Trans. Faraday Soc. 61, 2057 (1965).
115. Monk C.B., Amira M.F., Faraday Trans. 74, 1170 (1978).
116. Hamer W., in: The Structure of Electrolytic Solutions (ed. Hamer W.), 236, John Wiley (1959).
117. Christensen J.J., Izatt R.M., Hansen L.D., Partridge J.A., J. Phys. Chem. 70, 2003 (1966).
118. Izatt R.M., Eatough D., Christensen J.J., Bartholomew C.H., J. Chem. Soc.(A), 45 (1969).
119. Quist A.S., Franck E. U., Jolley H.R., Marshall W.L., J. Phys. Chem. 67, 2453, (1963).
120. Guggenheim E.A., Turgeon J.C., Trans Faraday Soc. 51, 747 (1955).
121. Helgeson H.C., J. Phys. Chem. 71, 3121 (1967).
122. Kortüm G., Treatise on Electrochemistry, Elsevier (1965).
123. Lietzke M.H., Stoughton R.W., J. Phys. Chem. 63, 1188 (1959).
124. Seward T.M., Personal Communications (1983), (H. Sakai, Okayama Univ.).
125. Ohmoto H., Lasaga A.C., Geochim. Cosmochim. Acta 46, 1727 (1982).
126. Malinin S.D., Khitarov N.I., Geochem. Intern. 6, 1022 (1969).
127. Gurney R.W., Ionic Processes in Solution, McGraw-Hill, N.Y. (1953).
128. Helgeson H.C., Kirkham D.H., Amer. J. Sci. 274, 1089 (1974).
129. Conway B.E., Ionic Hydration in Chemistry and Biophysics, Elsevier (1981).
130. Seward T.M., in: Chemistry and Geochemistry of Solutions at High Temperatures and Pressures (ed. Richard D.T., Wickman F.E.), Pergamon Press, 113 (1981).
131. Reed A.J., J. Soln. Chem. 11, 649 (1982).
132. Mesmer R.E., Baes C.F., J. Soln. Chem. 3, 307 (1974).
133. Ryzhenko B.N., Dokl. Akad. Nauk SSSR 149, 639 (1963), (see ref. 121).
134. Eugster H.P., in: Chemistry and Geochemistry of Solutions at High Temperatures and Pressures (ed. Richard D.T., Wickman F.E.), Pergamon Press, 461 (1981).
135. Gunter W.D., Eugster H.P., Contrib. Mineral. Petrol. 75, 235 (1980).

136. Burt D.M., Econ. Geol. 71, 665 (1976).
137. Morey G.W., Fournier R.O., Rowe J.J., Geochim. et Cosmochim. Acta 26, 1029 (1962).
138. Aagaard P., Helgeson H.C., Amer. J. Sci. 282, 237 (1982).
139. Lin F.C., Clemency C.V., Geochim. Cosmochim. Acta 45, 571 (1981).
140. Holdren Jr G.R., Berner R.A., Geochim. Cosmochim. Acta 43, 1161 (1979).
141. Fung P.C., Sanipelli G.G., Geochim. Cosmochim. Acta 46, 503 (1982).
142. Shade J.W., Econ. Geol. 69, 218 (1974).
143. Hemley J.J., Am. J. Sci. 257, 241 (1959).
144. Ivanov I.P., Belyayevskaya O.N., Potekhin V.Yu., Dokl. Akad. Nauk SSSR 219, 164 (1974).